Design and Development of Efficient Photosensitizers for Ln^{3+} ions based on Aromatic Carboxylates

Thesis submitted to

The University of Kerala

for the award of the degree of

Doctor of Philosophy in Chemistry

Under The Faculty of Science

By

RAMYA A. R.

NATIONAL INSTITUTE FOR INTERDISCIPLINARY

SCIENCE AND TECHNOLOGY (NIIST)

COUNCIL OF SCIENTIFIC AND INDUSTRIAL RESEARCH (CSIR)

THIRUVANANTHAPURAM-695 019

KERALA, INDIA

2014

Dedicated to.....

My Teachers

DECLARATION

I hereby declare that the Ph.D. thesis entitled **"Design and Development of Efficient Photosensitizers for Ln^{3+} ions based on Aromatic Carboxylates"** is an independent work carried out by me at the Materials Science and Technology Division, National Institute for Interdisciplinary Science and Technology (NIIST), CSIR, Thiruvananthapuram, under the supervision of **Dr. M. L. P. Reddy**, it has not been submitted anywhere else for any other degree, diploma or title.

Ramya A. R.

Thiruvananthapuram
October, 2014

NATIONAL INSTITUTE FOR INTERDISCIPLINARY SCIENCE AND TECHNOLOGY (NIIST)

Council of Scientific & Industrial Research (CSIR)
(Formerly Regional Research Laboratory)
Industrial Estate P.O., Trivandrum - 695 019
Kerala, INDIA

ISO 9001 REGISTERED

Dr. M. L. P. Reddy
Chief Scientist & Head
Materials Science and Technology Division

Tel: 91-471-2515 360
Fax: +91-471-2491 712
E-mail: mlpreddy55@gmail.com

CERTIFICATE

This is to certify that the work embodied in the thesis entitled **"Design and Development of Efficient Photosensitizers for Ln^{3+} ions based on Aromatic Carboxylates"** has been carried out by **Ms. Ramya A. R.** under my supervision at the Materials Science and Technology Division of National Institute for Interdisciplinary Science and Technology (NIIST), CSIR, Thiruvananthapuram and the same has not been submitted elsewhere for any other degree.

Dr. M. L. P. Reddy
(Thesis supervisor)

Thiruvananthapuram
October, 2014

Acknowledgements

It gives me great pleasure to place on record my deep sense of respect, regard and gratitude to my research supervisor Dr. M. L. P. Reddy for his excellent guidance, support and constant encouragement throughout the course of my work.

I would like to thank Dr. Suresh Das, Director, Dr. T. K. Chandrasekhar and Dr. B. C. Pai, former Directors, NIIST, for providing all the research facilities to carry out my work.

I am grateful to Dr. D. Ramaiah, former Head, Chemical Sciences and Technology Division, for his help and support. I am also grateful to all scientists and staffs of CSTD and MSTD for the help they rendered.

My sincere thanks to Prof. Alan H. Cowley, Dr. Kalyan V. Vasudevan, (Department of Chemistry and Biochemistry, University of Texas at Austin) and Prof. Srinivasan Natarajan, Dr. Debajit Sarma (Indian Institute of Science, Bangalore) and Dr. Sunil Varughese for helping to acquire single crystal X-ray data.

My sincere thanks to Ms. Soumini Mathew, Mr. B. Adarsh , Mr. Preethanuj, Ms. Viji, Mr.Kiran and Ms. Lucy Paul for their help in recording, ^{1}H NMR, ^{13}C NMR , FAB-MS , TEM and SEM analysis.

Words are inadequate to thank my dear friends Linda and Usha for their care, love, support and encouragement, which made my life in NIIST memorable.

I thank all the members of the division and in particular, Dr. Biju S., Dr. Ambili Raj, Dr. Shyni Raphael, Dr. Vishnu V. S., Dr. Giable George, Dr. Balamurugan, Dr. Divya , Dr. Sarika, Mr. Biju Francis, Ms. Aiswaria, Ms. Sheethu, Mr. Bejoy, Mr. George, Ms. Lucky, Mr. Thejus, Mr. Ali, Ms. Anaswara and Ms. Surya for their help and cooperation. I would like to thank Dr. Prathish, Aneesh, Dr. Sindhu, Dr. Danya and Milja for the help they rendered. I also thank all the former and present colleagues in my division for their help and support.

I would like to extend my thanks to Maneesh, Vaishakan Thampi and Bineesh for their friendship, help and care.

I cannot forget the companionship of my dear friends Dr. Suneesh, Suchitra, Sudheesh, Sajna, Derry, Vijay, Anupama, Sumi, Shubha, Mahesh, for their help and support.

I would also like to extend my thanks and appreciation to all my teachers for their help and blessings.

I am deeply indebted to my parents, sister Reshma and brother-in-law Sandeep for their love, care, patience and constant support throughout my research career. I owe my deep regards to my husband Nikesh, who has been constant source of inspiration during the entire period of my research.

I acknowledge the Council of Scientific and Industrial Research (CSIR) and Department of Science and Technology for the financial assistance.

Ramya

CONTENTS

List of Tables

List of Schemes **Page**

List of figures **Page**

ABBREVIATIONS

1.	$BaSO_4$	Barium Sulphate
2.	$CHCl_3$	Chloroform
3.	CH_3CN	Acetonitrile
4.	CH_2Cl_2	Dichloromethane
5.	CH_3OH	Methanol
6.	CIE	Commission internationale de l'éclairage
7.	DMF	N,N′-dimethylformamide
8.	DMSO	Dimethyl sulphoxide
9.	DSC	Differential Scanning Calorimeter
10.	EtOH	Ethanol
11.	FAB-MS	Fast Atom Bombardment Mass Spectrometer
12.	FT-IR	Fourier Transform Infra-Red
13.	ILCT	Intraligand Charge Transfer
14.	IR	Infrared
15.	ISC	Inter System Crossing
16.	KBr	Potassium bromide
17.	K_2CO_3	Potassium carbonate
18.	LMCT	Ligand-to-Metal Charge Transfer
19.	Ln^{3+}	Lanthanide ion
20.	MD	Magnetic Dipole
21.	MOF	Metal Organic Framework
22.	NMR	Nuclear Magnetic Resonance
23.	OLED	Organic Light Emitting Diode
24.	PL	Photoluminescence
25.	PMMA	poly(methyl methacrylate)

26.	ppm	Parts per million
27.	RGB	Red Green Blue
28.	S_1	Singlet
29.	SEM	Scanning Electron Microscopy
30.	T_1	Triplet
31.	TEM	Transmission Electron Microscopy
32.	TGA	Thermogravimetric analysis
33.	UV-Vis	Ultra Violet-Visible
34.	Xe	Xenon
35.	XRD	X-Ray Diffraction

PREFACE

Lanthanides possess intrinsic luminescence that originates from f–f electron transitions in the $4f^n$ shell of the [Xe] $5s^25p^6$ configuration and offer unique properties for potential applications in lighting, optical communications, photonics and biomedical devices. First, due to shielding by the 5s and 5p orbitals, the 4f orbitals do not directly participate in chemical bonding. The emission wavelengths of lanthanides are thus minimally perturbed by the surrounding matrix and ligand field, resulting in sharp, line-like emission bands with the same fingerprint wavelengths and narrow peak widths of the corresponding free Ln^{3+} salts. Second, the f–f transitions are formally forbidden by the spin and Laporte rule and feature long excited-state lifetimes in the milli- to microsecond range. Although the excited-state lifetimes of Ln^{3+} complexes are long, the forbidden f–f transitions suffer the consequence of weak intrinsic luminescence due to low molar absorptivity. Attachment of a light-harvesting antenna circumvents this limitation by sensitizing the Ln^{3+} ion in what has been termed as the antenna effect. In particular, when modified with light-harvesting moieties, benzoates have proven to be efficient sensitizers for lanthanide ions. Therefore the objective of the current research work is to design and develop efficient light emitting materials based on lanthanide aromatic benzoates with superior photophysical properties.

The present thesis has been divided into four chapters. In the first chapter, general principles for improving the light harvesting feature in the design of luminescent Eu^{3+} and Tb^{3+} complexes were discussed with a specific emphasis on how to take advantage of it for developing “robust antenna

molecules" based on various derivatives of benzoic acid. Of special importance was to demonstrate the key point of design of lanthanide benzoate coordination compounds with intriguing structural features and unique photoluminescent properties for potential utility in various photonic materials. The generation of white light emission from mixed lanthanide complexes are also described in the introduction chapter. These white light-emitting materials and devices have potential applications in solid-state lighting, low-cost back-lighting and full-color displays. Furthermore, the objectives of the thesis are also briefly presented in this chapter.

Three new binuclear lanthanide complexes of general formula $[Ln_2(L)_6(H_2O)_4]$ (Ln = Tb (**1**), Eu (**2**) and Gd (**3**)) supported by the novel aromatic carboxylate ligand 4-(dibenzylamino)benzoic acid (HL) have been synthesized, characterized and investigated their photophysical properties and these results are described in chapter 2. Complexes **1** and **2** were structurally characterized by single-crystal X-ray diffraction. Both **1** and **2** crystallize in the triclinic space group Pī and their molecular structures consist of homodinuclear species that are bridged by two oxygen atoms from two carboxylate ligands *via* different coordination modes. The discrete bridged dimer of **1** is centrosymmetric and features 8-coordinate terbium atoms, each of which adopts a distorted square-antiprismatic geometry. Both coordination spheres comprise two η^2-chelating benzoates, two μ-η^1:η^1-carboxylate interactions from the bridging benzoates, and two water molecules. By contrast, in complex **2** the Eu^{3+} ion coordination environment is best described as a distorted tricapped-trigonal prism, each europium ion being coordinated to three η^2-chelating

benzoate ligands and two water molecules. One of the η^2-carboxylate ligand is involved in a further interaction with an adjacent metal, thus rendering the overall binding mode bridging tridentate, μ-η^2:η^1. The Tb^{3+} complex **1** exhibits high green luminescence efficiency in the solid state with a quantum yield of 82%. On the other hand, poor luminescence efficiency has been noted for Eu^{3+} - 4-(dibenzylamino)benzoate complex.

A new aromatic carboxylate ligand, namely, 4- (dipyridin-2-yl)aminobenzoic acid (HL), has been designed and employed for the construction of a series of lanthanide complexes (Eu^{3+} = 1, Tb^{3+} = 2 and Gd^{3+} = 3). Complexes of **1**, **2** and **3** were structurally authenticated by single-crystal X-ray diffraction and were found to exist as infinite 1D coordination polymers with the general formulas $\{[Eu(L)_3(H_2O)_2]\}_n$ (**1**), $\{[Tb(L)_3(H_2O)].(H_2O)\}_n$ (**2**) and $\{[Gd(L)_3(H_2O)_2]\}_n$ (**3**). The photophysical properties demonstrated that the developed 4-(dipyridin-2-yl)aminobenzoate ligand is well suited for the sensitization of Tb^{3+} emission. On the other hand, the corresponding Eu^{3+} complex shows weak luminescence efficiency due to poor matching of the triplet state of the ligand with that of the emissive excited states of the metal ion. Furthermore, in this work, a mixed lanthanide system featuring Eu^{3+} and Tb^{3+} ions with the general formula $\{[Eu_{0.5}Tb_{0.5}(L)_3(H_2O)_2]\}_n$ (4) was also synthesized, and the luminescent properties were evaluated and compared with those of the analogous single-lanthanide ion systems (**1** and **2**). These results have been incorporated in chapter 3.

The fourth chapter describes the synthesis of a series of isostructural mixed Ln^{3+}-4-(dipyridin-2-yl)aminobenzoate coordination polymers [Ln^{3+} =

Eu^{3+} (**1**), Tb^{3+} (**2**), and Gd^{3+} (**3**)], their characterization and photophysical properties. The results demonstrated that by gently tuning the excitation wavelength of these mixed lanthanide complexes, white light emission can be realized with the Commission Internationale de I'Eclairage coordinates (0.32, 0.34). Furthermore, by changing the concentration profiles of lanthanide ions stiochiometrically in mixed-lanthanide complexes and exciting at particular wavelength, various emission colours can also be successfully obtained. The antenna ligand, 4-(dipyridin-2-yl)aminobenzoic acid provides an efficient energy transfer for the sensitization of Eu^{3+} and Tb^{3+} complexes and exhibits red and green emissions, respectively. Most importantly, due to the high energy (32150 cm^{-1}) of the Gd^{3+} ion lowest-lying emission level, the corresponding Gd^{3+} complex displays ligand-centered visible emission in blue light region, and hence it acts as a blue emitter. Therefore, Eu^{3+} and Tb^{3+} complexes in conjunction with Gd^{3+} complex is a suitable choice to obtain tunable white-light-emission from Ln^{3+} coordination polymers. The morphological analyses of the mixed lanthanide coordination polymers by Transmission Electron Microscopy (TEM) discloses that these compounds exist as unique crystalline nano-rods with an average diameter of 200 nm. The developed mixed lanthanide complexes also exhibit high thermal stability (~ 420 °C).

CHAPTER 1

Lanthanide luminescence: An overview

Lanthanides possess intrinsic luminescence that originates from f–f electron transitions in the $4f^n$ shell of the $[Xe]5s^25p^6$ configuration and offer unique properties for potential applications in many areas including solid state lighting and biomedicine (Figure 1.1) (Heffern *et al*. 2014; Bünzli and Eliseeva 2013; Feng and Zhang 2013; Bünzli 2010; Eliseeva and Bünzli 2010; Rocha *et al.* 2011; Brunet *et al.* 2007; de Bettencourt-Dias 2007; Kido and Okamoto 2002; Yan 2012; Armelao *et al.* 2010). First, due to shielding by the 5s and 5p orbitals, the 4f orbitals do not directly participate in chemical bonding. The emission wavelengths of lanthanides are thus minimally perturbed by the surrounding matrix and ligand field, resulting in sharp, line-like emission bands with the same fingerprint wavelengths and narrow peak widths of the corresponding free Ln^{3+} salts. Second, the f–f transitions are formally forbidden by the spin and Laporte rule and feature long excited-state lifetimes in the milli to microsecond range.

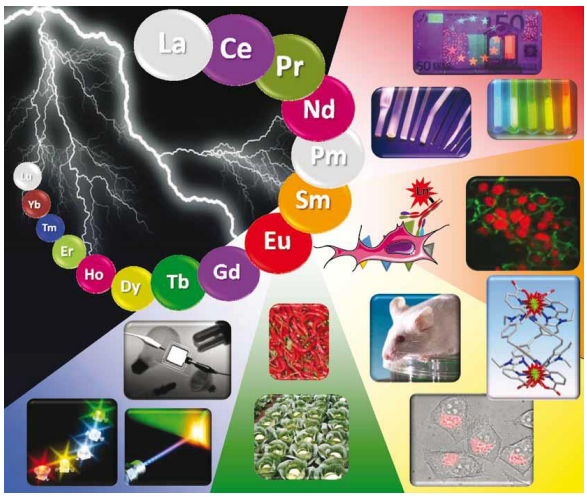

Figure 1.1. Applications of lanthanide luminescence.

Despite these useful features, obtaining the necessary excited states for lanthanide luminescence in a material can be difficult. Due to their parity-forbidden nature, the absorption coefficients for f–f-transitions are very low, which mostly gives ineffective luminescence. Different lanthanide elements in their trivalent state show diverse luminescence colours and characteristics. This results in easily predictable and very narrow emissions, as excited and ground states do hardly differ except in energy, covering a range from UV to NIR that is characteristic of Ln^{3+} ions, as shown in Figure 1.2 (Heine and Muller-Buschubaum 2013). A large number of luminescent lanthanide compounds are based on Tb^{3+} and Eu^{3+} which provide green or red 4f–4f-emissions, respectively. Additionally, Tb^{3+} and Eu^{3+} ions feature an energy gap between their main emissive and receiving states that is large enough to avoid pronounced vibrational quenching. Lanthanide ions such as Nd^{3+}, Er^{3+} or Yb^{3+} can provide f–f-emissions in technologically relevant ranges such as NIR or show upconversion effects where two or more NIR photons are combined into one shorter wavelength. Yet, lanthanides show much richer photophysics than this, as they are not generally restricted to metal-centred f–f-luminescence. As an exception, Ce^{3+} can show 5d–4f-transitions as emission in the visible range, as the energetic level of the d states is reduced by ligand and crystal fields. These transitions show a much higher dependence on the coordination environment of the metal ion than f–f transitions, due to participation of d states. They provide broad absorption and emission bands that do not require an antenna effect to improve brightness, as the transitions f–d and d–f are parity allowed. This is also observed for divalent lanthanide ions like Eu^{2+}, as they can

also commit 5d levels in luminescence processes. Reduction of energy of 5d states depending on chemical surrounding and the crystal field dominates broad band processes that are parity allowed and therefore as strong as for Ce^{3+}. Hence, transitions involving d and f states significantly differ from f–f transitions.

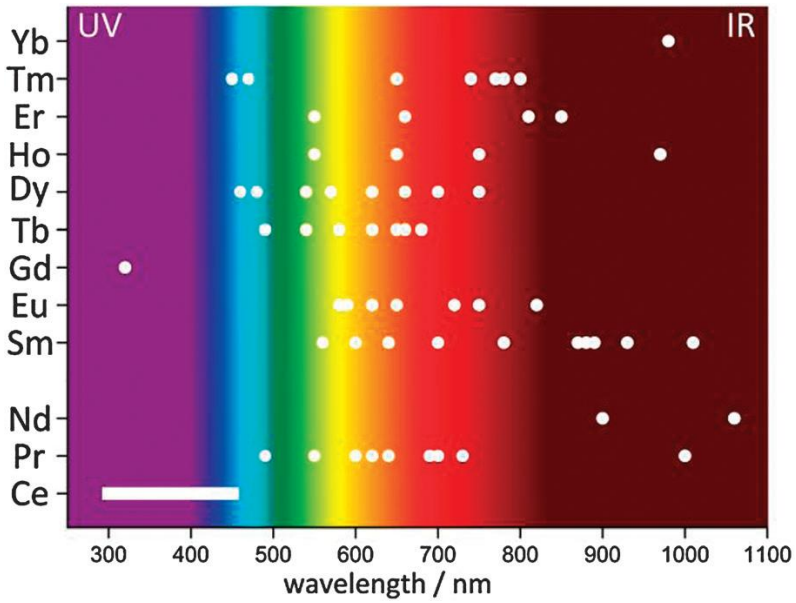

Figure 1.2. Wavelength of the main emissive transitions of the trivalent lanthanide coordination compounds in the near-UV to near-IR range.

1.1. The Antenna Effect

Although the excited-state lifetimes of Ln^{3+} complexes are long, the forbidden f–f transitions suffer the consequence of weak intrinsic luminescence due to low molar absorptivity. Intense light sources such as lasers are required to populate the excited states of Ln^{3+} ions by direct excitation and are impractical for the majority of biological imaging. Attachment of a light-harvesting antenna circumvents this limitation by sensitizing the Ln^{3+} ion in what has been termed

as the antenna effect (Figure 1.3(A)) (Heffern *et al*. 2014; Lehn 1990; Sabbatini *et al.* 1993). Light absorbed to the short-lived singlet excited state of the antenna ($S_0 \rightarrow S_1$) can undergo intersystem crossing to the longer-lived triplet excited state ($S_1 \rightarrow T_1$). Sensitization occurs by population of the lowest ^5D_J excited state of the lanthanide through energy transfer from the T_1 state of the antenna. Energy transfer can also occur from the S_1 state, but energy transfer from the T_1 state is generally accepted as the mechanism due to its longer lifetime. Electronic transitions from the ^5D_J excited state to the ^7F_J ground state of the lanthanide emit photons characterized by a series of bands in the visible (Eu^{3+} and Tb^{3+}) and near-IR (Dy^{3+} and Sm^{3+}) wavelengths. Figure 1.3(B) (Heffern *et al*. 2014) depicts the $^5D_0 \rightarrow {}^7F_J$ transitions (ΔJ = 0, 1, 2, 3, 4, and 5) for Eu^{3+} and the $^5D_4 \rightarrow {}^7F_J$ transitions (ΔJ = 2, 3, 4, 5, 6) for Tb^{3+} with commonly observed wavelengths.

The overall quantum yield ($\Phi_{overall}$) for a lanthanide complex treats the system as a "black box" in which the internal process is not considered explicitly. Given that the complex absorbs a photon (i.e., the antenna is excited), the overall quantum yield can be defined as follows (Comby *et al.* 2004; Xiao *et al.* 2001):

$$\Phi_{overall} = \Phi_{ISC}\Phi_{ET}\Phi_{Ln}$$

where Φ_{ISC} and Φ_{ET} are the respective efficiencies of intersystem crossing (ISC) and ligand-to-Ln^{3+} energy transfer (ET), and Φ_{Ln} is the intrinsic quantum yield of the Ln^{3+} ion.

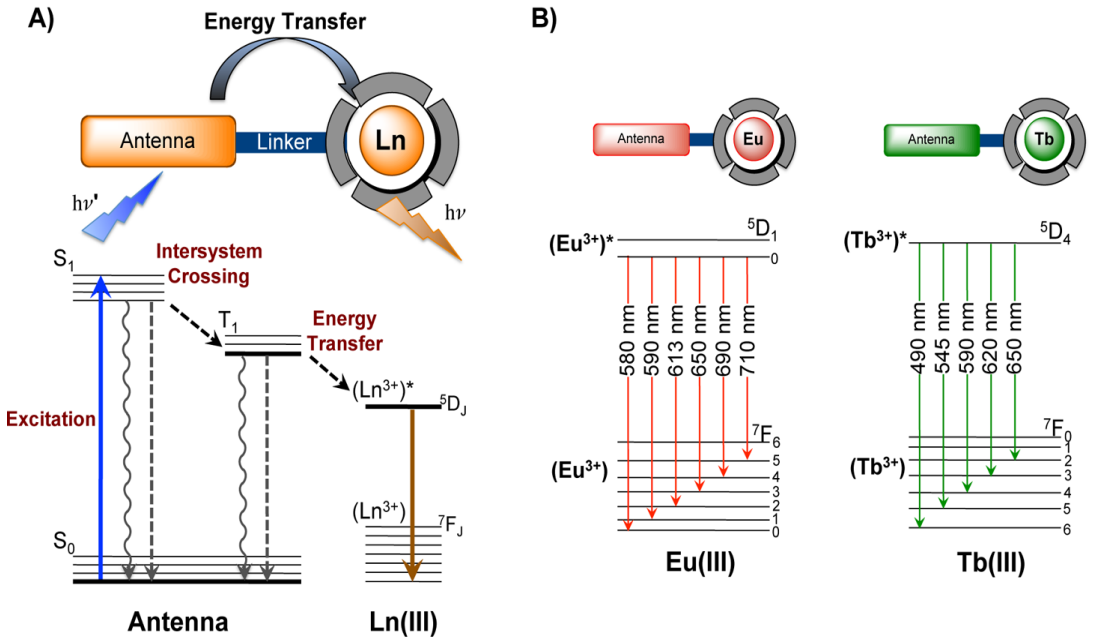

Figure 1.3. (A) The antenna effect. (B) Luminescent 4f–4f transitions of europium and terbium complexes and commonly observed emission wavelengths to emit red and green light, respectively.

1.2. Sensitizing Antennae

The antenna should possess a high molar absorptivity (high ε_{Ant}) for the $S_0 \rightarrow S_1$ transition. Ideal excitation wavelengths (λ_{ex}) should be > 340 nm to permit the use of quartz optics and minimize interfering excitation by chromophores in biological media. Antennae for luminescent lanthanides are generally limited to excitations < 420 nm due to energy requirements, namely a sufficiently small singlet–triplet state energy gap for efficient ISC and a triplet state energy that is greater than that of the Ln^{3+} excited state. Upon absorption, ISC from the S_1 into the T_1 state must be favoured over competing radiative (antenna fluorescence) and non-radiative relaxation back to the S_0 ground state to achieve a high Φ_{ISC}. This is most efficient when the ΔE between the T_1 and S_1 is < 8000 cm^{-1}

(Steemers *et al*. 1995; De Silva *et al.* 2008). The Ln^{3+} ion in the chelate serves as a sensitizer for ISC to the triplet state (in addition to being an energy acceptor) due to the increased spin–orbit coupling from the heavy-atom effect, making ISC faster in a chelated lanthanide than with the free chromophore. The Φ_{ET} of the T_1(antenna) → ^5D_J (Ln) transfer is determined by the energy gap between the two states (Latva *et al*. 1997). The energy of the triplet state must be slightly higher in energy than the ^5D_J of the lanthanide (20400 cm^{-1} for the $^5D_4$ of the Tb^{3+} ion and 17250 cm^{-1} for the $^5D_0$ of the Eu^{3+} ion) but with sufficiently large ΔE to minimize back-energy transfer. Such thermal repopulation of the T_1 manifold can be avoided with ΔE ≥ 1850 cm^{-1}. At short ranges of 10 Å or less, when an antenna molecule is within the bonding distance to the lanthanide ion, a direct electron exchange *via* a Dexter mechanism is possible. At longer ranges of up to 10 nm, for example when an antenna molecule or a complex is embedded as a guest within the framework of a lanthanide-based MOF, a dipole–dipole exchange *via* a Förster transfer may be observed (Bünzli and Piguet 2005; Dexter 1953).

The 'design' of suitable antenna ligands is a vital parameter. A number of principles have emerged from the study of luminescent lanthanide complexes that can help to guide the search for an appropriate ligand antenna. To achieve optimal luminescence quantum yields, a ligand with a T_1 state of appropriate energy equalling or slightly lower than the excited Ln-state should be chosen so that the energy difference between the ligand's triplet state and the excited lanthanide states is around 2500–3500 cm^{-1} (Latva *et al*. 1997). Aromatic carboxylic acids (Raphael *et al.* 2007; Raphael *et al.* 2008; Shavaleev *et al.* 2009;

Shavaleev 2010; Shavaleev *et al.* 2009; Zhan *et al.* 2012) and *β*-diketones (Binnemans 2009; Biju *et al.* 2009; Biju *et al.* 2009; Biju *et al.* 2006; Biju *et al.* 2009; Raj *et al.* 2010; Raj *et al.* 2008; Raj *et al.* 2010; Divya *et al*. 2010) are particularly valuable in this context because such ligands can absorb ultraviolet light and transfer the absorbed energy to the central lanthanide ions in an appropriately effective manner. In particular, when aromatic carboxylic acids are employed as the antenna ligands, the coordinated lanthanide ions exhibit higher luminescent stabilities than those ligated with other organic ligands. This enhanced stability is of obvious practical importance in terms of device performance and stability. A number of lanthanide benzoate coordination complexes with unique photophysical properties and intriguing structural features have been disclosed in our recent review article (Reddy and Sivakumar 2013).

1.3. Lanthanide complexes derived from various derivatives of benzoic acid

A new family of lanthanide (Eu^{3+}, Tb^{3+}, and Gd^{3+}) carboxylate complexes: $[Ln_2(L1)_6(MeOH)_4]_n$, $[Ln(L1)_3(DMF)]_n$ (L1 = benzoic acid), $[Ln(L2)_3(MeOH)_2]_n$ (L2 = 4-trifluoromethylbenzoic acid), $[Ln(L3)_3(MeOH)_2]_n$ (L3 = 4-trifluoromethoxybenzoic acid), $[Ln(L4)_3(DMF)(H_2O)]_2$ (L4 = 4-ethoxybenzoic acid), and $[Ln(L5)_2(NO_3)(MeOH)_2]_n$ (L5 = 4-*n*-propoxybenzoic acid), based on benzoic acid and its derivatives (L1-L5, Figure 1.4) have been developed by Wong and co-workers (Wong *et al.* 2003). The molecular structures of the isolated complexes are established by X-ray crystallography, which revealed that various chelating modes of benzoate ligands are present in the metal

coordination environment, resulting in the formation of dimeric and polymeric skeletons. Molecular structures of complexes (Eu^{3+}, Gd^{3+}, and Tb^{3+}) are found to be isostructural with a particular benzoic acid ligand. Comparison of the photoluminescence properties of lanthanide complexes with various benzoate ligands indicated that the electron-donating groups such as ethoxy and propoxy substituted on the fourth position of the benzoic acid increases the stability of the complexes, resulting in longer lifetimes and stronger luminescent intensities as compared with simple lanthanide benzoate complex. On the other hand, relatively shorter lifetimes and weak luminescent intensities were noted for electron-withdrawing groups such as trifluoromethyl and trifluoromethoxy substituted ligands. The triplet state energies of benzoic acid derivatives with *para*- and *ortho*- substituted –OH and $–NH_2$ groups are found to be in the range of 23 500 – 25 500 cm^{-1}, which is above the emission level of $^5D_0$ for Eu^{3+} and $^5D_4$ for Tb^{3+} ions (Georges and Arnaud 2000). This therefore supports the observation of stronger sensitization of terbium complexes than of the europium complexes because of the smaller overlap between the ligand triplet and Eu^{3+} ion excited states. Based on the above triplet state energy values, Wong and co-workers (Wong *et al.* 2003) concluded that aromatic benzoate ligands are in general sensitizes Tb^{3+} effectively than Eu^{3+}.

Ana de Bettencourt-Dias and co-workers (de Bettencourt-Dias and Viswanathan 2006) have synthesized several complexes of Eu^{3+} and Tb^{3+} with *o*, *m*, *p*-nitrobenzoic acid anions as ligands (L6–L8, Figure 1.5) and investigated their photophysical properties (Table 1.1). Single crystal X-ray analysis discloses that Eu^{3+}-*o*-nitrobenzoate complex is molecular, with two

homometallic molecules in the unit cell. On other hand, the formation of coordination polymers is noted with *m*- and *p*-nitrobenzoate complexes of Eu^{3+} and Tb^{3+}.

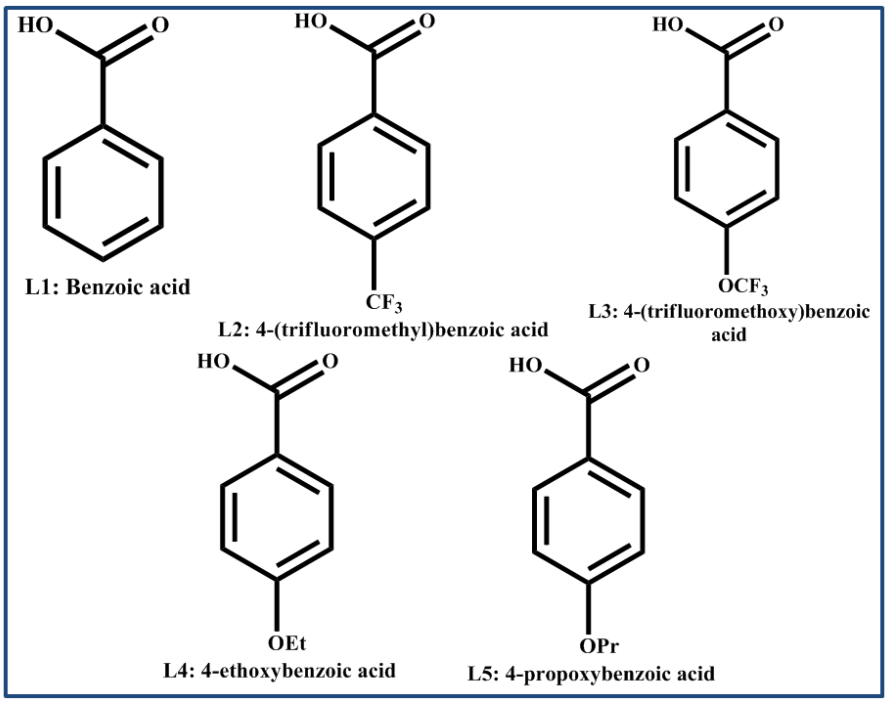

Figure 1.4. Structure of ligands L1–L5.

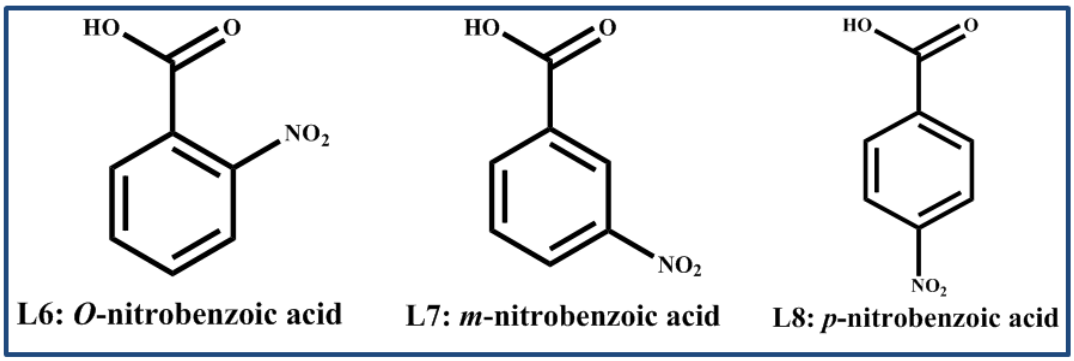

Figure 1.5. Structure of ligands L6–L8.

Relatively short Ln–Ln distances are seen in the complexes which display a triply coordinated carboxylate as a bridging bidentate ligand. These complexes are weakly luminescent in solid state, showing a metal-to-ligand ratio of 1:3. In solution, experimental evidence points to the formation of only 1:1 species. The quantum yields are ~1% and 3% for Eu^{3+}-and Tb^{3+}, respectively, in methanolic solution. The moderate quantum yield observed in methanol solution has been explained by the small stability constant of these species in solution as well as the large energy gaps between singlet and triplet levels of the ligand, and triplet level of the ligand and the emissive excited state of the lanthanide ion. Despite the strong electron-withdrawing effects of the $–NO_2$ group, for spectroscopic purposes its effect is not strongly dependent on the relative position of this functional group in the benzoic acid, as triplet and singlet states of ligands in solution with Ln^{3+} are relatively close. It is also interesting to note that while $–COO^-$ derivatization of benzene leads to a lowering of triplet energy by ~2600 cm^{-1}, $–NO_2$ derivatization to a lowering of ~8700 cm^{-1} and the presence of both functional group on benzene leads to a decrease of ~4500 cm^{-1} (Lewis and Kasha 1944).

The first example of luminescent lanthanide complexes with an *o*-nitrobenzoic acid based ligand, namely, 2-nitro-4-thiophen-3-yl benzoic acid (L9, Figure 1.6), was reported by Ana de Bettencourt-Dias and co-workers (de Bettencourt-Dias and Viswanathan 2004). The structural analysis of Eu^{3+} and Tb^{3+}-complexes of 2-nitro-4-thiophen-3-yl benzoic acid revealed that these complexes are isostructural and crystallize in a triclinic centrosymmetric unit cell. Each complex molecule is dimeric, containing two Ln^{3+} ions surrounded by

six ligands. The ligand shows three different coordination modes to the Ln^{3+} ions: bidentate, bridging bidentate, and bidentate with an oxygen atom bridging two metal atoms and another oxygen atom coordinating to one of the ions (triply coordinating). The coordination polyhedron around the Ln^{3+} ions can be described both as a distorted tricapped trigonal prism and as a monocapped square-antiprism. However, the authors stated that it is difficult to distinguish these two geometries in these complexes. The quantum yield of the red emitting Eu^{3+} complex in methanol solution is found to be 1.4%, while the green emitting solution shows an efficiency of 8.2% (Table 1.1). In the later studies these authors have evaluated various thiophenyl- derivitized *o*, *m*, *p*-nitro benzoic acid ligands (L10–L16, Figure 1.6) as possible sensitizers for Eu^{3+} and Tb^{3+} luminescence (Viswanathan and de Bettencourt-Dias 2006). The resulting solution and solid-state species were isolated and characterized by X-ray crystallography and luminescence spectroscopy. The molecular structure of the complexes is reported as homobimetallic with six ligands in the complex. Four of these ligands connect the two metal ions. Two of the ligands have μ-COO^{-} - bridging moiety, and the other two are triply coordinated, the triply coordinated fashion corresponds to a carboxylate moiety showing bidentate coordination to one metal ion. The fourth ligand coordinates to only one metal ion in a bidentate fashion. The coordination number of nine around each metal ion is completed by two solvent molecules in the coordination sphere. The main differences between these complexes are in the form of different torsion angles, Ln-O bond lengths, metal-metal distances and coordination polyhedra around the metal ions. Moderate solution quantum yields between 0.9 and 3.1% for Eu^{3+}

containing and 4.7 and 9.8% for Tb^{3+} containing solutions were reported (Table 1.1).

Table 1.1. Solution state photophysical properties of complexes of ligands L6-L16.

Ligands	E^a (^1S)/cm^{-1}	E^b (^3T)/cm^{-1}	$\Phi_{overall}$ (%)	
			Eu	Tb
o-nitrobenzoic acid (L6)	32 760	25 620	0.97	3.00
m-nitrobenzoic acid (L7)	32 720	25 590	1.09	3.14
p-nitrobenzoic acid (L8)	32 590	25 020	0.99	2.91
2-nitro-4-thiophen-3-yl-benzoic acid (L9)	31 820	21680	1.40	8.20
2-nitro-5-thiophen-3-yl-benzoic acid (L10)	32570	20110	1.40	9.80
5-nitro-2-thiophen-3-yl-benzoic acid (L11)	33090	19770	0.90	weak
4-nitro-2-thiophen-3-yl-benzoic acid (L12)	32220	not observed	1.60	4.70
3-nitro-5-thiophen-3-yl-benzoic acid (L13)	32930	26080	weak	weak
2-nitro-3-thiophen-3-yl-benzoic acid (L14)	33130	22600	1.70	7.90
3-nitro-4 -thiophen-3-yl-benzoic acid (L15)	32910	25760	2.30	weak
3-nitro-2 -thiophen-3-yl-benzoic acid (L16)	33450	23600	3.10	weak

[a] = singlet energy, [b] = triplet energy

The reasons for smaller quantum yields noted in these complexes have been explained by the smaller stability constant of the species in solution, as well as

the unfavourable energy gaps between triplet level of the ligand and emissive excited state of the lanthanide ion. Finally the authors concluded that the strong electron-withdrawing effect of the nitro group and its position relative to the coordinating carboxylate moiety do not seem to influence strongly the photophysical properties of the sensitizer as its effect is counter balanced by the moderate electron-donating thiophene.

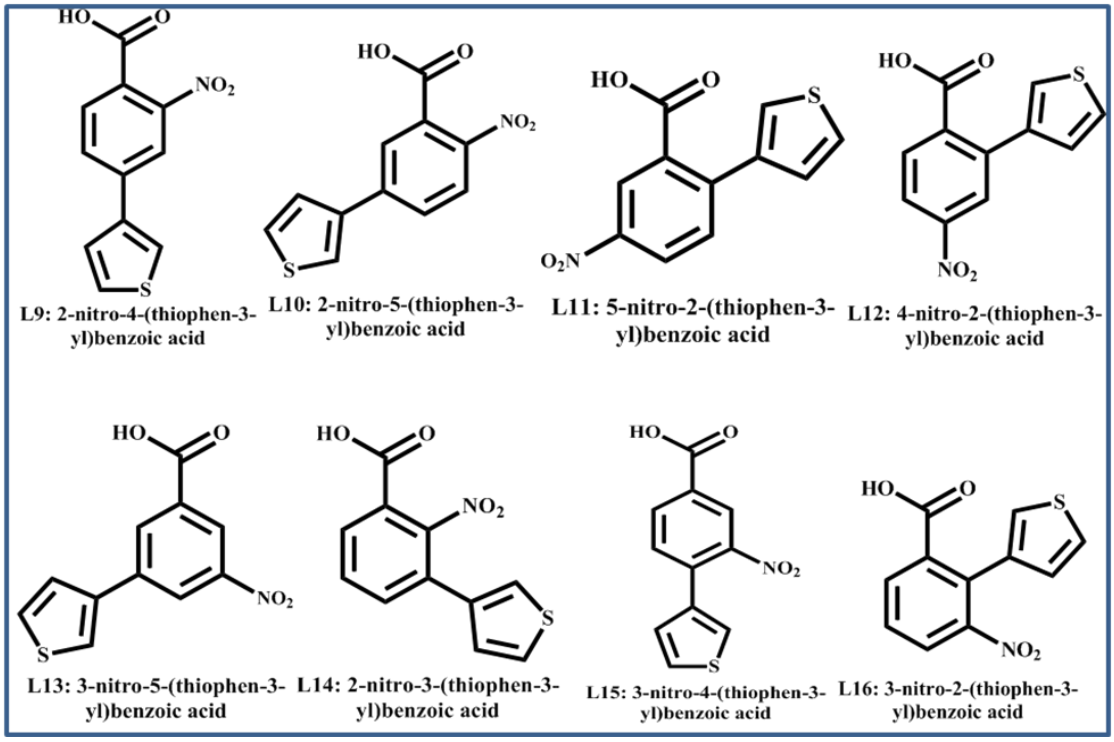

Figure 1.6. Structure of ligands L9–L16.

A new 3D rare-earth hybrid material Eu(L17) has been synthesised by a hydrothermal route from europium nitrate and the rigid precursor, 4-phosphonobenzoic acid (Figure 1.7) by Jaffrès and co-workers (Jaffrès *et al.* 2009). The structure of Eu(L17) has been solved by X-ray diffraction on a powder sample and is described as an inorganic network in which both

carboxylic and phosphonic acid groups are linked to Eu^{3+} ions forming a three-dimensional architecture. Thermal analysis performed on this compound has underlined its remarkable stability up to 510 °C. The emission spectrum of the rare earth hybrid material excited at 310 nm exhibits characteristic peaks of Eu^{3+} transitions. This indicates that energy transfer from ligand to Eu^{3+} ion is efficient. The presence of a single peak for the $^5D_0 \rightarrow {}^7F_0$ transition is consistent with one crystallographic site for Eu^{3+} ion which is consistent with the crystal structure.

In order to modulate the light harvesting properties of benzoic acid ligands, herein a novel aromatic carboxylate ligand, namely, 4-((1H-benzo[*d*]imidazol-1-yl)methyl)benzoic acid (L18, Figure 1.7) has been formulated by anchoring benzimidazole moiety at the 4th position of the benzoic acid through an alkyl linkage and utilized for the development of a series of new lanthanide complexes featuring Eu^{3+}, Gd^{3+} and Tb^{3+} (Lucky *et al.* 2011).

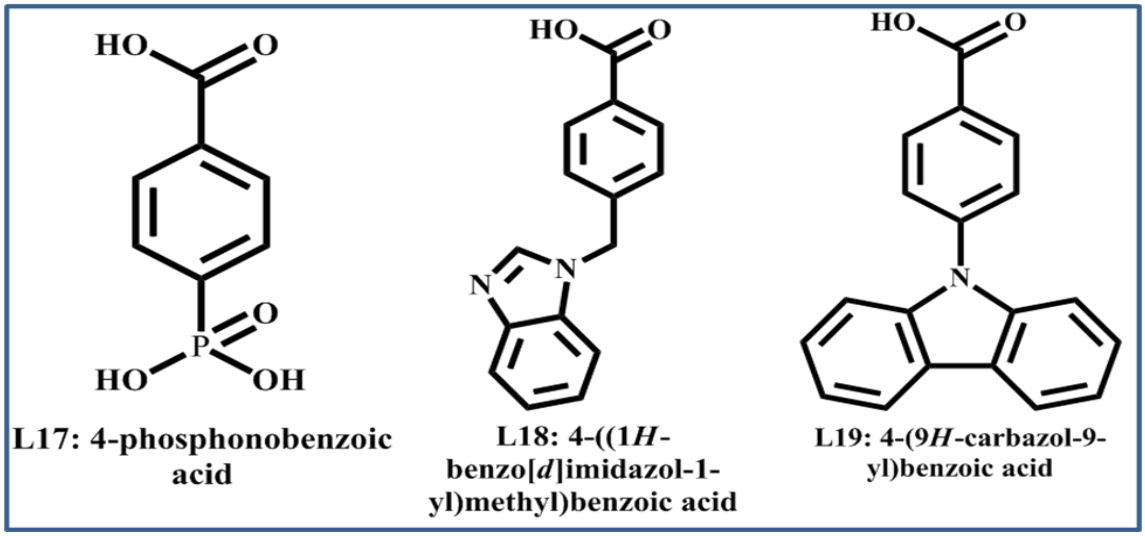

L17: 4-phosphonobenzoic acid

L18: 4-((1*H*-benzo[*d*]imidazol-1-yl)methyl)benzoic acid

L19: 4-(9*H*-carbazol-9-yl)benzoic acid

Figure 1.7. Structure of ligands L17–L19.

The X-ray single crystal analysis discloses that the Eu^{3+}-complex forms a 1D helical chain like coordination polymer, consisting of unique unsymmetrical dinuclear building blocks (Figure 1.8). It is interesting to mention that the ligand adopts bridging coordination mode around the Eu1 center. On other hand, carboxylates ligands adopt three different coordination modes around Eu2: bidentate chelating, bridging, and monodentate. Interestingly, the two europium centers are inter connected by four aromatic carboxylte groups in a bridging mode resulting in the dinuclear paddle-wheel building blocks with Eu1·····Eu1 separation of 4.104 Å.

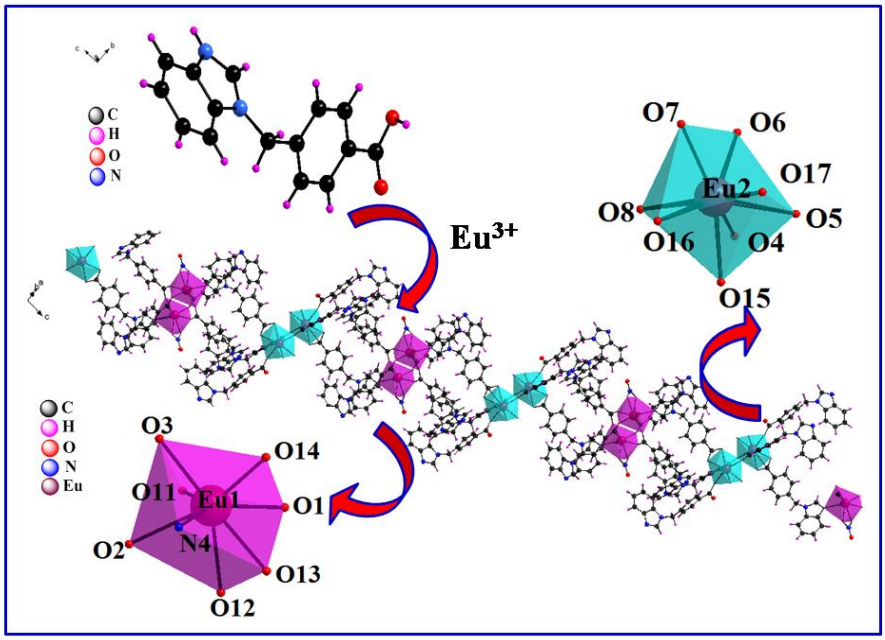

Figure 1.8. The 1D coordination polymer chain of Eu^{3+}-4-((1H-benzo[*d*]imidazol-1-yl)methyl)benzoate and polyhedra (pink and blue) showing unsymmetrical dinuclear Eu^{3+} building blocks.

In a similar fashion, the two Eu2·····Eu2 centers are also connected by two bridging carboxylte groups to give other type of dinuclear paddle-wheel

building blocks with Eu2·····Eu2 separation of 4.869 Å. Finally these two unsymmetrical bulding blocks are inter connected *via* one of the carboxylate group through the nitrogen atom of the benzimidazole moiety to form an infinite one-dimensional (1D) coordination polymer in a helical arrangement. The 1D chains are further linked by intermolecular hydrogen bonding interactions to form a two dimensional supra molecular network. The Tb^{3+}-complex exhibits bright green luminescence efficiency in the solid state with a quantum yield of 15%. On the other hand, poor luminescence efficiency has been observed for Eu^{3+}-benzoate complex.

It is well documented that carbazole moiety incorporated into *β*-diketone ligand acts as an efficient photosensitizer for lanthanides (Raj *et al*. 2010; Zheng *et al*. 2008; Kon *et al*. 2001; Nie *et al*. 2007). On the other hand, ligands in which carbazole grafted into an aromatic carboxylate ligands are scarce. Carbazole possesses a number of desirable properties, which include good chemical stability, modest cost, and the ability to tune the optical and electrical properties by appending with a wide variety of functional groups. A new carboxylate ligand, 4-(9*H*-carbazol-9-yl) benzoic acid (L19, Figure 1.7) has been synthesized for the first time by grafting a carbazole group as a hole-transporting moiety to a benzoic acid and utilized for the development of two lanthanide complexes, $Tb(L19)_3(H_2O)_2$ and $Eu(L19)_3(H_2O)_2$ (Bo *et al.* 2006). The composition of the complexes has been determined by various spectroscopic techniques. The PL studies demonstrated that 4-(9*H*-carbazol-9-yl) benzoic acid could sensitize Tb^{3+} luminescence efficiently at room temperature. On the other hand, the luminescent intensity of the Eu^{3+}-complex is very weak. Obviously, the

triplet state of the ligand is too near to the Eu^{3+} energy level that allows the back energy transfer happened easily. Based on the good luminescent intensity and thermal stability of the Tb^{3+}-complex, it should be considered as a potential emitting material for the fabrication of OLEDs.

Reddy *et al*. prepared a series of 4-benzyloxy benzoic acid derivatives to investigate the influence of electron-releasing and electron-withdrawing substituents on the photoluminescent properties of corresponding Eu^{3+} and Tb^{3+} complexes (Sivakumar *et al*. 2010). With this aim three novel ligands: 4-benzyloxy benzoic acid; 3-methoxy-4-benzyloxy benzoic acid; 3-nitro-4-benzyloxy benzoic acid (L20–L22, Figure 1.9) have been designed and utilised for the construction of lanthanide coordination compounds.

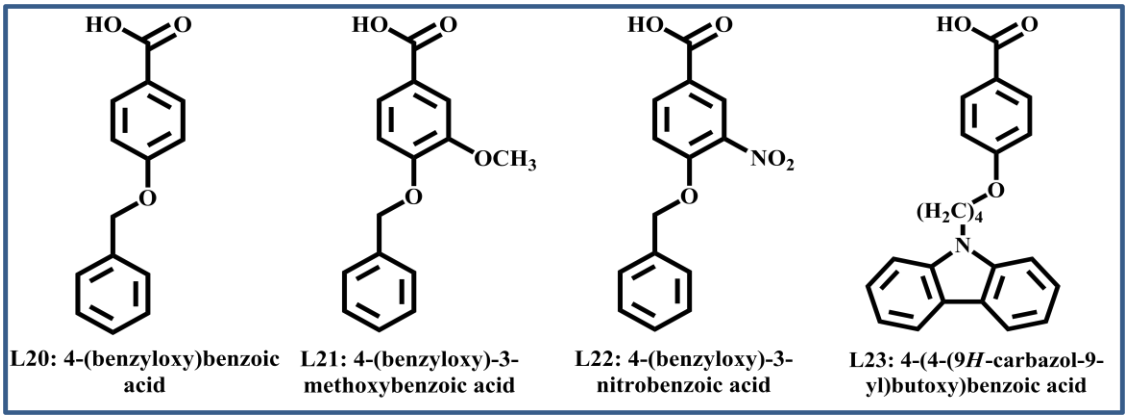

Figure 1.9. Structure of ligands L20–L23.

The molecular structures of the Tb^{3+}-4-benzyloxy benzoate and Tb^{3+}-3-methoxy-4-benzyloxy benzoate complexes have been investigated by single-crystal X-ray diffraction. Interestingly, the Tb^{3+}complex based on 4-benzyloxy benzoate consist of homodinuclear species that are bridged by two oxygen atoms from two benzoate ligands. By contrast, the X-ray structure of Tb^{3+}-3-

methoxy-4-benzyloxy benzoate reveals that each Tb^{3+} ion is connected to two neighboring ions by four methoxy substituted benzoates *via* the carboxylate groups in bridging mode to form an infinite one-dimensional coordination polymer. The incorporation of an electron-releasing substituent on position 3 of 4-benzyloxy benzoic acid increases the electron density of the ligand and consequently improves the photoluminescence of the Tb^{3+} complexes ($\Phi_{overall}$ = 33%) (Table 1. 2).

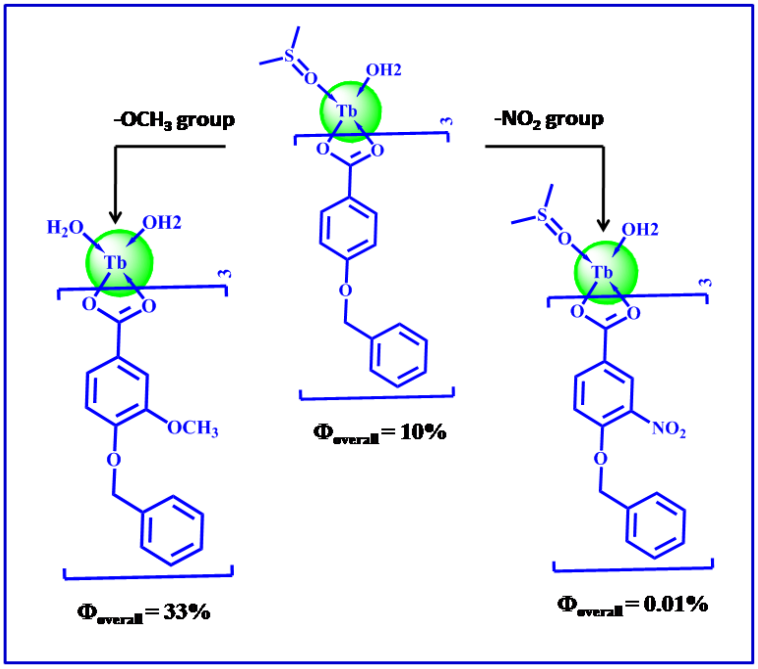

Figure 1.10. Schematic diagram showing the effect of electron-releasing ($-OCH_3$) and electron-withdrawing ($-NO_2$) groups on photophysical properties of Tb^{3+}-benzyloxy benzoate complexes.

On the other hand, the presence of an electron-withdrawing group at this position dramatically decreases the overall sensitization efficiency of the Tb^{3+}-centered luminescence due to dissipation of the excitation energy by means of a π*-n transition of the NO_2 substituent along with the participation of the ILCT

bands ($\Phi_{overall}$ = 0.10%) (Figure 1.10). Given the substantial energy gaps between the triplet states of the various benzoate ligands and the emissive level of Eu^{3+}, it is not surprising that the Eu^{3+} benzoates exhibit poor luminescence intensities (Table 1.2) (Latva *et al*. 1997).

A unique, green luminescent solvent-free terbium coordination polymer based on a new aromatic carboxylate ligand, 4-[4-(9H-carbazol-9-yl)butoxy]benzoate (L23, Figure 1.9) has been synthesized and structurally solved by single-crystal X-ray diffraction (Raphael *et al*. 2012). The polymer exhibits an unusually low coordination number for a terbium cation (CN = 6). The incorporation of a bulky carbazolylbutyl group in the *p*-hydroxy benzoate ligand appears to be responsible for the exclusion of solvent from the derived structure, by inducing the second order steric crowding within the immediate coordination environment (de Lill and Cahill 2006; Fomina *et al*. 2012; Buskamp *et al*. 2007; Cotton 2006; Rao *et al*. 2004). The structural data revealed that, the terbium atoms in the coordination polymer reside in an octahedral ligand environment that is somewhat unusual for a lanthanide (Figure 1.11). It is interesting to note that, each carboxylate group exhibits only a bridging-bidentate mode, with a complete lack of complex connectivities that are commonly observed for extended lanthanide-containing solid-state structures. Examination of the packing diagram of the crystal structure revealed the existence of two-dimensional molecular arrays held together by means of CH-π interactions. Photophysical investigations revealed that the presence of bidentate nitrogen donor ligands significantly enhances the quantum yields of both the Eu^{3+} and Tb^{3+} benzoate complexes (Table 1.2). This observation can be

explained on the basis of additional energy transfer from the ancillary ligand to the carboxylate ligand in the ternary complexes, which in turn enhances the overall sensitization efficiency of the complex molecule. This result may be further explained on the basis of the minimization of nonradiative decay rates in monomeric complexes in comparison with those of polymeric species.

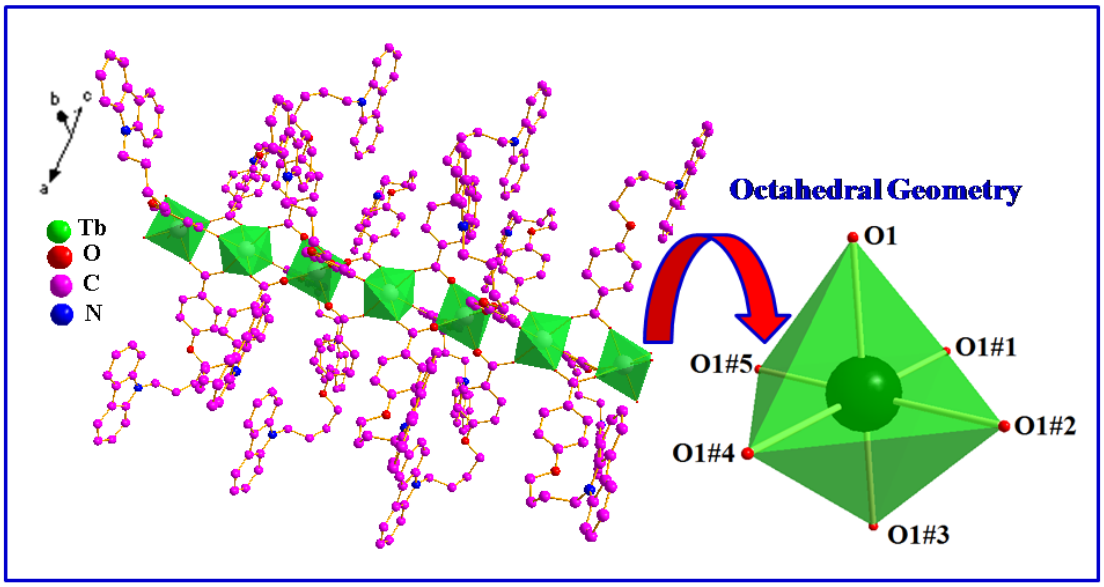

Figure 1.11. The solvent-free 1D coordination polymer chain in Tb^{3+}-4-[4-(9H-carbazol-9-yl)butoxy]benzoate complex and the polyhedra showing octahedral geometry. All hydrogen atoms were omitted for clarity.

It is evident from the photophysical data that europium coordination polymer displays poor quantum yield ($\Phi_{overall}$ = 0.11%) as compared to terbium analogue ($\Phi_{overall}$ = 2.0%), which can be explained on the basis of larger energy gap (ΔE = $^3\pi\pi^* - {}^5D_0$ = 6673 cm^{-1}) between the excited state level of the Eu^{3+} cation and the triplet energy level of the ligand (Latva *et al*. 1997). On the other hand, due to the smaller energy gap between the $^5D_4$ excited state level of the Tb^{3+} cation and the triplet state of the ligand (ΔE = $^3\pi\pi^* - {}^5D_4$ = 3423 cm^{-1}) Tb^{3+}-complex shows

an improved quantum yield. However, the overall quantum yields and the sensitization efficiency noted for both the lanthanide compounds in the current study are found to be somewhat inferior as compared with various lanthanide benzoate complexes reported earlier in our laboratory (Sivakumar *et al*. 2010; Lucky *et al*. 2011). The fact that both the lanthanide complexes derived from 4-[4-(9H-carbazol-9-yl)butoxy]benzoate exhibit residual ligand emission in 375-475 nm region as can be noted from the respective emission spectra, which indicates that modest efficiency of energy transfer from the ligand to the Ln^{3+}center. These spectral features are further supported from the crystal structure of the Tb^{3+}-complex that the appended carbazole moiety of the new ligand is away from the central Tb^{3+} ion (11.6 Å). Thus the carbazole moiety may not be able to efficiently transfer energy to the central lanthanide ion, which results in the residual emission of the ligand. However, incorporation of the bidentate nitrogen donors phen or tmphen breaks the coordination polymer into discrete monomeric complexes while simultaneously serving to enhance the overall quantum yields of these complexes.

The Tb^{3+} complex of 2,6-dihydroxy benzoic acid (L24, Figure 1.12) has been isolated, structurally characterized and investigated the photophysical properties by Santos and group (Santos *et al*. 2003). The single-crystal X-ray diffraction studies revealed the molecular structure of the Tb^{3+}-complex as $[n\mathrm{Bu_4N}]_2[\mathrm{Ln(L24)_5(H_2O)_2}]$. The crystal structure contains one crystallographically unique metal center coordinated to five 2,6-dihydroxy benzoate ligands and two water molecules, in a geometry which is best described as a distorted tricapped trigonal prism. The Tb^{3+}-complex shows

intense photoluminescence in both solid state and ethanol solution. Surprisingly, when ground by hand in daylight, single crystals of Tb^{3+}-complex exhibits green triboluminescence detectable by the naked eye. The Tb^{3+} complex is a non-centrosymmetric ionic complex and it has been suggested (Chen *et al*. 1999; Rheingold and King 1989) that triboluminescence arises from charge separation by partial fracture along oppositely charged planes. Given its triboluminescence behaviour, the Tb^{3+} complex is a potential candidate for the development of optical sensors.

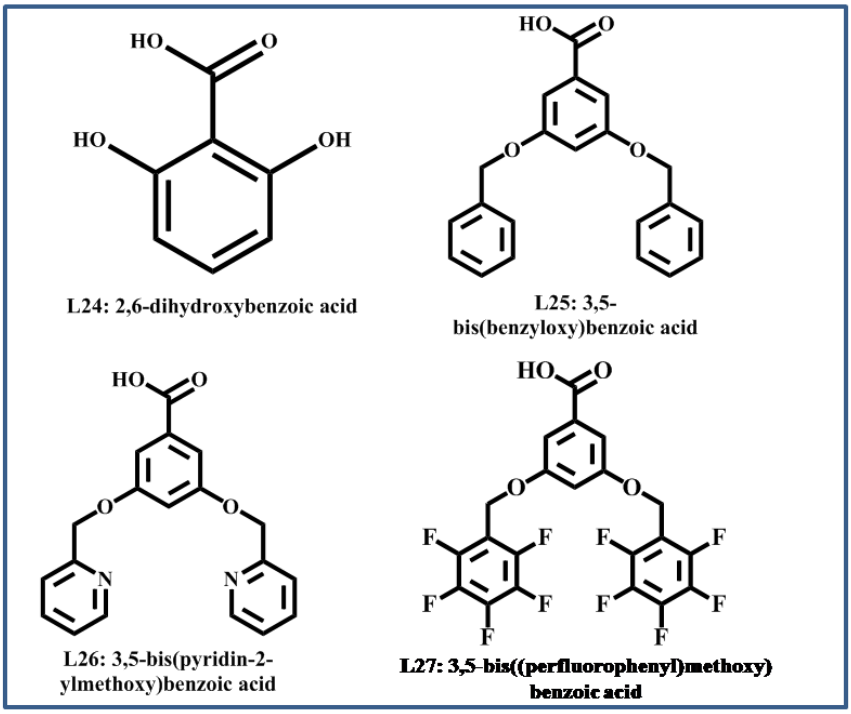

Figure 1.12. Structure of ligands L24–L27.

Reddy and co-workers have designed two novel photosensitizers for Ln^{3+} ions, namely, 3,5-bis(benzyloxy)benzoic acid and 3,5-bis(pyridine-2-ylmethoxy)benzoic acid, which were synthesized by replacing the hydroxyl hydrogens of 3,5-dihydroxy benzoic acid with benzyl and pyridyl moieties,

respectively (L25-L26, Figure 1.12) (Sivakumar *et al*. 2011). The anions derived from the above ligands have been used for the support of a series of lanthanide coordination compounds [Eu^{3+}, Tb^{3+} or Gd^{3+}] and the resultant complexes were characterized on the basis of variety of spectroscopic techniques in conjunction with the assessment of their photophysical properties. Lanthanide complexes, which were synthesized from 3,5-bis(pyridine-2-ylmethoxy)benzoic acid, were structurally authenticated by single-crystal X-ray diffraction. All the compounds are found to exist as infinite one-dimensional (1-D) coordination polymers of the general formula $\{[Ln(L26)_3(H_2O)_2]\cdot xH_2O\}_n$ (Figure 1.13). The Ln center is coordinated to four carboxylate oxygen atoms of the bridging 3,5-bis(pyridine-2-ylmethoxy)benzoate ligands, two carboxylate oxygen atoms of the chelating benzoate ligand, and two water molecules. Furthermore, the Ln centers are doubly bridged by the carboxylate groups of the 3,5-bis(pyridine-2-ylmethoxy)benzoate ligands thereby forming an infinite 1-D chain. The most striking feature of these compounds is the presence of free Lewis basic pyridyl sites within the 1-D coordination polymer (Figure 1.13), this in turn, augurs well for the potential utility of these compounds for the recognition and sensing of metal ions. Scrutiny of the packing diagrams of these coordination polymers revealed the existence of interesting two-dimensional molecular arrays held together by intermolecular hydrogen-bonding interactions. The newly designed 3,5-bis benzyloxy benzoate derivatives are found to be adequate sensitizers for the Tb^{3+} ion.

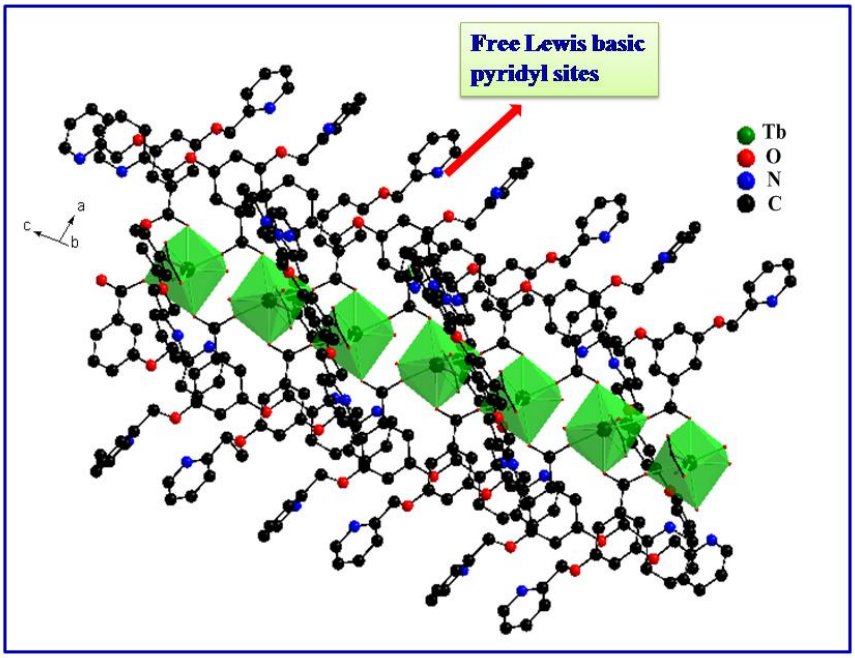

Figure 1.13. The 1D coordination polymer chain of $\{[Tb(L26)_3(H_2O)_2]\cdot xH_2O\}_n$ showing free Lewis basic pyridyl sites.

Indeed, their excited states lie at sufficiently high energies in comparison with that of the $^5D_4$ state to obviate back transfer of energy. As a result, even in the presence of metal-bound water molecules, the solid state quantum yields ($\Phi_{overall}$ = 27-60%) and lifetimes (τ_{obs} = 1.16-1.38 ms) of the sensitized Tb^{3+} complexes are appreciably higher (Table 1.2). In contrast to the foregoing, the Eu^{3+}-complexes show poor luminescence efficiencies because of the larger energy gap between the triplet states of the ligands and $^5D_0$ excited state level of Eu^{3+} ion (7259 cm^{-1}) (Latva et al. 1997). Terbium complex based on 3,5-bis(benzyloxy)benzoic acid exhibits higher quantum yield ($\Phi_{overall}$ = 60%) and efficient ligand-to-metal energy transfer (Φ_{sen} = 60%) than Tb^{3+}-3,5-bis(pyridine-2-ylmethoxy)benzoate because of the better match of the triplet energy level of the 3,5-bis(benzyloxy)benzoic ligand to that of the Tb^{3+} emitting

level.[18] The introduction of highly conjugated benzyl groups in 3,5-bis(benzyloxy)benzoic acid lowers the triplet energy to 24509 cm^{-1}, and therefore it exhibits superior quantum yields (60%) for Tb^{3+} ion as compared to 4-benzyloxybenzoic acid ($\Phi_{overall}$ = 10%). The sensitizing ligands containing high-energy oscillators, such as C–H, O–H, and N–H bonds, quench the metal excited states nonradiatively leading to decreased luminescence intensities and shorter excited-state lifetimes in lanthanide coordination compounds (Artizzu *et al*. 2007; Biju *et al*. 2006; Biju *et al*. 2009). Accordingly, to eliminate such quenching effects, highly fluorinated antenna chromophores have been reported for the sensitization of near-IR emissive lanthanides such as Er^{3+}, Nd^{3+} and Yb^{3+} (Glover *et al*. 2007; Mech *et al*. 2010; Chen *et al*. 2006; Norton *et al*. 2009). Approaches involved alkyl chain C-F substitution of *β*-diketonate ligands are well known for the sensitization of emitting Ln^{3+}-ions (Sun *et al*. 2006). However, the effect of fluorination on the luminescence intensities of visible emitting lanthanide–benzoate complexes (Eu^{3+} and Tb^{3+}) has not yet been examined.

Recently Reddy and co-workers have demonstrated that the replacement of high energy C-H vibrations with fluorinated phenyl groups in the 3,5-bis(benzyloxy benzoate) significantly improves the luminescence intensity and lifetime of Eu^{3+}-complex ($\Phi_{overall}$ = 6.5%; τ_{obs} = 615 μs; Φ_{sen} = 24%) [Sivakumar and Reddy 2012] as compared to the Eu^{3+}-complex of 3,5-bis(benzyloxy)benzoate ($\Phi_{overall}$ = 1.1%; τ_{obs} = 426 μs; Φ_{sen} = 3.6%) (Sivakumar *et al*. 2011).

Table 1.2. Solid state photophysical properties of complexes of ligands L20–L29.

Ligands	E^a (^1S)/cm^{-1}	E^b (^3T)/cm^{-1}	τ_{obs} (μs)		Φ_{Ln} (%)		Φ_{sen} (%)		$\Phi_{overall}$ (%)	
			Eu	Tb	Eu	Tb	Eu	Tb	Eu	Tb
L20	32573	26178	420	1180	15	77	00.90	13.00	00.14	10.00
L21	29239	24813	400	1240	25	93	01.90	35.00	00.49	33.00
L22	35842	24937	380	1040	24	82	00.17	<0.01	00.04	00.10
L23	23923	28089	344	986	17	62	00.64	02.32	00.11	02.00
L23(phen)			1098	1006	41	82	24.00	19.00	10.00	14.00
L23(tmphen)			1176	1262	43	88	49.00	37.00	19.10	33.00
L25	30581	24509	426	1160	41	~100	03.60	60.00	01.50	60.00
L26	31152	25253	426	1377	17	~100	05.90	27.00	01.00	27.00
L27	30675	24038	615	1151	16	~100	24.00	52.00	06.50	52.00

[a] = singlet energy, [b] = triplet energy

A new antenna chromophore 3,5-bis(perfluorophenyl)methoxy)benzoic acid (L27, Figure 1.12) was designed by replacing the hydroxyl hydrogen atoms in 3,5-dihydroxy benzoic acid with highly fluorinated phenyl groups for the sensitization of visible emitting Ln^{3+} ions. It is interesting to note that the designed fluorinated carboxylate is well-suited for the sensitization of Tb^{3+}-emission (Φ_{sen} = 52%) (Figure 1.14), thanks to a favorable position of the triplet state of the ligand [ΔE ($^3\pi\pi^*$– $^5D_4$) = 3538 cm^{-1}] as investigated in the Gd^{3+} complex. On the other hand, the corresponding Eu^{3+}-complex shows weak luminescence efficiency (Φ_{sen} = 24%) due to poor match of the triplet state of the ligand with the emissive excited states of the metal ion [(ΔE = ($^3\pi\pi^*$– $^5D_0$) =

6788 cm^{-1}] (Table 1.2). It is also noted that, the Eu^{3+}-complex is associated with a large value of non-radiative decay rates (A_{NR} = 1468 s^{-1}), which may quench the effective radiative decay rates thereby decreasing the sensitization efficiency and overall quantum yield value. Further efforts have also been made to isolate luminescent molecular terbium plastic materials by combining the unique optical properties of lanthanides with that of mechanical, thermal stability, flexibility and film forming tendency of polymers (PMMA). The emission spectra of PMMA doped with the Tb^{3+}-compound at a variety of concentrations (6, 8, 10 and 12% w/w) and excited at 320 nm exhibit well defined emission peaks characteristic of the $^5D_4 \rightarrow {}^7F_J$ (J = 6-3) transitions of Tb^{3+} ion in the 480-650 nm region (Figure 1.14). The luminescent intensity of Tb^{3+}emission at 545 nm increases with increasing concentrationTb^{3+}-compound and reaches a maximum at 8%. The further increase in the terbium content decreases the luminescent intensity. The energy transfer between the lanthanide ions themselves is a non-radiative process, which is responsible for the decrease in the Tb^{3+} emission, especially at high metal concentrations (Biju *et al*. 2009; Kai *et al*. 2008). Notably, these terbium molecular plastic materials derived from highly fluorinated benzoate ligand display bright green luminescence efficiency with high quantum yields (63-65%) (Figure 1.14) and lifetime values (1.20-1.49 ms) as compared to precursor Tb^{3+}-compound, thus making these polymer films an interesting candidate for practical applications as polymer optical fibers or as dopant in organic light-emitting devices. In Tb/PMMA polymer films, the long chain of PMMA molecule enwraps the Tb^{3+}-3,5-bis(perfluorophenyl)methoxy)benzoate complex making the distance

between donor and acceptor closer, resulting in efficient intermolecular energy transfer thereby enhancing the overall quantum yield of Tb^{3+}-doped polymer films.

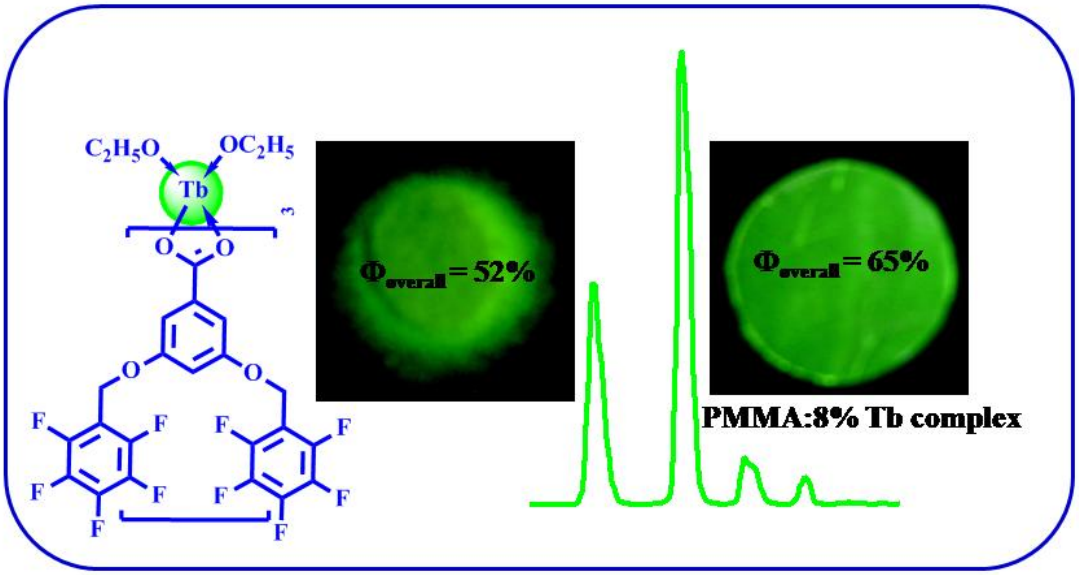

Figure 1.14. Photograph of Tb^{3+}-3,5-bis(perfluorophenyl)methoxy)benzoate complex and PMMA polymer film doped with 8% Tb^{3+}-complex.

Very high quantum yields have been reported for Tb^{3+}-*p*-aminobenzoate complex, which is somewhat surprising in view of the coordination of both $-NH_2$ and $-OH_2$ as ligands, as they are essential vibrational deactivators of the excited state (Fiedler *et al*. 2007). However, it should be noted that both Ln-OH_2 distance (261 pm) and Ln-NH_2 distance (276 pm) are fairly long in the Tb^{3+}-*p*-aminobenzoate complex and multiphoton emission may thus be of secondary importance only, which is even more pronounced due to fairly strong hydrogen bonding.

1.4. Tunable white light emission in lanthanide metal–organic frameworks

The interest in white light-emitting materials and devices stems from their potential applications in solid-state lighting, low-cost back-lighting and full-color displays. (Reineke *et al*. 2009; Zhu *et al*. 2011; Liu *et al*. 2012; Farinola and Ragni 2011). High quality white light illumination requires a source with the Commission internationale de l'éclairage) (CIE) coordinates (0.333; 0.333), with correlated color temperature (CCT) between 2500 and 6500 K, and color rendering index (CRI) above 80.159. In principle, white emission should ideally be composed of two (blue and yellow) or three (blue, green, and red) primary colors and cover the whole visible range from 400 to 700 nm, and the emitters should have the ability to emit primary colors simultaneously and be comparable in intensity to produce white light and the pure colors separately in a tunable way (Figure 1.15). Different approaches have been reported to obtain efficient white-light-emitting materials. They mainly focus on metal-doped or hybrid inorganic materials, nano-materials, organic molecules, and metal complexes. However, the emission from organic or inorganic luminescent materials can only cover part of the visible spectrum. Recently, lanthanide-containing materials, especially, metal organic frameworks or also known as coordination polymers (CPs) or coordination networks, which exhibit excellent sharp-emission luminescence properties with suitable sensitization, have attracted considerable interest and been effectively used in designing of white-emitting materials (Song *et al*. 2013; Ma *et al.* 2013; Kerbellec *et al.* 2009; Rao *et al.* 2012; Tang *et al.* 2014; Zhang *et al.* 2014).

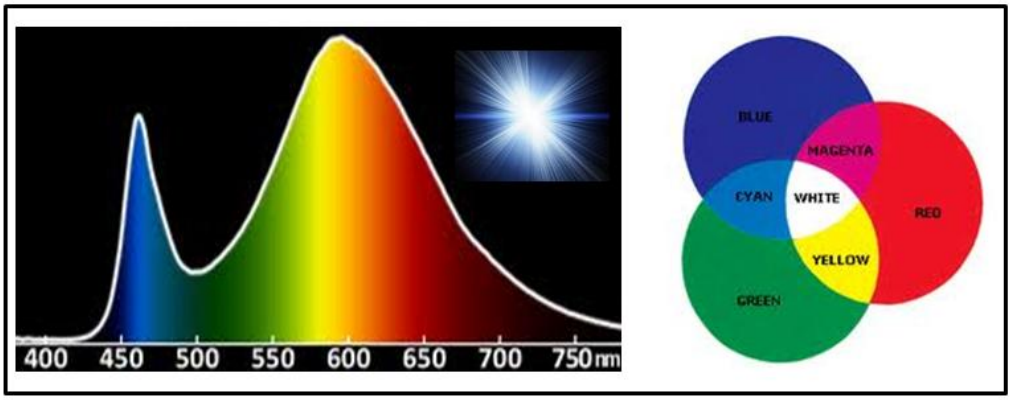

Figure 1.15. Representation of white emission.

Interestingly, Eu^{3+} and Tb^{3+} based metal complexes exhibit intense red and green emissions, respectively. On the other hand, Gd^{3+} complex emits in the blue region in view of its high lowest emitting level (32,150 cm^{-1}). Consequently, mixed lanthanide complexes (Gd^{3+}, Tb^{3+} and Eu^{3+}) have potential applications in generating white-light emission (Ma *et al.* 2012; Zhang *et al.* 2013) . The relative luminescence intensity between the lanthanide ions and antenna chromophore strongly depends on the nature of the energy transfer, thus allowing the fine-tuning of the MOFs emission color across the CIE diagram. In addition, the emission color can also be readily modulated both by chemical factors (Ln^{3+} types and concentration, ligand structure, coordination status, guest species) and by physical parameters (excitation wavelength and temperature).

Isostructurality of the complexes in a series of lanthanide complexes is a prerequisite to achieve efficient doping and thus to obtain lanthanide codoped systems with tunable emission characteristics, especially white light. For example, making use of the isostructurality in Gd^{3+}, Eu^{3+} and Tb^{3+} complexes $\{[Ln_3(bidc)_4(phen)_2(NO_3)]\cdot 2H_2O\}_n$ (bidc = benzimidazole-5,6-dicarboxylic acid;

phen = 1,10-phenanthroline) variations in the relative intensities of blue, green and red was achieved by adjusting the doping ratios of Gd^{3+}, Tb^{3+} and Eu^{3+}, respectively. By changing the relative amount of Gd^{3+}, Eu^{3+} and Tb^{3+} in the doped complexes blue, red and green light emitting components were systematically incorporated into the materials; with the molar ratio of 98.5:0.5:1 (Gd^{3+}:Eu^{3+}:Tb^{3+}), (**1**) (Figure 1.16) white light emission with CIE chromaticity coordinates (0.322, 0.328) was attained (Ma *et al*. 2012).

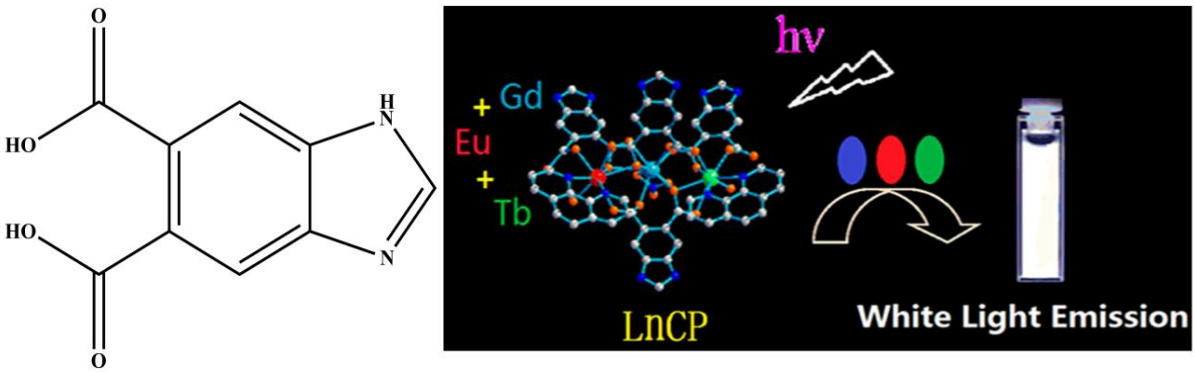

Figure 1.16. Representation of tunable white-light emission observed in **1.**

Using the aforesaid strategy, stoichiometric ratio of the lanthanide ions in isostructural mixed-lanthanide complexes $[Gd_{1-x-y}Eu_xTb_y$(pyridine-2,6-dicarboxylate)$_3]$.$(H_2NMe_2)_3$ (**2**) was adjusted to bring about a fluent change of emission colors within the full color region including green, blue-green, blue, pink, white, yellow, orange and red; it is in fact a rare example for obtaining full-colour luminescent materials based on lanthanide–organic complexes. Also was attained a strong white light-emission with CIE coordinates of (0.331, 0.337) and high quantum yield up to 62%. In the doped complex Eu^{3+} and Tb^{3+} emitting

species acted as red and green light source while pyridinedicarboxylate linker served as the blue emitter. The inefficient blue emitting power of the carboxylate linker was compensated by maintaining a much higher composition percentage of Gd^{3+} (for example, Gd:Eu:Tb ratio of 0.9365: 0.0370: 0.0265) over the other two Ln components. This allowed for the dilution of the other two rare earth ions in the solid state and also to maximize the blue emission (Figure 1.17) (Zhang *et al*. 2013).

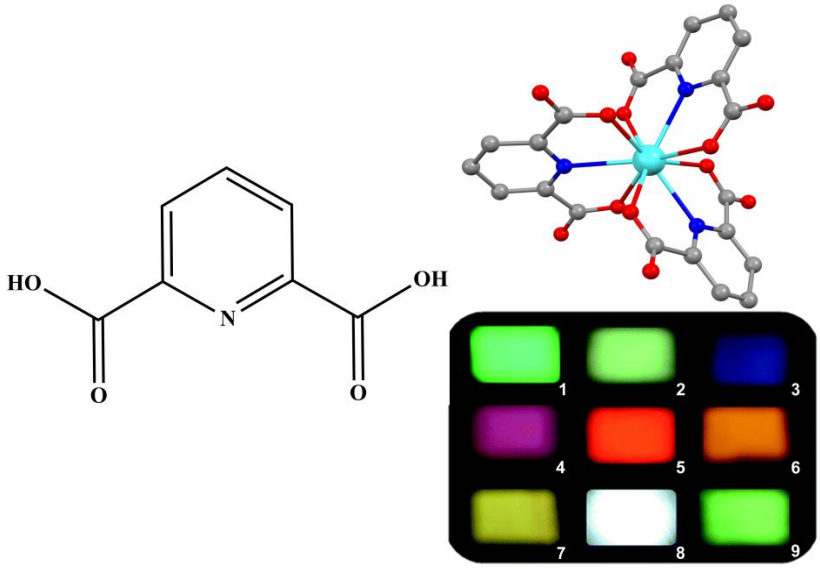

Figure 1.17. The coordination sphere of **2** and the photographs of the emission colors obtained by varying the lanthanide composition (excited using a Xe lamp).

In a yet another example, the emission color of the complex $[Eu_{0.0040}Tb_{0.0460}Gd_{0.9500}$(1,3,5-tris(4-carboxyphenyl)-benzene))$(DMSO)_2].H_2O$ (**3**) switched between blue, white and yellow emission chromaticity, by varying the excitation wavelength; a rare example of its type in mixed-lanthanide MOF family (Figure 1.18). Thus, with λ_{ex} = 315 nm the material exhibited an orange

emission with CIE coordinates of (0.41, 0.41), a white emission (0.36, 0.32) at λ_{ex} = 347 nm and a blue emission (0.19, 0.13) at λ_{ex} = 365 nm. This excitation-dependent photoluminescence tuning and the reversible on–off switching in the blue, yellow and white regions was proposed to be controlled by different energy transfer processes. The reversible emission switching indicates non-destructive readout ability in the solid state (Zhang *et al*. 2014).

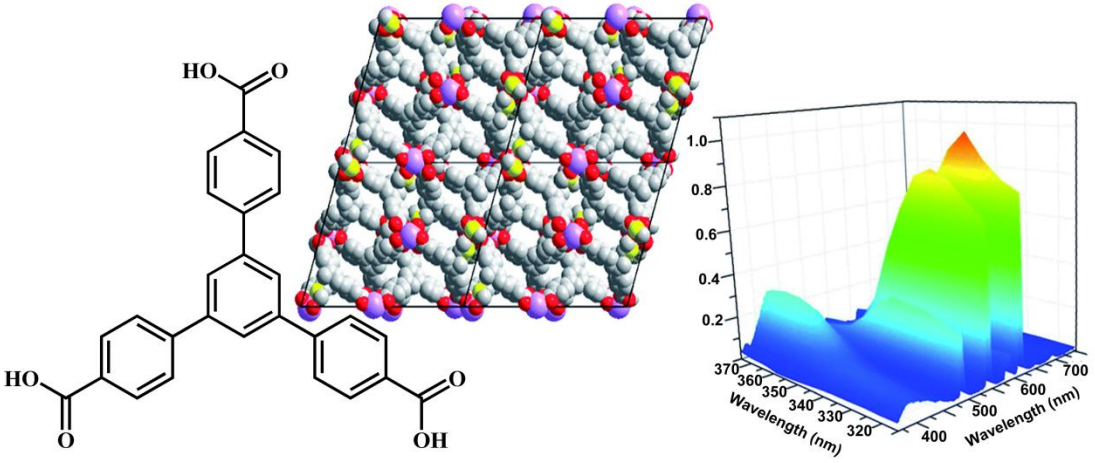

Figure 1.18. Coordination network formed in **3**, together with its solid state PL spectrum obtained by varying excitation wavelength.

Besides Gd complexes, La complexes also exhibit ligand based blue emission which could be used as a source of blue light to attain white light emission. Thus, in isostructural complexes of $\{[Ln_2(5\text{-}(3,5\text{-dicarboxybenzyloxy})isophthalic\ acid))_2]\cdot(H_2O)_3\cdot(Me_2NH_2)_2\}_n$ (Ln = La, Ce, Pr, Nd, Sm, Eu, Gd, Tb, Ho, Er) (**4**) the blue-emission of La-complex and the intense emission from Eu^{3+} and Tb^{3+} ions were employed to tune the emission color. Accordingly, the materials with the composition $Eu_{0.17}Tb_{0.18}La_{0.65}(L)$ and

$Eu_{0.16}Tb_{0.19}La_{0.65}$(L) (Figure 1.19) were found to have the CIE coordinates (0.330, 0.334) and (0.332, 0.338), respectively (Ma *et al*. 2013).

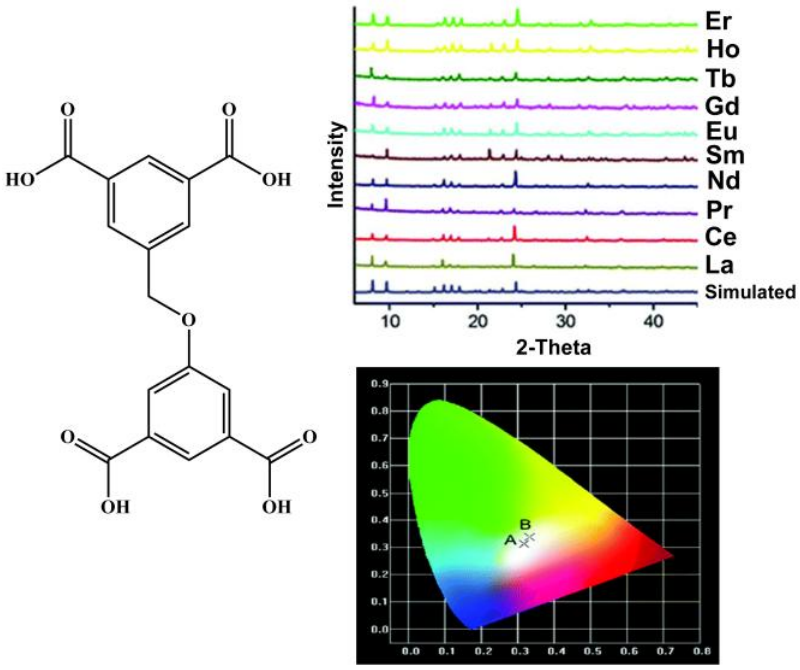

Figure 1.19. PXRD patterns confirming the isostructurality of the series of complexes. The CIE coordinates characteristic to the emission for $Eu_{0.17}Tb_{0.18}La_{0.65}$(L) and $Eu_{0.16}Tb_{0.19}La_{0.65}$(L).

In Tb^{3+}/Eu^{3+} doped [La_2(pyridine-2,6-dicarboxylate)$_3$(H_2O)$_5$] (**5**) closer triplet state of ligand (T_1 = 25,000 cm^{-1}) and the emitting excited state of Tb^{3+} ($^5D_4$ = 20,400 cm^{-1}) invoked an efficient ligand to metal energy transfer and an enhanced metal-specific emission. Thus, together with the ligand-centered blue emission, the emission colors were systematically by varying the concentration of the Tb^{3+} and Eu^{3+} from 0.1% to 10% molar percentage. For the compositions **5**: 1.0% Tb^{3+}, 2.0% Eu^{3+} and **5**: 1.5% Tb^{3+}, 2.0% Eu^{3+} the complexes emitted in white light region with the corresponding CIE coordinate (0.3269, 0.3123) and (0.3109, 0.3332), respectively (Rao *et al*. 2012).

1.5. Objectives of the present investigation

The luminescence quantum yield is an important parameter to characterize the lanthanide luminescence, defined as the ratio between the number of emitted photons divided by the number of absorbed photons. For luminescent lanthanide complexes, the overall luminescence quantum yield is determined by the efficiency of sensitization and by the intrinsic quantum yield of the lanthanide luminescence. The intrinsic quantum yield is the quantum yield of the lanthanide-centered luminescence upon direct excitation into the 4f levels, which reflects the extent of nonradiative relaxation processes occurring both in the inner- and in the outer-coordination spheres of the lanthanide ion and depends on the energy gap between the emissive state and the highest sub level of the ground state of lanthanide ion. It is well documented that due to the presence of high-energy C–H, N–H and O–H oscillators in the ligands and solvents, which significantly quench the metal excited states nonradiatively, leading to decreased luminescence intensities in lanthanide coordination polymer complexes. To alleviate nonradiative decays in luminescent lanthanide complexes, a variety of strategies have been adopted in the current work to shield the ion excited levels to high nonradiative transition probability by O–H, C–H and N–H oscillators. Recently, among aromatic carboxylate acids, especially, benzoates have proven to be efficient sensitizers for lanthanide ions when modified with light-harvesting moieties (Reddy and Sivakumar 2013). Further, the benzoate ligands were selected on the basis of the fact that carboxylate groups interact strongly with the oxophilic lanthanides and the

delocalized π-electron system provides a strongly absorbing chromophore. Therefore, the primary objective of the present work is to design and develop novel efficient light emitting materials based on lanthanide benzoates and investigate their photophysical properties. Yet another objective of the present investigation is to structural authentification of the designed lanthanide antenna complexes by X-ray single crystal analysis. Furthermore, the photoluminescence properties of the designed lanthanide benzoates will be systematically evaluated and correlate with the triplet energy level of the newly developed benzoate molecules.

White-light-emitting materials have broad applications in displays and solid-state lighting. Obtaining such materials has been a considerable challenge. With judiciously chosen red-(Eu^{3+}) and green-(Tb^{3+}) emissive ions, doped in an appropriate blue emitting host, it is possible to obtain phosphors which emit light across the entire visible spectrum with high color purity. Thus another objective of the present investigation is to develop white-light emitting materials based on isostructural lanthanide benzoate complexes.

CHAPTER 2

Synthesis, Crystal Structure and Photoluminescence of Homodinuclear Lanthanide 4-(Dibenzylamino)benzoate Complexes

2.1. ABSTRACT

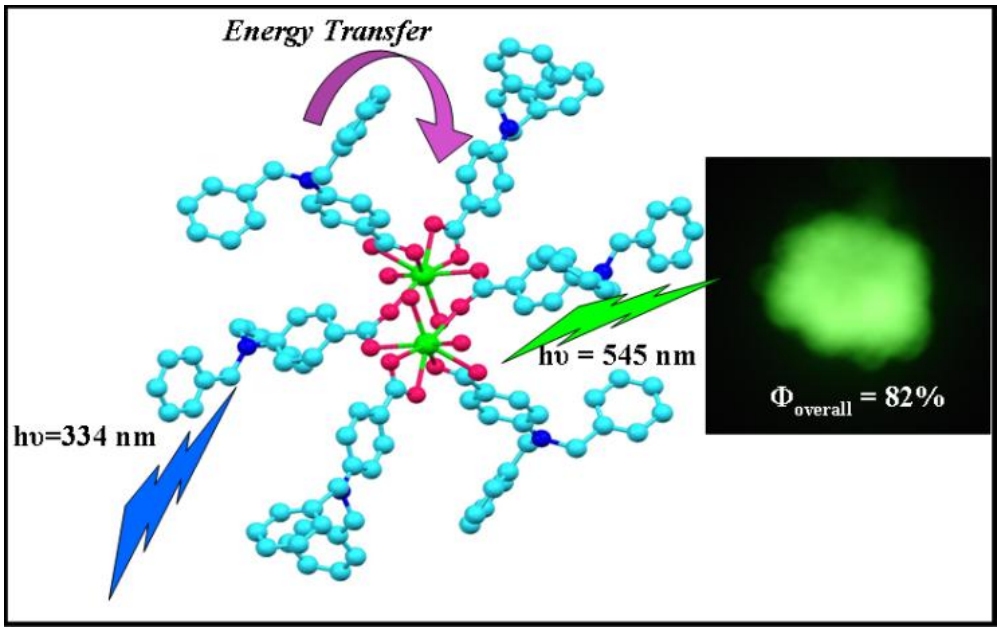

Three new binuclear lanthanide complexes of general formula $[Ln_2(L)_6(H_2O)_4]$ (Ln = Tb (**1**), Eu (**2**) and Gd (**3**)) supported by the novel aromatic carboxylate ligand 4-(dibenzylamino)benzoic acid (HL) have been synthesized. Complexes **1** and **2** were structurally characterized by single-crystal X-ray diffraction. Both **1** and **2** crystallize in the triclinic space group Pī and their molecular structures consist of homodinuclear species that are bridged by two oxygen atoms from two carboxylate ligands *via* different coordination modes. The discrete bridged dimer of **1** is centrosymmetric and features eight-coordinate terbium atoms, each of which adopts a distorted square-antiprismatic geometry. Both

coordination spheres comprise two η^2-chelating benzoates, two μ-η^1:η^1-carboxylate interactions from the bridging benzoates, and two water molecules. By contrast, in complex **2** the Eu^{3+} ion coordination environment is best described as a distorted tricapped-trigonal prism, each europium ion being coordinated to three η^2-chelating benzoate ligands and two water molecules. One of the η^2-carboxylate ligands is involved in a further interaction with an adjacent metal, thus rendering the overall binding mode bridging tridentate, μ-η^2:η^1. Scrutiny of the packing diagrams for **1** and **2** revealed the existence of a one-dimensional molecular array that is held together by intermolecular hydrogen-bonding interactions. The Tb^{3+} complex **1** exhibits high green luminescence efficiency in the solid state with a quantum yield of 82%. On the other hand, poor luminescence efficiency has been noted for Eu^{3+}–4-(dibenzylamino)benzoate complex.

Ramya, A. R.; Reddy, M. L. P.; Cowley, A. H.; Vasudevan, K. V. *Inorganic Chemistry.,* **2010**, *49*, 2407 - 2415.

2.2. INTRODUCTION

The unique electronic structures of lanthanide cations ligated with conjugated organic ligands continue to stimulate an ever increasing number of important technological applications in fields as diverse as biomedicine and materials science (Binnemans 2009; Brunet *et al.* 2007; Bünzli 2006; Bünzli and Piguet 2005; de Bettencourt-Dias 2007; Gunnlaugsson and Leonard 2005; Kuriki *et al.* 2002; Moore *et al*. 2009; Pandya *et al.* 2006; Parker 2004; Picot *et al.* 2008). Moreover, the long excited-state lifetimes and the high chromaticities of the lanthanides are also pertinent to applications in the domain of solid-state photonic materials. For instance, Tb^{3+}, Eu^{3+}, and Tm^{3+} cations are used as green, red, and blue emitters, respectively, in multicolor displays and organic light-emitting diodes (OLEDs) (Justel *et al*. 1998; Hao *et al*. 2001). However, since f–f transitions are parity forbidden, unligated luminescent lanthanide cations have extremely low molar extinction coefficients hence direct lanthanide excitation results only in modest luminescence intensities (Carnall *et al*. 1962; Carnall 1963; Carnall *et al*. 1965; Kim *et al*. 2006). Therefore, over the past few years, efforts have been made to augment the absorption coefficients and thereby obtain significantly more intense lanthanide ion emissions. Fortunately, this objective can be accomplished by prudent selection and synthesis of organic ligands with conjugated motifs. Aromatic carboxylic acids (Louise *et al*. 2007; Chen *et al.* 2007; Eddaudi *et al.* 2001; Pan *et al.* 2004; Bredol *et al*. 1991) and *β*-diketones (Biju *et al.* 2006; Binnemans 2009; de Sá *et al.* 2000; Zheng *et al.* 2008; Fratini *et al*. 2008; Binnemans and Gorller-Walrand 2002) are particularly valuable in this context because such ligands can absorb ultraviolet

light and transfer the absorbed energy to the central lanthanide ions in an appropriately effective manner (the so-called antenna effect) (Bünzli and Piguet 2002; Lehn 1990; Parker 2000; Petoud *et al.* 2003; Piguet and Bünzli 1999). In particular, when aromatic carboxylic acids are employed as the antenna ligands, the coordinated lanthanide ions exhibit higher luminescent stabilities than those ligated with other organic ligands (Raphael *et al.* 2008; Raphael *et al.* 2007). This enhanced stability is of obvious practical importance in terms of device performance and stability.

A number of lanthanide benzoate coordination complexes with unique photophysical properties (Hilder *et al.* 2009; Song *et al*. 2008; Tsaryuk *et al.* 2006) and intriguing structural features (Busskamp *et al.* 2007; Deacon *et al.* 2007; Zhong *et al.* 2008; Chen *et al*. 2007) have been disclosed recently. The benzoate ligands were selected on the basis that carboxylate groups interact strongly with the oxophilic lanthanoids and the fact that the delocalized π-electron system provides a strongly absorbing chromophore (de Bettencourt-Dias and Viswanathan 2006; Hilder *et al.* 2009; Tsaryuk *et al.* 2006). Prior results suggested that derivatization of the benzoic acid analogues with thiophene had a beneficial effect in terms of tuning the triplet state of the antenna. In particular, the enhanced emission quantum yield originated from a better match between the pertinent ligand orbitals and lanthanide ion excited states (Viswanathan and de Bettencourt-Dias 2006). The intense fluorescent emissions of homodinuclear lanthanide complexes of 4-cyanobenzoic acid imply that the ligand-to-Ln^{3+} energy transfer is efficient and that coordinated water molecules do not quench the luminescence by nonradiative dissipation of

energy (Li *et al.* 2006). Very high quantum yields (88%) have been reported with terbium–aminobenzoate complexes, which is somewhat surprising in view of the coordination of both $-NH_2$ and OH_2 ligands (Fiedler *et al.* 2007), since such moieties usually function as vibrational deactivators of the excited state (Sabbatini *et al.* 1993).

Given the important potential applications of lanthanide carboxylates and the fascinating properties of benzoate ligands, we were prompted to prepare a new series of lanthanide complexes featuring the 4-(dibenzylamino)benzoic acid ligand (Figure 2.1) by replacing the hydrogens of the $-NH_2$ group with benzyl groups. The highly conjugated benzoic acid functionality has a significant influence on the distribution of π-electron density within the ligand system. Accordingly, the effective charges on the atoms coordinated to the Ln^{3+} ions can be changed and the interaction of the ligand with metal ion can be modified. As a consequence, the energies of the ligand–metal charge transfer states (LMCTs) and the position of the triplet level are changed, which in turn has profound effects on the luminescent properties of various Ln^{3+} ions. In the present work, a new derivative of benzoic acid has been designed, characterized and utilized for the synthesis of the desired Tb^{3+}, Eu^{3+} and Gd^{3+} complexes. Two of the new lanthanide 4-(dibenzylamino)benzoates have been structurally characterized by single-crystal X-ray diffraction and the photophysical properties of all three of the new lanthanide benzoate complexes have been investigated and correlated with the triplet energy levels of the designed ligand.

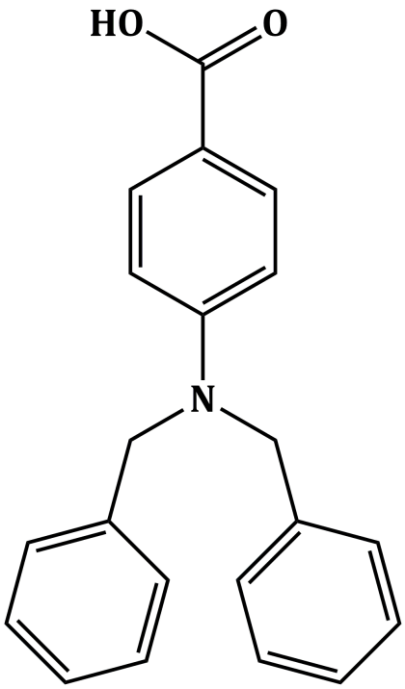

Figure 2.1. Structure of the ligand 4-(dibenzylamino)benzoic acid.

2.3. EXPERIMENTAL SECTION

2.3.1. Materials

Europium(III) nitrate hexahydrate, 99.9%, terbium(III) nitrate hexahydrate, 99.9% and gadolinium(III) nitrate hexahydrate, 99.9% were procured from Triebacher. Methyl 4-aminobenzoate, 98%, and benzyl bromide, 99.9% were purchased from Sigma-Aldrich and used without further purification. All the other chemicals used were of analytical reagent grade.

2.3.2. Characterization and spectroscopic techniques

Elemental analyses were performed with a Perkin-Elmer Series 2 Elemental Analyzer 2400. A Perkin-Elmer Spectrum One FT-IR spectrometer was used to obtain the IR spectral data (neat KBr) and a Bruker 500 MHz NMR spectrometer was used to record the ^{1}H NMR and ^{13}C NMR (125 MHz) spectra of the ligand in

$CDCl_3$ solution. The mass spectra were recorded on a JEOL JSM 600 fast atom bombardment high resolution mass spectrometer (FAB–MS) and the thermogravimetric analyses were performed on a TG/DTA-6200 (SII Nano Technology Inc., Japan). The absorbance of the ligand were measured in $CHCl_3$ solution on a UV–vis spectrophotometer (Shimadzu, UV-2450) and the photoluminescence (PL) spectra were recorded on a Spex-Fluorolog FL22 spectrofluorimeter equipped with a double grating 0.22 m Spex 1680 monochromator and a 450W Xe lamp as the excitation source operating in the front face mode. The lifetime measurements were carried out at room temperature using a Spex 1040D phosphorimeter.

The overall quantum yields ($\Phi_{overall}$) were measured using an integrating sphere in a SPEX Fluorolog spectrofluorimeter. The PL quantum yields of thin films ($\Phi_{overall}$) were determined using a calibrated integrating sphere system. A Xe-arc lamp was used to excite the thin film samples that were placed in the sphere. All samples were prepared by drop casting the material placed between two quartz cover slips. The quantum yields were determined by comparing the spectral intensities of the lamp and the sample emission as reported in the literature (de Mello *et al.* 1997; Shah *et al.* 2006; Palsson and Monkman 2002). Using this experimental setup and the integrating sphere system, the solid state fluorescence quantum yield of a thin film of the standard green OLED material tris-8-hydroxyquinolinolato aluminum (Alq_3) was determined to be 0.19, which is consistent with previously reported values (Cölle *et al.* 2003; Saleesh Kumar *et al*. 2008). Each sample was measured several times under slightly different experimental conditions. The

estimated error for the quantum yields is (±10%) (Eliseeva *et al.* 2008). For measuring the quantum yield by the relative method, the diffuse reflectance spectra of the new lanthanide complexes and the standard phosphor were recorded on a Shimadzu, UV-2450 UV–vis spectrophotometer using $BaSO_4$ as a reference. The overall quantum yields ($\Phi_{overall}$), were measured at room temperature using the technique for powdered samples described by (Bril and De Jager-Veenis 1976), along with the following expression:

$$\Phi_{overall} = \frac{1-r_{st}}{1-r_X} \times \frac{A_x}{A_{st}} \times \Phi_{st}$$

where r_x and r_{st} represent the diffuse reflectance of the complexes and the standard phosphor, respectively (with respect to a fixed wavelength), and Φ_{st} is the quantum yield of the standard phosphor. The terms A_x and A_{st} represent the areas under the complex and the standard emission spectra, respectively. To acquire absolute intensity values, $BaSO_4$ was used as a reflecting standard. The standard phosphor used was pyrene (Aldrich), the emission spectrum of which comprises a large broadband peaking around 471 nm, with a constant Φ value (Φ_{st} = 61%, λ_{ex} = 313 nm) (Melhuish 1964). Three measurements were carried out for each sample, and the reported $\Phi_{overall}$ value corresponds to the arithmetic mean value of the three values. The errors in the quantum yield values associated with this technique were estimated to be within ±10% (Carlos *et al.* 2003; De Mello Donega *et al.* 1996).

The X-ray diffraction data were collected at 153 K on a Nonius Kappa CCD diffractometer equipped with an Oxford Cryostream low-temperature

device and a graphite-monochromated Mo Kα radiation source (λ = 0.71073 Å). Corrections were applied for Lorentz and polarization effects (Sheldrick 1994). Both structures were solved by direct methods and refined by full-matrix least-squares cycles on F^2. All of the non-hydrogen atoms were allowed anisotropic thermal motion, and the hydrogen atoms were placed in fixed, calculated positions using a riding model (C-H, 0.96 Å). X-ray crystallographic information files can be obtained free of charge *via* www.ccdc.cam.ac.uk/consts/retrieving.html (or from CCDC, 12 Union Road, Cambridge CB2 1EZ, U.K.; fax: +44 1223 336033; e-mail: deposit @ccdc.cam.ac.uk). The CCDC numbers are 743231 and 746200 for **1** and **2**, respectively. A molecule of DMSO has been added to the molecular formulas of **1** and **2** since in each case it was removed via "Squeeze" due to the extreme disorder which could not be solved. Furthermore, the water protons were not located, and the hydroxyl protons have been placed in the positions that were calculated on the basis of optimum hydrogen bonding.

2.3.3. Synthesis and characterization of the ligand

2.3.3.1. Synthesis of Methyl 4-(dibenzylamino)benzoate. Potassium carbonate (0.68 g, 4.92 mmol) was added to a solution of methyl 4-amino benzoate (0.25 g, 1.65 mmol) in freshly distilled DMF (50 mL). The resulting reaction mixture was refluxed for 30 min, following which benzyl bromide (0.56 g, 3.29 mmol) was added and the solution was refluxed at 78 ^{o}C for an additional 48 h. The reaction mixture was then poured into water and the resulting precipitate was filtered off, washed with water and dried. The resulting residue

was purified by silica gel column chromatography using hexane/ethyl acetate, thereby affording the desired product as a white solid. Yield, 0.2 g (36.4%). ^{1}H NMR (500 MHz, $CDCl_3$): δ (ppm) 7.85 (d, 2H, J = 9 Hz, Ar–H), 7.34 (t, 4H, J = 7 Hz, Ar–H), 7.27 (t, 2H, J = 7.5 Hz, Ar–H), 7.21 (d, 4H, J = 7 Hz, Ar–H), 6.72 (d, 2H, J = 9 Hz, Ar–H), 4.71 (S, 4H, $-NCH_2$), 3.83 (S, 3H, $-OCH_3$). ^{13}C NMR (125 MHz, $CDCl_3$): δ (ppm) 167.26, 152.54, 137.37, 131.48, 128.83, 127.24, 126.45, 117.93, 111.26, 53.98, 51.53. FAB-MS: m/z = 332.53 $(M+1)^+$. FT-IR (KBr): ν_{max} 1690 (ν_{as}(C=O)), 1432 (ν_s(C=O)), 1600, 1530, 1313, 1280, 1174, 1113, 834, 768 cm^{-1}.

2.3.3.2. Synthesis of 4-(Dibenzylamino)benzoic acid (HL). Methyl 4-(dibenzylamino)benzoate (0.3 g, 0.902 mmol) was refluxed for 24 h in a solution of KOH (0.15 g, 2.67 mmol) in 50 mL of ethanol. The reaction mixture was poured into ice cold water, acidified with dilute HCl, and the resulting precipitate was filtered, washed, dried and recrystallized from CH_2Cl_2. Yield, 0.25 g (87%) (Scheme 2.1). ^{1}H NMR (500 MHz, $CDCl_3$): δ (ppm) 7.92 (d, 2H, J = 9.5 Hz, Ar–H), 7.36 (t, 4H, J = 7 Hz, Ar–H), 7.29 (t, 2H, J = 7 Hz, Ar–H), 7.23 (d, 4H, J = 7 Hz, Ar–H), 6.74 (d, 2H, J = 9 Hz, Ar–H), 4.74 (s, 4H, $-NCH_2$). ^{13}C NMR (125 MHz, $CDCl_3$): δ (ppm) 172.06, 153.17, 137.21, 132.26, 128.87, 127.29, 126.43, 116.92, 111.27, 53.99. FAB-MS: m/z = 318.57 $(M+1)^+$. Elemental analysis (%): Calcd (found) for $C_{21}H_{19}O_2N$ (317.38): C, 79.47 (79.00) ; H, 6.03 (6.27); N, 4.41 (4.36). FT-IR (KBr) : ν_{max} 1663 (ν_{as}(C=O)), 1450 (ν_s(C=O)), 1599, 1557, 1529, 1450, 1413, 1363, 1288, 723, 694 cm^{-1}.

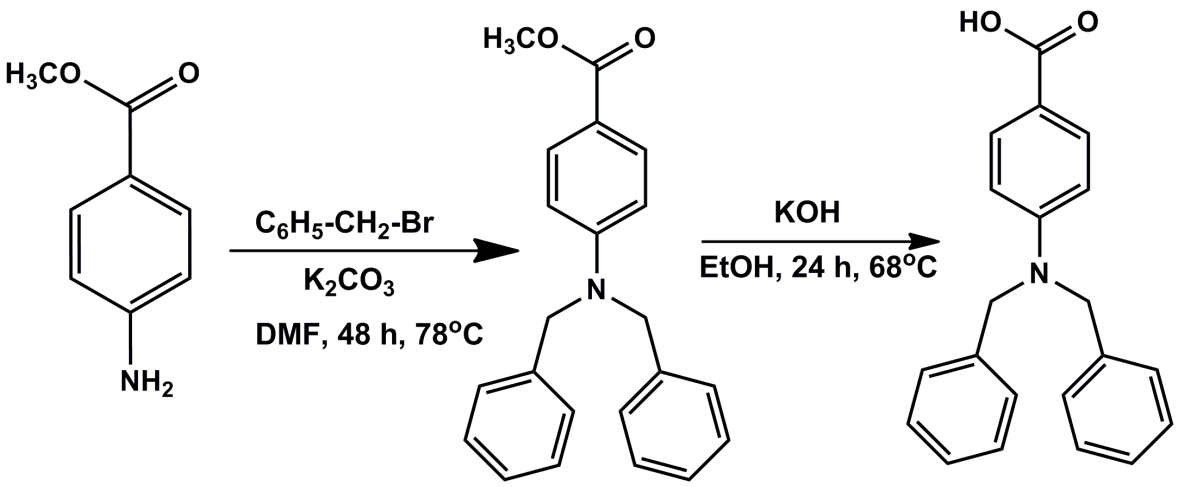

Scheme 2.1. Synthesis of the ligand 4-(dibenzylamino)benzoic acid (HL).

2.3.4. Syntheses of lanthanide complexes

In a typical procedure, an ethanolic solution of $Ln(NO_3)_3{\cdot}6H_2O$ (0.5 mmol) (Ln = Eu, Tb, or Gd) was added to a solution of 4-(dibenzylamino)benzoic acid (1.5 mmol) in ethanol in the presence of NaOH (1.5 mmol). Precipitation took place immediately, and the reaction mixture was stirred subsequently for 10 h at room temperature. The crude product was filtered, washed with ethanol and dried. The resulting complexes were then purified by recrystallization from a dichloromethane/methanol solvent mixture. Single crystals of the terbium and europium complexes suitable for X-ray study were obtained from a dimethylsulfoxide/ethanol/dichloromethane solvent mixture after storage for 3 weeks at ambient temperature.

$Tb_2(L)_6(H_2O)_4$ (1). Elemental analysis (%): calcd (found) for $C_{126}H_{116}N_6O_{16}Tb_2$ (2288.15): C, 66.14 (66.38); H, 5.11 (4.75); N, 3.67 (3.89). FT-IR (KBr): ν_{max} 3429 (ν(O–H)), 1603 (ν_{as}(C=O)), 1572 (ν_{as}(C=O)), 1402 (ν_s(C=O)), 1358

(ν_s(C=O)), 1503, 1221, 1199, 1072, 783 cm^{-1}. FAB-MS: m/z = 1109.06 $(Tb(L)_3)$+1.

$Eu_2(L)_6(H_2O)_4$ (2). Elemental analysis (%): calcd (found) for $C_{126}H_{116}N_6O_{16}Eu_2$ (2274.23): C, 66.54 (66.82); H, 5.14 (4.84); N, 3.70 (3.91). FT-IR (KBr) ν_{max}: 3413 (ν(O–H)), 1604 (ν_{as}(C=O)), 1518 (ν_{as}(C=O)), 1403 (ν_s(C=O)), 1358 (ν_s(C=O)), 1495, 1225, 1121, 783 cm^{-1}. FAB-MS: m/z = 1124.70 $(Eu(L)_3$ + Na) +1.

$Gd_2(L)_6(H_2O)_4$ (3). Elemental analysis (%): calcd (found) for $C_{126}H_{116}N_6O_{16}Gd_2$ (2284.79): C, 66.24 (66.60); H, 5.12 (4.85); N, 3.68 (3.84). FT-IR (KBr): ν_{max} 3414 (ν(O–H)), 1603 (ν_{as}(C=O)), 1574 (ν_{as}(C=O)), 1395 (ν_s(C=O)), 1356 (ν_s(C=O)), 1513, 1226, 1199, 1078, 946 cm^{-1}. FAB-MS: m/z = 1130.49 $(Gd(L)_3$+Na)+1.

2.4. RESULTS AND DISCUSSION

2.4.1. Synthesis and characterization of ligand and Ln^{3+} complexes 1–3

The ligand 4-(dibenzylamino)benzoic acid (HL) was synthesized in 87% yield according to the method described in Scheme 2.1. The ligand was characterized by FT-IR, ^{1}H NMR, and ^{13}C NMR spectroscopy as well as by mass spectroscopy (FAB-MS) and elemental analysis. The synthetic procedures for the Ln^{3+} complexes **1–3** are described in the Experimental Section. The microanalyses of complexes **1–3** revealed that each Ln^{3+} ion had reacted with the HL ligand in a metal-to-ligand mole ratio of 1:3. The FT-IR spectra of the coordinated ligand HL exhibits two intense bands at

approximately 1450 and 1663 cm^{-1}, which are attributable to the symmetric ν_s(C=O) and *anti*-symmetric ν_{as}(C=O) vibration modes, respectively. In each case, coordination of the ligand HL to the respective lanthanide ion was confirmed by the absence of the ν(COOH) absorption bands of the ligand at ~1660 cm^{-1}. Moreover, the asymmetric and symmetric stretching vibrational modes of the carboxylic acid in complexes **1–3** are further split into two peaks [ν_s(C=O): 1402, 1358 cm^{-1}; ν_{as}(C=O) : 1603, 1572 cm^{-1} in **1**; ν_s(C=O) : 1403, 1358 cm^{-1} ; ν_{as}(C=O): 1604, 1518 cm^{-1} in **2**; ν_s(C=O) :1395, 1356 cm^{-1}; ν_{as}(C=O) : 1603, 1574 cm^{-1} in **3**]. The difference between the asymmetric and symmetric stretching vibration modes ($\Delta\nu_{(C=O)} = \nu_{as} - \nu_s$) fall in the ranges 245–247 and 170–179 cm^{-1}, which in turn implies that the carboxylate groups are coordinated to the Tb^{3+} or Gd^{3+} ions in two different ways, namely, *via* chelating and bidentate bridging (Figure 2.2) (Deacon and Phillips 1980; Teotonio *et al.* 2005). On the other hand, the difference between the asymmetric and symmetric stretching vibration modes is 246 and 115 cm^{-1} in the case of complex **2**, indicating that the coordination of Eu^{3+} with carboxylate groups in chelating and tridentate bridging modes (Deacon and Phillips 1980; Teotonio *et al.* 2005). Furthermore, the IR spectra of **1–3** exhibit a broad band at approximately 3400 cm^{-1} which is characteristic of an O–H stretching vibration, thereby indicating the presence of water molecules in the coordination sphere of each complex.

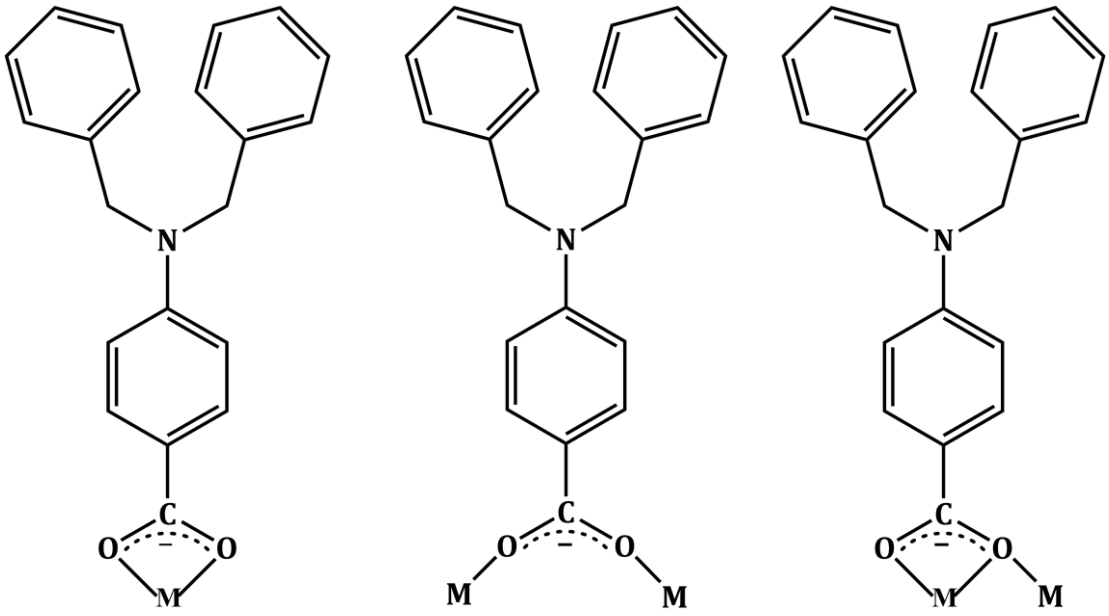

η^2 - chelating (μ-$\eta^1 : \eta^1$) bridging bidentate (μ-$\eta^2 : \eta^1$) bridging tridentate

Figure 2.2. Different types of binding modes for the ligand HL observed in Tb and Eu complexes **1** and **2**.

The thermal stabilities of complexes **1** and **2** were examined by TGA in the 30-1000 ^{o}C range, and the corresponding thermograms are depicted in Figure 2.3. It is clear from the thermogravimetric analysis data for **1** and **2** (Figure 2.3) that each complex undergoes a mass loss of approximately 3% (calcd ~ 3.14%) in the first step (120–240 °C), which corresponds to elimination of the coordinated water molecules (Mahata *et al.* 2008). Subsequent thermal decomposition of **1** and **2** takes place in two steps in the temperature region 240–900 °C which is attributed to the thermal decomposition of three ligand molecules. The quantity of residue for each

complex represents approximately 16% of the initial mass and corresponds to formation of the respective lanthanide oxide.

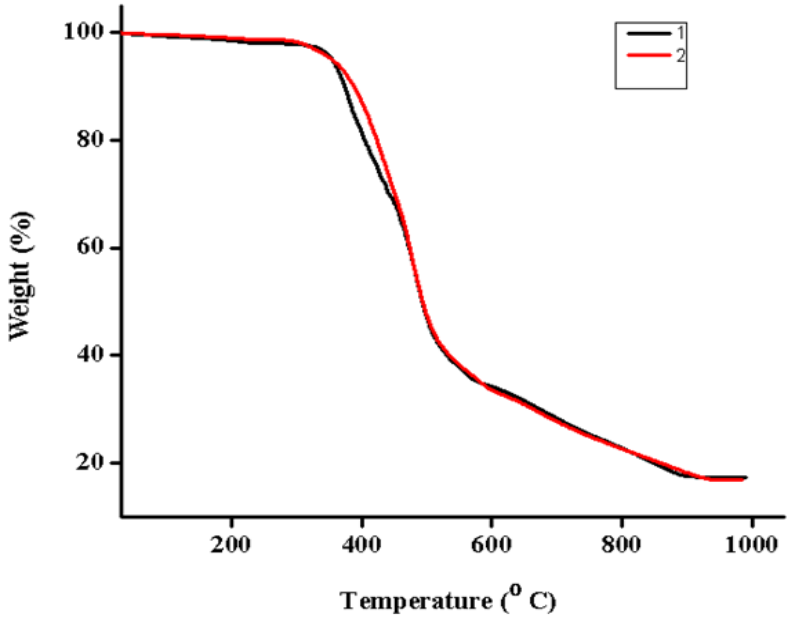

Figure 2.3. TG analysis of complexes **1**–**2**.

2.4.2. X-ray crystal structures

The solid state structures of $Tb_2(L)_6(H_2O)_4$ (**1**) and $Eu_2(L)_6(H_2O)_4$ (**2**) were determined by single-crystal X-ray diffraction. Figures 2.4 and 2.6 depict the molecular structures of complexes **1** and **2**, respectively. The pertinent data collection parameters and a listing of significant bond distances and bond angles for the metal coordination environments are presented in Tables 2.1 and 2.2, respectively. Compounds **1** and **2** crystallize in the triclinic space group *P*ī and their molecular structures consist of homodinuclear species that are bridged by two oxygen atoms from two carboxylate ligands in different coordination modes. It is interesting to note that the dimeric structures of the Ln^{3+}–4-(dibenzylamino)benzoate complexes possess an inversion center of symmetry,

thus indicating that the Ln(1) and Ln(2) centers reside in equivalent chemical environments. The distance between the Tb(1) and Tb(2) cations in compound **1** is equal to 4.347 Å while the corresponding Eu-Eu distance in **2** is 4.309 Å. These distances fall within the range of 3.785–4.532 Å that has been observed for other Ln^{3+} carboxylate complexes that feature both bidentate and tridentate bridging coordination modes. In the case of complex **1**, each terbium atom is coordinated to two η^2-bidentate chelating benzoates, two η^1-carboxylate interactions from the bridging benzoates (the coordination modes can be viewed in Figure 2.2), which is in good agreement with the IR data. The coordination polyhedra can be described best as distorted square antiprisms, in which six oxygen atoms are furnished by the four benzoate moieties and two oxygen atoms are provided by the two water molecules.

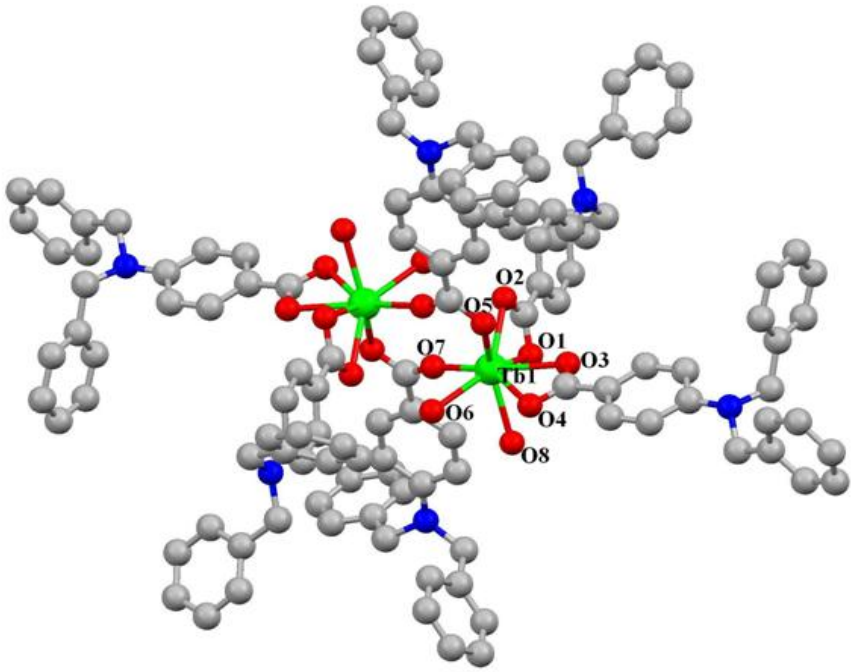

Figure 2.4. ORTEP diagram of complex **1**.

Table 2.1. Crystallographic and refinement data for **1** and **2**.

	1	**2**
formula	$C_{130}H_{136}N_6O_{22}S_2Tb_2$	$C_{130}H_{128}N_6O_{18}S_2Eu_2$
fw	2516.41	2430.42
cryst sys	Triclinic	Triclinic
space group	*P*ī	*P*ī
cryst size	0.25 × 0.22 × 0.15	0.24 × 0.20 × 0.13
Temp/K	153(2)	153(2)
a/(Å)	9.829(5)	9.879(5)
b/(Å)	17.180(5)	17.259(5)
c/(Å)	17.816 (5)	17.896 (5)
α (°)	84.917 (5)	85.264(5)
B (°)	82.794 (5)	83.206 (5)
γ (°)	87.271(5)	88.609 (5)
V/Å^3	2971.2 (19)	3019(2)
Z	1	1
D_{calcd}, g cm^{-1}	1.406	1.337
μ/(Mo,Kα)mm^{-1}	1.288	1.131
F(000)	1296	1252
R1 [*I*> 2σ(*I*)]	0.0396	0.0521
w*R2* [*I*> 2σ(*I*)]	0.0872	0.1146
R1 (all data)	0.0532	0.0996
w*R2* (all data)	0.0915	0.1246
gof	1.093	1.093

Table 2.2. Selected bond lengths (Å) and angles (°) for **1** and **2**.

1		**2**	
Tb1–Tb2	4.347	Eu1–Eu2	4.309
Tb1–O1	2.458(2)	Eu1–O1	2.483(3)
Tb1–O2	2.420(2)	Eu1–O2	2.435(3)
Tb1–O3	2.358(2)	Eu1–O3	2.390(3)
Tb1–O4	2.560(2)	Eu1–O4	2.577(3)
Tb1–O5	2.332(3)	Eu1–O5	2.362(3)
Tb1–O6	2.377(2)	Eu1–O6	2.410(3)
Tb1–O7	2.330(2)	Eu1–O7	2.830(3)
Tb1–O8	2.421(3)	Eu1–O8	2.455(3)
		Eu1–O7#	2.369(3)
O1–Tb1–O2	53.75(8)	O1–Eu1–O2	53.25(10)
O3–Tb1–O4	52.85(7)	O3–Eu1–O4	52.23(10)
O8–Tb1–O6	77.51(8)	O8–Eu1–O6	78.21(10)
O5–Tb1–O7	116.08(9)	O5–Eu1–O7	49.29(9)
O2–Tb1–O5	79.53(8)	O7–Eu1–O7#	68.34(11)
O7–Tb1–O6	74.56(8)	O7–Eu1–O6	75.24(10)
O7–Tb1–O8	92.69(9)	O7–Eu1–O8	92.56(10)

The longest Tb–O bonds involve the oxygen atoms of the bidentate chelating ligands [Tb(1)–O(1): 2.458 Å; Tb(1)–O(2): 2.420 Å; Tb(1)–O(4): 2.560 Å; Tb(1)–O(3): 2.358 Å] and the shortest such bonds are associated with the bridging carboxylate ligand [Tb(1)–O(7): 2.330 Å; Tb(1)–O(5): 2.332 Å]. On the other hand, the Tb-O bond distances for the coordinated water molecules

[Tb(1)–(O8): 2.421 Å and Tb(1)–O(6): 2.377 Å, respectively] are shorter than those for the bidentate chelating benzoates (Sun *et al*. 2004).

Scrutiny of the packing diagram for **1** revealed the presence of a 1D molecular array that is oriented along the *c* axis. This feature is illustrated by the intermolecular hydrogen bonding interaction between C28 and O8 through H28 with a H···O distance of 2.650 Å and a C–H···O angle of 154.97° (Figure 2.5) (Remya *et al.* 2008; Roesky and Andruh 2003).

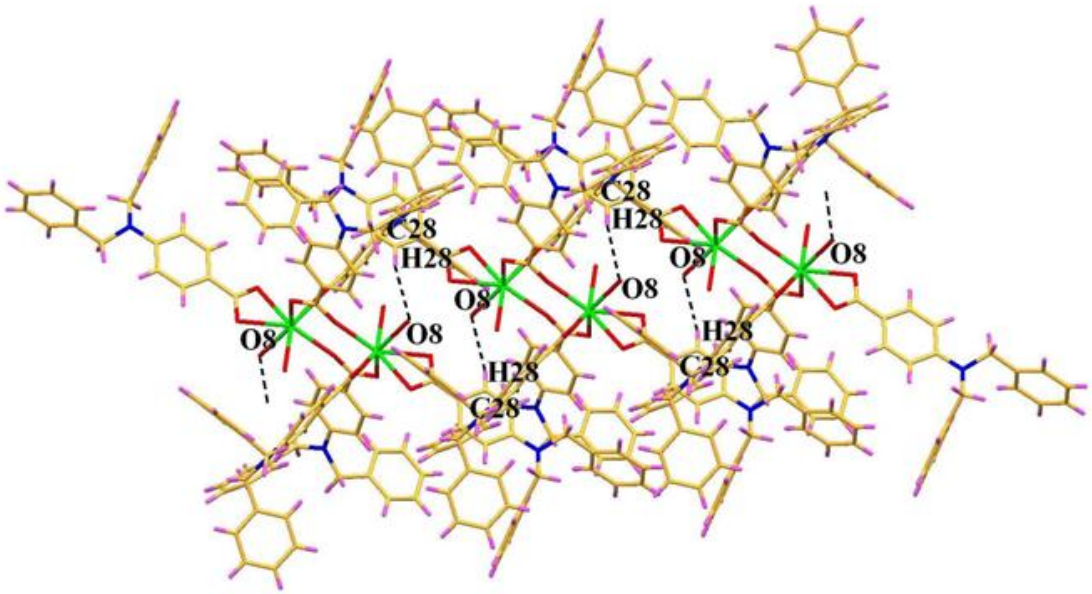

Figure 2.5. View of complex **1** showing the intermolecular hydrogen bonding interactions involving C28–H28 of the phenyl moiety and O8 of the water molecule.

In the case of complex **2**, the 4-(dibenzylamino)benzoate ligands exhibit two different coordination modes to the Eu^{3+} ions, namely bidentate chelating (η^2-chelating benzoates) and bidentate chelating with an oxygen atom bridging two metal ions and another oxygen atom coordinating to one of the ions (triply coordinated; η^2-η^1-chelating benzoates) as illustrated in Figure 2.6, thus

corroborating the IR data. The Eu^{3+} ions are nine coordinate and feature two bidentate chelating carboxylates and one tridentate bridging carboxylate ligand.

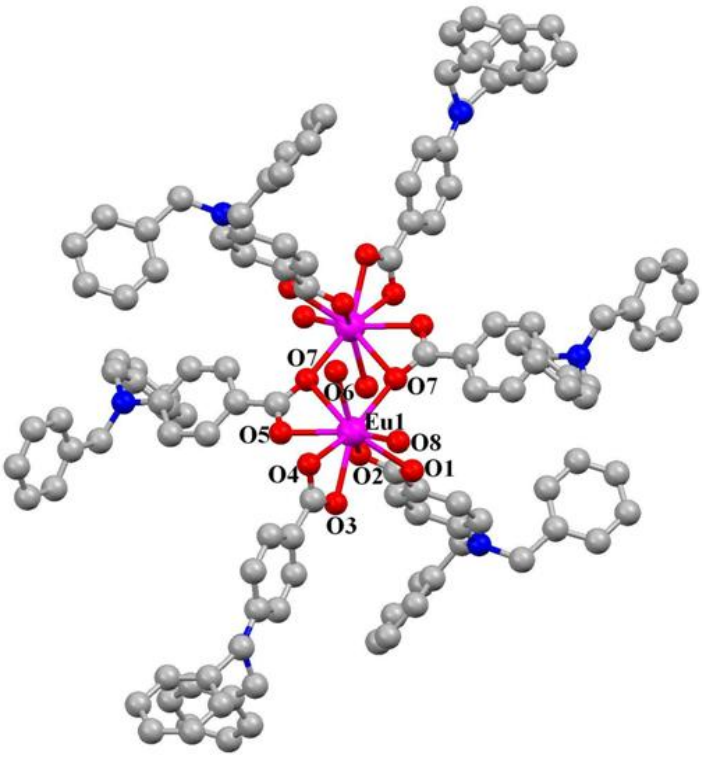

Figure 2.6. ORTEP diagram of complex **2**.

The coordination sphere is completed by the presence of two water molecules. The coordination sphere can be described best as a tricapped trigonal prism in which seven oxygen atoms are provided by four 4-(dibenzylamino)benzoate ligands and two oxygen atoms are furnished by two water molecules. The Eu–O bond lengths range from 2.362 to 2.830 Å and thus fall within the range anticipated for this type of complex (Raphael *et al.* 2007; Viswanathan and de Bettencourt-Dias 2006). The longest Eu–O bonds involve the oxygen atoms of one of the triply coordinated ligands [Eu(1)–O(7): 2.830 Å].

The packing diagram for **2** reveals the presence of a one-dimensional array that is aligned along the *c* axis and which involves an intermolecular hydrogen bonding interaction between the C(28)–H(28) bond of a phenyl ring of one of the carboxylate ligands and O(8) of a water molecule with a separation of 2.684 Å [H(28)---O(8)] and an angle of 154.44° [C(28)–H(28)–O(8) (Figure 2.7).

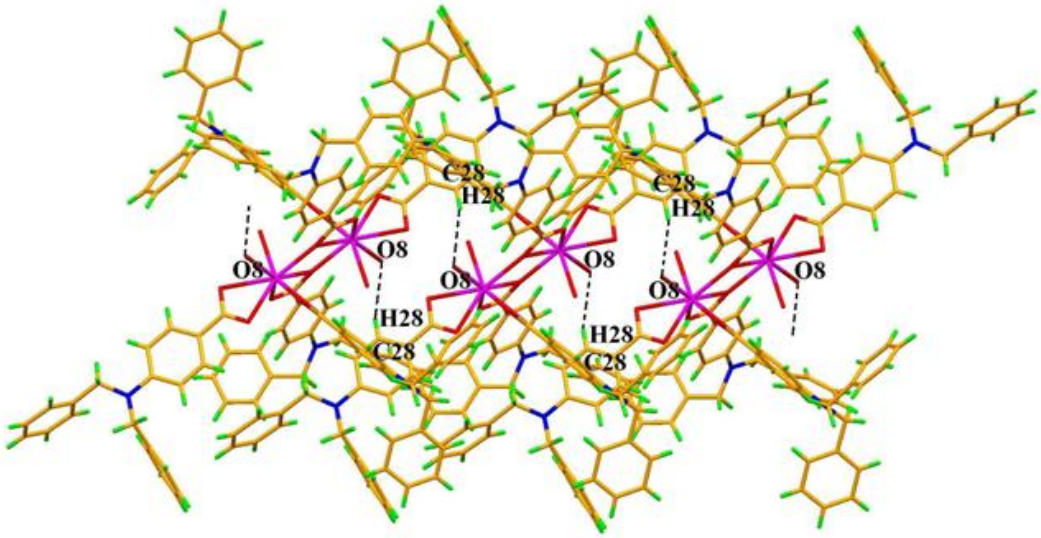

Figure 2.7. View of complex **2** showing the intermolecular hydrogen bonding interactions involving C28–H28 of the phenyl moiety and O8 of the water molecule.

2.4.3. Electronic states of the ligand and complexes

The UV-vis absorption spectrum of the free ligand HL and those of the corresponding complexes **1**–**3** were measured in $CHCl_3$ solution (c = 2 × 10^{-6} M) and are displayed in Figure 2.8. The absorption maxima for **1**–**3** (309 nm), which are attributable to singlet-singlet $^1\pi$-π^* absorptions of the aromatic rings, are slightly blue-shifted with respect to that of the free ligand HL (λ_{max} = 311 nm). No significant changes are apparent in the shapes of the absorption bands

upon formation of the lanthanide complexes, therefore suggesting that the coordination of the Ln^{3+} ion does not have a significant influence on the $^1\pi$-π^* transition.

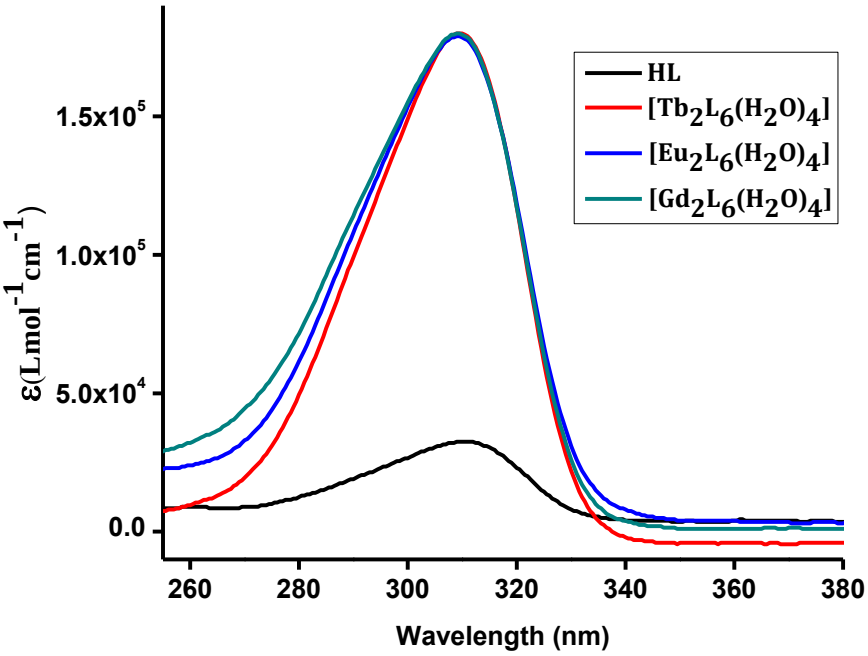

Figure 2.8. UV–visible absorption spectra of the ligand, HL and Ln^{3+}–complexes in $CHCl_3$ solution (2×10^{-6} M).

However, a small blue shift that is discernible in the absorption maximum of all three complexes is attributable to the perturbation induced by the metal coordination. The molar absorption coefficient values for complexes **1**–**3** at 309 nm of 1.8×10^5, 1.78×10^5 and 1.79×10^5 L mol$^-$ cm^{-1}, respectively, are approximately six times higher than that of the HL ligand (3×10^4 at 311 nm), which is consistent with the presence of six carboxylate ligands in each complex. Note also that the large molar absorption coefficient for the HL ligand indicates that it has a strong ability to absorb light.

2.4.4. Photophysical properties

In order to understand the energy transfer processes in the new Ln^{3+} complexes, it was necessary to determine the singlet and triplet energy levels of the ligand, 4-(dibenzylamino)benzoic acid (HL). The singlet ($^1\pi\pi^*$) energy level of this ligand was estimated by reference to the wavelength of the UV–vis absorption edge of the Gd^{3+} complex **3**. The pertinent value was found to be 331 nm (30221 cm^{-1}) in the case of the HL ligand. The triplet energy level ($^3\pi\pi^*$) of this ligand was calculated by reference to the lower wavelength emission edge (423 nm: 23640 cm^{-1}) from the low-temperature phosphorescence spectra of the Gd^{3+} complex of the 4-(dibenzylamino)benzoic acid (Figure 2.9).

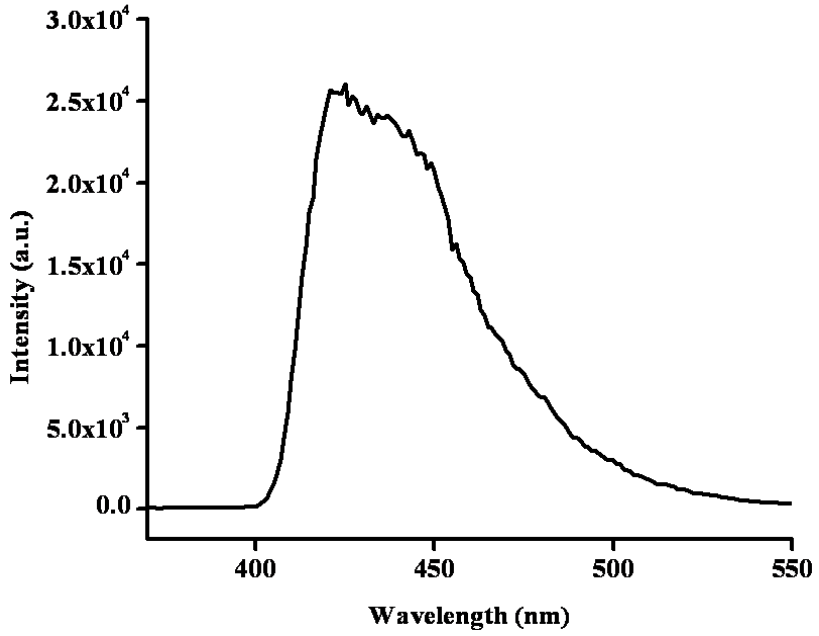

Figure 2.9. Phosphorescence spectrum of gadolinium complex **3** at 77 K.

According to Reinhoudt's empirical rule, the intersystem crossing process becomes effective when ΔE ($^1\pi\pi^*$– $^3\pi\pi^*$) is at least 5000 cm^{-1} (Steemers *et al.*

1995). The energy gap ΔE ($^1\pi\pi^* - {}^3\pi\pi^*$) for the ligand HL is 6581 cm^{-1}; hence, our new complexes amply satisfy this condition. As a consequence, the intersystem crossing process is effective for this ligand. The triplet energy level of HL appears at appreciably higher energy than $^5D_4$ for Tb^{3+} or $^5D_0$ for Eu^{3+}, thus indicating that the designed new ligand can act as antenna for the photosensitization of trivalent Ln^{3+} ions.

The solid-state excitation and emission spectra of complex **1** recorded at room-temperature are displayed in Figure 2.10. The excitation spectrum monitored at the characteristic emission of the Tb^{3+} ion in the solid state overlaps with the absorption spectrum in the 250–360 nm regions (Figure 2.8), which indicate that energy transfer from the ligand to the metal ion is operative (Kawa and Frechet 1998; Sabattini *et al*. 1991; Li *et al*. 2002). The excitation spectrum of **1** exhibits a broad band between 250 and 380 nm which is attributable to the π-π^* transition of the aromatic carboxylate ligand. The absence of any absorption bands due to the f–f transitions of the Tb^{3+} cation proves that luminescence sensitization *via* excitation of the ligand is effective. The room-temperature emission spectrum of complex **1** exhibits the characteristic emission bands of the Tb^{3+} cation (λ_{ex} = 334 nm) centered at 488, 545, 585, and 620 nm which result from deactivation of the $^5D_4$ excited state to the corresponding ^7F_J ground state of the Tb^{3+} cation (J = 6, 5, 4, 3) (Carnall 1987; Dieke 1968; Biju *et al.* 2009; Raphael *et al.* 2008; Raphael *et al.* 2007; Sivakumar *et al.* 2010; Xia *et al.* 2007). Interestingly, no emission bands from the organic ligand were observed, which leads to the conclusion that energy transfer from the ligand to the Tb^{3+} center is very efficient.

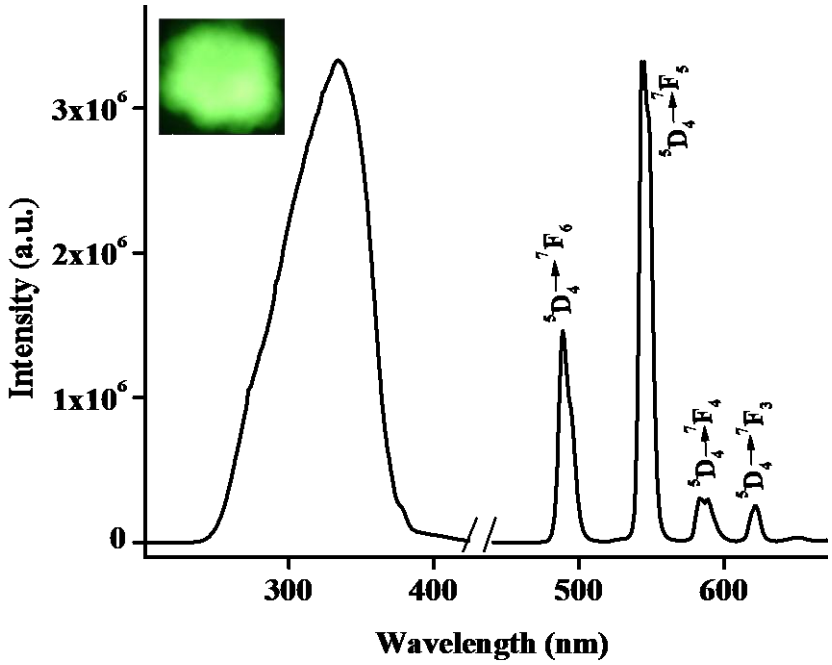

Figure 2.10. Room-temperature excitation and emission spectra for complex **1** (λ_{ex} = 334 nm) with emission monitored at approximately 545 nm.

The solid-state excitation and emission spectra for the Eu^{3+} complex **2** at room- temperature are shown in Figure 2.11. The excitation spectrum of the Eu^{3+} complex of HL has negligible contributions from the ligand and exhibits a series of sharp lines that are characteristic of the Eu^{3+} energy-level structure and can therefore be assigned to transitions between the $^7F_{0,1}$ and $^5L_6$ and $^5D_{2,1}$ levels. (Raj *et al.* 2009; Biju *et al.* 2006; Pavithran *et al.* 2005; Steemers *et al.* 1995). Accordingly, luminescence sensitization of the Eu^{3+} complex *via* ligand excitation is not efficient in this case. The ambient-temperature emission spectrum of the Eu^{3+} complex is characteristic of the metal in the 550–700 nm region and exhibits well-resolved peaks that are attributable to transitions from the metal-centered $^5D_0$ excited state to the ^7F_J ground-state multiplet. Maximum peak intensities at 580, 593, 617, 652, and 694 nm, were observed for the J = 0,

1, 2, 3, and 4 transitions, respectively, and the J = 2 so-called "hypersensitive" transition is intense (Biju *et al.* 2009; Miyata *et al*. 2011; Pavithran *et al.* 2006; Raj *et al.* 2008; Werts *et al.* 2002; Fu *et al*. 2005; Zucchi *et al.* 2009).

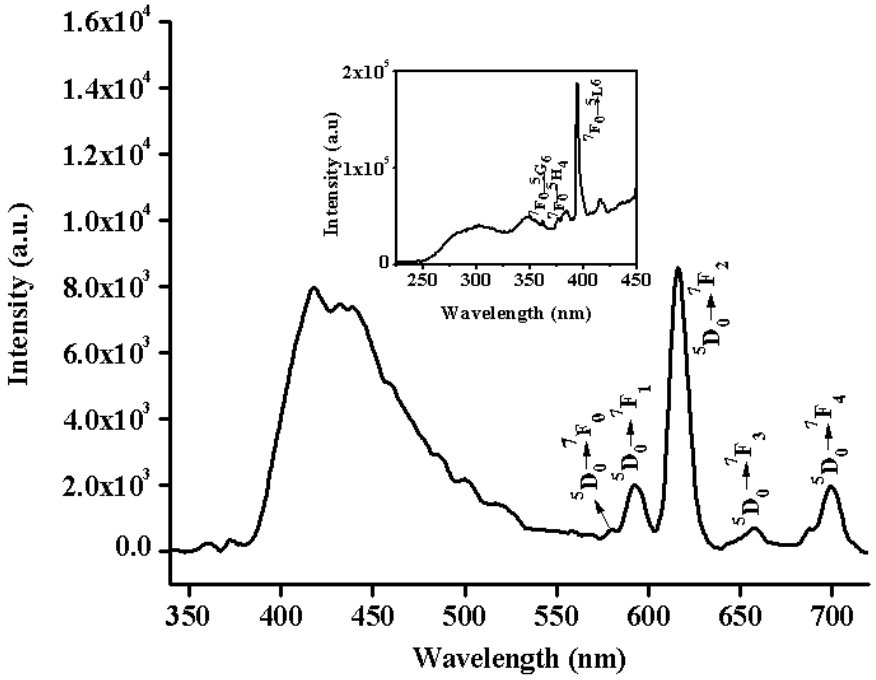

Figure 2.11. Room-temperature excitation (inset) and emission spectra for complex **2** (λ_{ex} = 308 nm) with emission monitored at approximately 612 nm.

The intensity of the $^5D_0 \rightarrow {}^7F_2$ transition (electric dipole) is greater than that of the $^5D_0 \rightarrow {}^7F_1$ transition (magnetic dipole), which indicates that the coordination environment of the Eu^{3+} ion is devoid of inversion center. Furthermore, an intense broad band in the region 400–500 nm due to a π-π^* transition of the ligand was evident in the emission spectrum of **2** (Stanley *et al*. 2010). Such an observation is typically diagnostic of poor sensitization of the ligand toward the Eu^{3+} ion.

The luminescent lifetimes of Ln^{3+} complexes were measured at both ambient (298 K) (complexes **1**–**2**) and low temperatures (77 K) (complex **1**) on

the basis of the respective luminescent decay profiles by fitting them with monoexponential decay curves (Figures 2.12 and 2.13). Collectively, these data imply the existence of a single chemical environment around the Ln^{3+} ion in each case. The pertinent values are summarized in Table 2.3. A longer $^5D_4$ lifetime value (τ_{obs} = 1.02 ms) was observed in the case of the Tb^{3+} complex **1** despite the presence of solvent molecules in the first coordination sphere, since such molecules are typically vibrational deactivators of the excited states of Ln^{3+} ions. It is somewhat surprising that the magnitude of the $^5D_4$ lifetime for complex **1** is not very high compared with some recently reported data for highly luminescent Tb^{3+} complexes ($\Phi_{overall}$ = 56%; τ_{obs} = 2.63 ms) (Samuel *et al*. 2008). On the other hand, there is a recent report of a $\Phi_{overall}$ value of 40% and τ_{obs} = 0.46 ms for Tb^{3+}-dipivaloylmethanato complexes (Eliseeva *et al.* 2008). Furthermore, our group also observed $\Phi_{overall}$ value of 72% and τ_{obs} = 0.92 ms for a Tb^{3+}-4-isobutyryl-3-phenyl-5-isoxazolonate complex (Biju *et al.* 2009). The lifetime is the inverse of the total deactivation rate, which in turn is the sum of the radiative and non-radiative rates. Therefore, the fact that a lanthanide complex is highly luminescent yet possesses a short lifetime does not represent a contradiction. It simply means that the radiative rate is rapid as observed in the case of Tb^{3+} complex **1.** Moreover, on account of its electronic structure, the Tb^{3+} cation has many energy levels that can mix with appropriate ligand wave functions, including a relatively low-lying 4f 5d state, which may explain why the lifetime is relatively short (i.e., it implies that the phosphorescence character of the transition is partly lost).

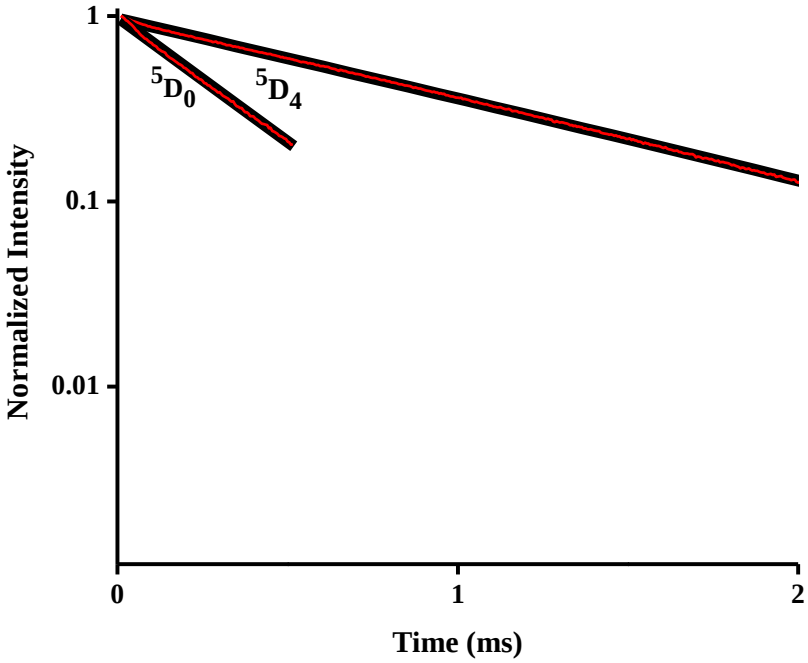

Figure 2.12. Room-temperature luminescence decay profiles for complexes **1** and **2** excited at 334 nm and 308 nm and monitored at 545 nm and 612 nm, respectively.

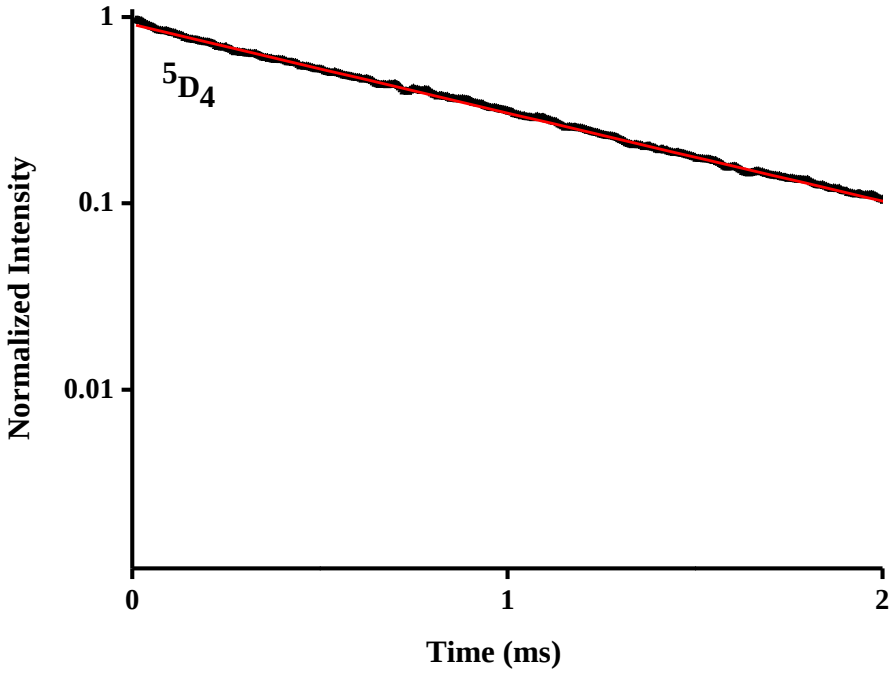

Figure 2.13. Low temperature (77 K) luminescence decay profile of Tb-complex excited at 334 nm and monitered at approximately 545 nm.

The somewhat shorter $^5D_0$ lifetime value (τ_{obs} = 0.33 ms) that was observed for the Eu^{3+} analogue may be due to the dominant non-radiative decay channels associated with vibronic coupling due to the presence of solvent molecules. Similar observations have been made for several europium complexes (Raj *et al.* 2008).

In order to gain a better understanding of the luminescence efficiencies of the new 4-(dibenzylamino)benzoate complexes **1** and **2**, it was appropriate to calculate the overall quantum yields. The overall quantum yield ($\Phi_{overall}$) for a lanthanide complex treats the system as a "black box" in which the internal process is not considered explicitly. Given that the complex absorbs a photon (i.e. the antenna is excited), the overall quantum yield can be defined as follows (Comby *et al.* 2004; Xiao and Selvin 2001; Quici *et al*. 2005):

$$\Phi_{overall} = \Phi_{sen}\,\Phi_{Ln} \qquad (1)$$

Here, Φ_{sen} represents the efficiency of the energy transfer from the ligand to the Ln^{3+} ion and Φ_{Ln} represents the intrinsic quantum yield of the Ln^{3+} ion, which can be calculated as from the following equation.

$$\Phi_{Ln} = \left(\frac{A_{RAD}}{A_{RAD} + A_{NR}} \right) = \frac{\tau_{obs}}{\tau_{RAD}} \qquad (2)$$

In the case of the Eu^{3+} complex **2**, the radiative lifetime (τ_{RAD}) can be calculated using Equation (3) (Kim *et al.* 2006; Viswanathan and de Bettencourt-Dias 2006), assuming that the energy of the $^5D_0 \rightarrow {}^7F_1$ transition (MD) and its oscillator strength are constant.

$$A_{RAD} = \frac{1}{\tau_{RAD}} = A_{MD,0}\ n^3\left(\frac{I_{TOT}}{I_{MD}}\right) \qquad (3)$$

Hence, $A_{MD,0}$ (14.65 s^{-1}) represents the spontaneous emission probability of the $^5D_0 \rightarrow {}^7F_1$ transition in vacuo, I_{TOT}/I_{MD} is the ratio of the total area of the Eu^{3+} emission spectrum to the area of the $^5D_0 \rightarrow {}^7F_1$ band and n is the refractive index of the medium. An average index of refraction equal to 1.5 was employed in the calculation (Pavithran *et al.* 2006). The intrinsic quantum yield for Tb^{3+} (Φ_{Tb}) was estimated by means of Equation 4 with the assumption that the decay process at 77 K in a deuterated solvent is purely radiative (Biju *et al.* 2009; Nasso *et al.* 2008; Sabbatini *et al.* 1993).

$$\Phi_{Tb} = \frac{\tau_{obs(298K)}}{\tau_{RAD\ (77K)}} \qquad (4)$$

The overall quantum yields ($\Phi_{overall}$), radiative (A_{RAD}) and nonradiative (A_{NR}) decay rates, intrinsic quantum yields (Φ_{Ln}) and energy transfer efficiencies (Φ_{sen}) for complexes **1** and **2** are presented in Table 2.3. In the solid state, the overall quantum yields for these complexes were determined according to the absolute method of Wrighton *et al*. (De Mello 1997; Wrington *et al*. 1974) and are correlated with the values obtained by relative method. A remarkably high quantum yield value of 82% has been observed for the Tb^{3+}-4-(dibenzylamino)benzoate complex **1**. This large value is particularly surprising in view of the presence of four H_2O molecules in the first coordination sphere,

since such solvent molecules typically serve as vibrational deactivators of the excited states of Ln^{3+} ions.

Table 2.3. Radiative (A_{RAD}) and nonradiative (A_{NR}) decay rates, $^5D_0/^5D_4$ lifetimes (τ_{obs}), radiative lifetimes (τ_{RAD}), intrinsic quantum yields (Φ_{Ln}), energy transfer efficiencies (Φ_{sen}), and overall quantum yields ($\Phi_{overall}$) for complexes **1** and **2.**

Complex	A_{RAD}/s^{-1}	A_{NR}/s^{-1}	$\tau_{obs}/\mu s$	$\tau_{RAD}/\mu s$	Φ_{Ln} (%)	Φ_{sen} (%)	$\Phi_{overall}$ (%)
1	---	---	1020 ± 0.8	1040 ± 0.8	98	84	82 ± 8[a]
						87	85 ± 8[b]
2	212	2812	330 ± 1	4720 ± 1	7.0	0.14	< 0.01[b]

[a] Absolute quantum yield; [b] Relative quantum yield

Only a few Tb^{3+} complexes have been reported to exhibit higher quantum yields in the solid state (Feidler *et al*. 2007; Zucchi *et al*. 2009; Kajiwara *et al*. 2008). Recently, our group reported another case of a high quantum yield (72%) for a 4-isobutyryl-3-phenyl-5-isoxazolonate complex of Tb^{3+} that also features solvent molecules in the primary coordination sphere (Biju *et al*. 2009). The energy gap between the luminescent state and the ground state manifold is approximately 12000 cm^{-1} for Eu^{3+} and 14800 cm^{-1} for Tb^{3+}. Relatively efficient coupling of the Eu^{3+} excited states occurs to the third vibrational overtone of proximate O–H oscillators ($\nu_{OH} \sim 3300–3500\ cm^{-1}$), and to the fourth harmonic in the case of Tb^{3+}, which is consistent with the observation of less efficient quenching for Tb^{3+}, when the Franck–Condon overlap factor is less favourable (Beeby *et al.* 1999; Døssing 2005).

It is well recognized that the energy-level match between the triplet states of the ligands to the ^5D_J state of the Ln^{3+} cation is one of the key factors that governs the luminescence efficiency of Ln^{3+} complexes (Shi *et al.* 2005; Xin *et al.* 2004). Latva's empirical rule states that an optimal ligand-to-metal energy transfer process for Ln^{3+} requires ΔE ($^3\pi\pi^*$– $^5D_4$) = 2500–4500 cm^{-1} for Tb^{3+} and 2500–4000 cm^{-1} for Eu^{3+} (Latva *et al.* 1997). On this basis it can be concluded that the energy transfer to the Tb^{3+} ion will be more effective for the ligand 4-(dibenzylamino)benzoic acid, since ΔE ($^3\pi\pi^*$– $^5D_4$) for **1** is 3140 cm^{-1}. The very high intrinsic quantum yield (Φ_{Ln}) and energy transfer efficiency (Φ_{sen}) for complex **1** further confirms the view that 4-(dibenzylamino)benzoic acid is an efficient sensitizer for the Tb^{3+} ion. Poor luminescence efficiency ($\Phi_{overall} < 0.01$) is also apparent in complex **2**, and may be due to the weak sensitization efficiency (Φ_{sen} = 0.14%) of 4-(dibenzylamino)benzoic acid with respect to the Eu^{3+} ion. The latter observation can be explained on the basis of the large energy gap between the triplet state of the ligand (6340 cm^{-1}) and the $^5D_0$ emitting level of the Eu^{3+} ion (17300 cm^{-1}).

2.5. CONCLUSIONS

- Three new binuclear lanthanide complexes of general formula $[Ln_2(L)_6(H_2O)_4]$ (Ln = Tb (**1**), Eu (**2**) and Gd (**3**)) supported by the novel aromatic carboxylate ligand 4-(dibenzylamino)benzoic acid (HL) have been synthesized, characterized and their photophysical properties were investigated.

- The single-crystal X-ray structures of novel $[Ln_2(L)_6(H_2O)_4]$ (Ln = Tb (**1**) and Eu (**2**)) complexes was established.
- Compounds **1** and **2** crystallize in the triclinic space group *P*ī and their molecular structures consist of homodinuclear species that are bridged by carboxylate ligands in different coordination modes.
- The complexes possess intermolecular hydrogen bonding interactions forming a 1D array.
- The sensitization mechanism for the complexes involves a usual triplet pathway, in which the transfer of energy absorbed by the ligand to the metal ion takes place from the ligand-centered triplet excited state.
- The Tb^{3+} complex **1** exhibits high green luminescence efficiency in the solid state with a quantum yield of 82%.
- On the other hand, poor luminescence efficiency has been noted for Eu^{3+}-4-(dibenzylamino)benzoate complex.

CHAPTER 3

Highly Luminescent and Thermally Stable Lanthanide Coordination Polymers Designed from 4-(Dipyridin-2-yl)aminobenzoate: Efficient Energy Transfer from Tb^{3+} to Eu^{3+} in a Mixed Lanthanide Coordination Compound

3.1. ABSTRACT

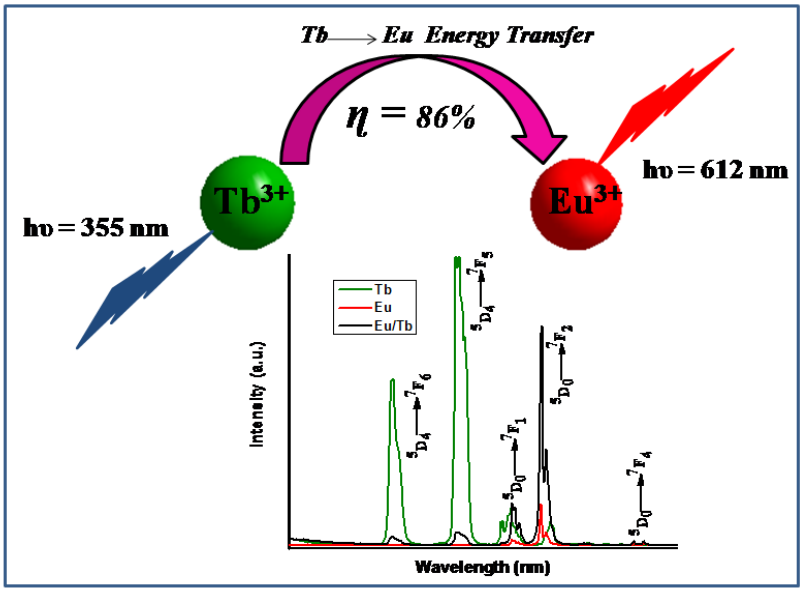

Herein, a new aromatic carboxylate ligand, namely, 4- (dipyridin-2-yl)aminobenzoic acid (HL), has been designed and employed for the construction of a series of lanthanide complexes (Eu^{3+} = **1**, Tb^{3+} = **2** and Gd^{3+} = **3**). Complexes **1** , **2** and **3** were structurally authenticated by single-crystal X-ray diffraction and were found to exist as infinite 1D coordination polymers with the general formulas $\{[Eu(L)_3(H_2O)_2]\}_n$ (**1**), $\{[Tb(L)_3(H_2O)]\}_n$ (**2**) and $\{[Gd(L)_3(H_2O)_2]\}_n$ (**3**). All the compounds crystallize in monoclinic space group C2/c. The photophysical properties demonstrated that the developed 4-(dipyridin-2-yl)aminobenzoate ligand is well suited for the sensitization of Tb^{3+}

emission ($\Phi_{overall}$ = 64%), thanks to the favourable position of the triplet state ($^3\pi\pi^*$) of the ligand [the energy difference between the triplet state of the ligand and the excited state of Tb^{3+} (ΔE) = $^3\pi\pi^* - {}^5D_4$ = 3197 cm^{-1}], as investigated in the Gd^{3+} complex. On the other hand, the corresponding Eu^{3+} complex shows weak luminescence efficiency ($\Phi_{overall}$ = 7%) due to poor matching of the triplet state of the ligand with that of the emissive excited states of the metal ion (ΔE = $^3\pi\pi^* - {}^5D_0$ = 6447 cm^{-1}). Furthermore, in the present work, a mixed lanthanide system featuring Eu^{3+} and Tb^{3+} ions with the general formula $\{[Eu_{0.5}Tb_{0.5}(L)_3(H_2O)_2]\}_n$ (**4**) was also synthesized, and the luminescent properties were evaluated and compared with those of the analogous single-lanthanide ion systems (**1** and **2**). The lifetime measurements for **4** strongly support the premise that efficient energy transfer occurs between Tb^{3+} and Eu^{3+} in a mixed lanthanide system (η = 86%).

Ramya, A. R.; Sharma, D.; Natarajan, S.; Reddy, M. L. P. *Inorganic Chemistry*., **2012**, *51*, 8818-8826.

3.2. INTRODUCTION

Carboxylate ligands are highly complementary toward lanthanide metal ions because of the oxophilic nature of the later (Busskamp *et al.* 2007; Deacon *et al.* 2007; Hilder *et al.* 2009). Accordingly, lanthanide benzoates and their derivatives are stable and have attracted considerable attention for their potential use in a wide variety of fields because of their novel luminescent and magnetic properties (Lam *et al.* 2003; Li *et al.* 2006; Lucky *et al.* 2011). In particular, when modified with light-harvesting moieties, benzoates have proven to be efficient sensitizers for lanthanide ions (Li *et al.* 2005; Viswanathan and de-Bettencourt-Dias 2006; Hilder *et al*. 2011). In the second chapter, it was demonstrated that replacement of the hydrogen atoms of the NH_2 moiety of p-aminobenzoic acid by benzyl groups had a significant influence on the distribution of the π-electron density within the ligand system and resulted in the development of a novel solid-state photosensitizer for Tb^{3+} with an overall quantum yield of 82% (Ramya *et al.* 2010). Subsequent investigations from our group also revealed that the presence of electron-releasing or -withdrawing groups on position 3 of the 4-benzyloxybenzoic acid ligand has a profound effect on the π-electron density of the ligands and consequently on the photosensitization of Ln^{3+} ions. Specifically, the presence of a methoxy substituent in this position results in a significant improvement in the photoluminescence (PL) efficiency of the terbium($^{3+}$) 3-methoxy-4-benzyloxybenzoate complex in comparison with that of the 4-benzyloxybenzoate complex (10 − 33%). By contrast, the introduction of a nitro group in the 3 position dramatically diminishes the PL efficiency of the

terbium($^{3+}$) 3-nitro-4-benzyloxybenzoate complex because of the presence of a channel that permits dissipation of the excitation energy *via* the π^*-n transition of the nitro group in conjunction with the intraligand charge-transfer (ILCT) band (Sivakumar *et al.* 2010). Our latest communication disclosed that the replacement of high-energy C−H vibrations with fluorinated phenyl groups in 3,5-bis(benzyloxy)benzoate effectively improves the luminescence intensity and lifetimes of lanthanide complexes (Sivakumar and Reddy. 2012). Inspired by the efficient sensitization of various lanthanide benzoates, herein, we have synthesized a new ligand, namely, 4-(dipyridin- 2-yl)aminobenzoic acid, (Figure 3.1) and utilized it for support of a series of new lanthanide coordination polymers featuring Eu^{3+}, Gd^{3+}, and Tb^{3+} cations. The designed 4-(dipyridin-2-yl)- aminobenzoate complexes of lanthanides were structurally characterized by single-crystal X-ray diffraction. The luminescent properties of the designed lanthanide benzoates have been systematically investigated and correlated with the triplet energy level of the newly developed benzoate molecule.

Energy-transfer processes involving two lanthanide ions in heterodinuclear complexes have been widely studied because they are proving useful in the design of miniature laser devices (Froidevaux and Bünzli 1994; Bettinelli and Flint 1990; Kellendonk and Blase 1981; Kim Anh and Strek 1988; Biju *et al.* 2009). Heterometallic lanthanide complexes are popular as they are potentially able to incorporate interesting luminescent properties by judicious choice of metal centers. Remarkable enhancements and quenching of the photoluminescent emissions have been found recently in various mixed lanthanide coordination polymers (Choi *et al.* 2011; Comby *et al.* 2006; Guo *et*

al. 2010). Cahill and co-workers reported terbium sensitization of europium in heterolanthanide coordination polymers (de Lill *et al*. 2007). The tunable emission of a widely varied family of lanthanide coordination polymers based on lanthanide terephthalate has been investigated, and it is proposed that Tb^{3+} can assist sensitization of Eu^{3+} (Kerbellec *et al*. 2009). Exploration of PL from polymer solid solutions has just started to emerge. Herein, we report energy transfer from 4-(dipyridin-2-yl)aminobenzoate-sensitized Tb^{3+} to Eu^{3+} in coordination polymers.

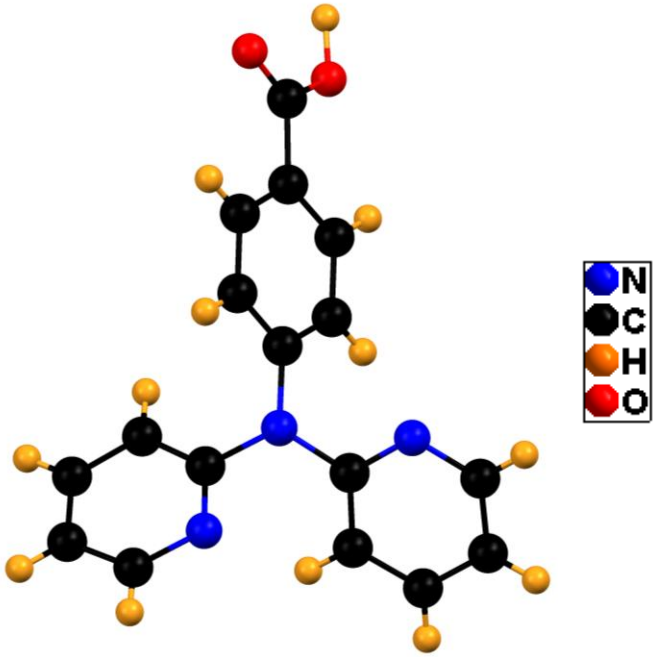

Fig. 3.1. Structure of the ligand 4-(Dipyridin-2-yl)aminobenzoic acid.

3.3. EXPERIMENTAL SECTION

3.3.1. Materials

Europium(III) nitrate hexahydrate, 99.9%, terbium(III) nitrate hexahydrate, 99.9% and gadolinium(III) nitrate hexahydrate, 99.9% were procured from Triebacher. Methyl 4-aminobenzoate, 98% and 2-bromopyridine, 99.9% were

purchased from Sigma-Aldrich and used without further purification. All the other chemicals used were of analytical reagent grade.

3.3.2. Characterization and spectroscopic techniques

Powder X-ray diffraction (XRD) patterns were recorded in the 2θ range of 10−70° using Cu Kα radiation (Philips X′pert). The quantitative microanalysis of the mixed lanthanide complex was carried out on an energy-dispersive spectrometer (Technai G^2 30LaB_6, ST with EDAX). UV−vis absorption spectra were recorded with a Shimadzu UV-2450 UV−vis spectrophotometer. All spectra were corrected for the background spectrum of the solvent. The absorbances of the ligand and complexes were measured in a CH_3CN/water mixture.

The single-crystal XRD data of complexes **1** and **2** were collected with a Bruker AXS Smart Apex CCD diffractometer at 293 K. The X-ray generator was operated at 50 kV and 35 mA using Mo Kα (λ = 0.71073 Å) radiation. The data were reduced using *SAINT+* (SMART 1994), and an empirical absorption correction was applied using the *SADABS* program (Sheldrick 1994). The structure was solved and refined by using *SHELXL−97* in the *WINGX* suit of programs (v.1.63.04a) (Sheldrick 1997). All of the hydrogen positions were initially located in the difference Fourier maps, and for the final refinement, the hydrogen atoms were placed in geometrically ideal positions and refined in the riding mode. Final refinement included the atomic positions of all of the atoms, anisotropic thermal parameters for all of the non-hydrogen atoms, and isotropic thermal parameters for all of the hydrogen atoms. Full-matrix least-squares refinement against F^2 was carried out using the *WINGX* package of programs

(Farrugia 1999). The X-ray diffraction data for ligand and complex **3** was collected on a Rigaku AFC-12 Saturn 724+ CCD diffractometer equipped with a graphite-monochromated Mo Kα radiation source (λ = 0.71073 Å) and a Rigaku XStream low temperature device cooled to 100 K. Corrections were applied for Lorentz and polarization effects. The structure was solved by direct methods and refined by full-matrix least-squares cycles on F^2 using the Siemens *SHELXTL PLUS 5.0* (PC) (Pflugrath 1999) software package and PLATON. All non-hydrogen atoms were refined anisotropically, and the hydrogen atoms were placed in fixed, calculated positions using a riding model. The CCDC numbers for the ligand and complexes **1**–**3** are 980347, 904386, 904387 and 975130 respectively. All other characterization techniques are discussed in chapter 2.

3.3.3. Synthesis and characterization of the ligand

3.3.3.1. Synthesis of Methyl 4-(di(pyridin-2-yl)amino)benzoate. The ester methyl 4-(di(pyridin-2-yl)amino)benzoate was synthesized by a modified procedure reported elsewhere (Kirin *et al*. 2007). Potassium carbonate (1g,), potassium iodide (0.1 g), $CuSO_4.5H_2O$ (0.1 g) and 1,10-phenanthroline (0.1 g) were added to a solution of methyl 4-amino benzoate (1 g, 6.6 mmol) in toluene (50 mL) followed by the addition of 2-bromopyridine (1.25 mL, 13.03 mmol). The resulting reaction mixture was refluxed for 24 h at 150 °C and the solvents were evaporated to dryness. The residue was then dissolved in dichloromethane and washed with water. The resulting aqueous layer was further extracted with dichloromethane and the combined organic extracts were dried with sodium sulphate, filtered and evaporated at reduced pressure.

The resulting residue obtained was purified by silica gel column chromatography using hexane/ethyl acetate, thereby affording the desired product as an off- white solid. Yield, 0.8 g (42%). ^{1}H NMR (500 MHz, $CDCl_3$): δ (ppm) 8.29 (m, 2H, Ar–H), 7.92 (d, 2H, J = 8.5 Hz, Ar–H), 7.54 (m, 2H, Ar–H), 7.10 (d, 2H, J = 9 Hz, Ar–H), 6.94 (m, 4H, Ar–H), 3.83 (s, 3H, $-OCH_3$). ^{13}C NMR (125 MHz, $CDCl_3$): δ (ppm) 165.56, 156.65, 148.31, 147.86, 136.92, 129.95, 124.80, 123.90, 118.20, 116.92, 50.96. FAB-MS: m/z = 306.61 $(M+1)^+$. FT-IR (KBr): ν_{max} 1715 (ν_{as}(C=O)), 1587, 1465 (ν_s(C=O)), 1430, 1289, 1172, 1106, 769, 703, 522 cm^{-1}.

3.3.3.2. Synthesis of 4-(Di(pyridin-2-yl)amino)benzoic acid (HL). Methyl 4-(di(pyridin-2-yl)amino)benzoate (0.8 g, 2.62 mmol) was stirred at room temperature for 24 h in a 50 mL methanolic solution of NaOH (0.63 g, 5.75 mmol). The reaction mixture was poured into ice cold water, and acidified with dilute HCl, and the resulting precipitate was filtered, washed, dried, and recrystallized from dichloromethane (Scheme 3.1). Yield, 0.6 g (77%). ^{1}H NMR (500 MHz, $CDCl_3$): δ (ppm) 8.40 (m, 2H, Ar–H), 7.93 (d, 2H, J = 8.5 Hz, Ar–H), 7.64 (m, 2H, Ar–H), 7.17 (d, 2H, J = 8.5Hz, Ar–H), 7.05 (m, 4H, Ar–H). ^{13}C NMR (125 MHz, $CDCl_3$): δ (ppm) 169.52, 157.49, 149.24, 148.69, 138.21, 131.60, 126.23, 125.28, 119.33, 118.07. FAB-MS: m/z = 292.59 $(M+1)^+$. Elemental analysis (%): Calcd (found) for $C_{17}H_{13}O_2N_3$ (291.31): C, 70.09 (70.05) ; H, 4.50 (4.31); N, 14.42 (14.22). FT-IR (KBr) ν_{max}: 1699 (ν_{as}(C=O)), 1598, 1466, 1434 (ν_s(C=O)), 1286, 1172, 1009, 770, 741, 520 cm^{-1}.

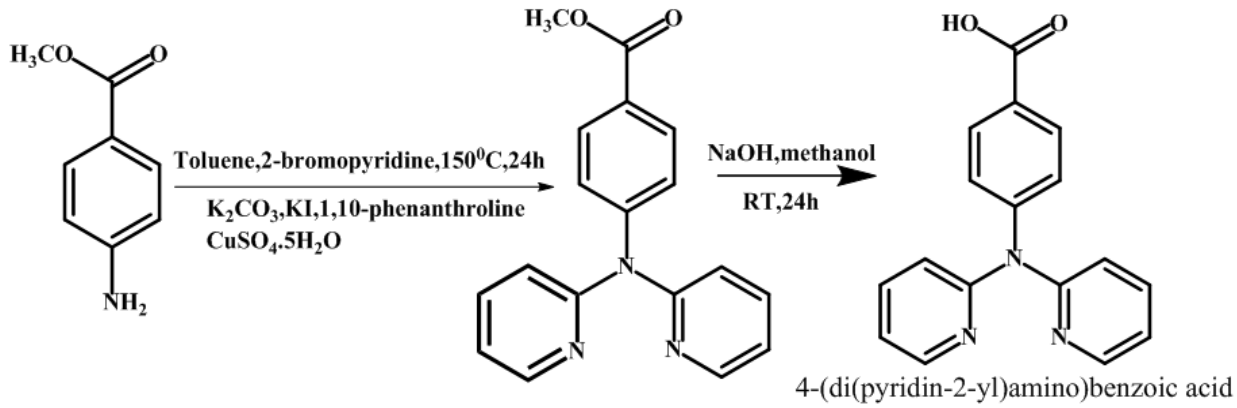

Scheme 3.1. Synthesis of ligand, HL.

3.3.4. Syntheses of lanthanide complexes. All metal complexes were prepared in a similar manner in air by mixing stoichiometric amounts of ligand (1.5 mmol) and $Ln(NO_3)_3{\cdot}6H_2O$ (0.5 mmol; Ln = Eu, Tb, or Gd) in ethanol in the presence of NaOH (1.5 mmol). Precipitation took place immediately, and the reaction mixture was stirred subsequently for 12 h at room temperature. The crude product was filtered, washed with ethanol and dried. The resulting complexes were then purified by recrystallization from a dichloromethane/methanol solvent mixture. Single crystals of the terbium and europium complexes suitable for single-crystal X-ray study were obtained from an ethanol/water solvent mixture after storage for 4 weeks at room temperature.

$[Eu(L)_3(H_2O)_2](H_2O)$ (1). Elemental analysis(%): Calcd (found) for $C_{51}H_{42}N_9O_9Eu$ (1076.91) : C, 56.88 (56.66); H, 3.93 (3.66); N, 11.70 (11.45). FT-IR (KBr): ν_{max} 3402 (ν(O–H)), 1643 (ν_{as}(C=O)), 1594 (ν_{as}(C=O)), 1469, 1426

(ν_s(C=O)), 1400 (ν_s(C=O)), 1321, 1274, 1154, 773 cm^{-1}. FAB-MS: m/z = 1022.22 $[Eu(L)_3]^+$.

$[Tb(L)_3(H_2O)](H_2O)$ (2). Elemental analysis (%): calcd (found) for $C_{51}H_{40}N_9O_8Tb$ (1065.86) : C, 57.46 (57.33); H, 3.78 (3.81); N, 11.82 (11.60). FT-IR (KBr): ν_{max} 3391 (ν(O–H)), 1643 (ν_{as}(C=O)), 1594 (ν_{as}(C=O)), 1469, 1424 (ν_s(C=O)), 1404 (ν_s(C=O)), 1321, 1274, 1154, 773 cm^{-1}. FAB-MS: m/z = 1046.64 $[Tb(L)_3.(H_2O)]^+$.

$[Gd(L)_3(H_2O)_2]$ (3). Elemental analysis (%): calcd (found) for $C_{51}H_{40}N_9O_8Gd$ (1063.75) : C, 57.57 (57.45); H, 3.79 (3.81); N, 11.85 (11.74). FT-IR (KBr): ν_{max} 3409 (ν(O–H)), 1643 (ν_{as}(C=O)), 1594 (ν_{as}(C=O)), 1468, 1428 (ν_s(C=O)), 1402 (ν_s(C=O)), 1294, 1153, 774 cm^{-1}. FAB-MS: m/z = 1046.83 $[Gd(L)_3.(H_2O)+1]^+$.

$[Eu_{0.5}Tb_{0.5}(L)_3(H_2O)_2]$ (4). Elemental analysis (%): calcd (found) for $C_{51}H_{40}N_9O_8Eu_{0.5}Tb_{0.5}$ (1062.38): C, 57.66 (57.49); H, 3.79 (3.57); N, 11.86 (12.00). FT-IR (KBr): ν_{max} 3401 (ν(O–H)), 1646 (ν_{as}(C=O)), 1595 (ν_{as}(C=O)), 1469, 1428 (ν_s(C=O)), 1405 (ν_s(C=O)), 1320, 1274, 1153, 854, 773 cm^{-1}. FAB-MS: m/z = 1041.36 $[Eu(L)_3.(H_2O)+1]^+$, 1028.85 $[Tb(L)_3]^+$. The 1:1 molar ratios of Tb^{3+}/Eu^{3+} in a mixed Ln^{3+} complex were further confirmed by energy-dispersive spectrometry (EDS) analysis (Eu / Tb = 1.02).

3.4. RESULTS AND DISCUSSION

3.4.1. Synthesis and characterization of ligand and Ln^{3+} complexes 1-4

The ligand 4-(di(pyridin-2-yl)amino)benzoic acid (HL) was synthesized (yield: 77%) in two steps starting from commercially available 4-aminobenzoate, as outlined in Scheme 3.1. The newly designed ligand was identified on the basis of ^{1}H and ^{13}C NMR spectroscopy, FAB-MS, FT-IR, and elemental analysis. The protocols used for the syntheses of lanthanide 4-(di(pyridin-2-yl)amino)benzoate complexes are summarized in the Experimental Section. The elemental analysis data of the complexes revealed that in each case the Ln^{3+} ion had reacted with the corresponding benzoate ligand in a metal-to-ligand mole ratio of 1:3. The FT-IR spectrum of the ligand evidenced intense absorption bands characteristic of the carboxylate groups at 1434 and 1699 cm^{-1}, which are assigned to the symmetric ν_s(C=O) and asymmetric ν_{as}(C=O) vibrations, respectively (Table 3.1). These bands in the spectrum of the free ligand, which are assigned to the stretching vibrations of the nonionised carboxylic group, are shifted in the FT-IR spectra of **1**–**4**, thus confirming that the ligand is completely ionised and, hence, in accordance with the single crystal X-ray structures. Moreover, the symmetric and asymmetric stretching vibrational modes of the carboxylate groups in complexes **1**–**4** are further split into two peaks. The differences between the asymmetric and symmetric stretching vibrational modes ($\Delta\nu_{(C=O)} = \nu_{as} - \nu_s$) fall in the ranges 239-243 cm^{-1} and 166-170 cm^{-1}, which

indicates that carboxylate groups are coordinated to Ln^{3+} ions in bidentate bridging and chelating modes (Deacon and Phillips. 1980; Raphael *et al.* 2008; Teotonio *et al.* 2005). The broad band observed at 3400 cm^{-1} for complexes **1**–**4** is attributed to the characteristic ν_{OH} stretching vibration and is indicative of the presence of water molecules.

Table 3.1. Infra-red vibrational frequencies for the carboxylate functionalities of the ligand and complexes **1**–**4**.

	υ_{as}(C=O) cm^{-1}	υ_{s}(C=O) cm^{-1}	$\Delta\upsilon$(C=O) cm^{-1}
HL	1699	1434	----
1	1643, 1594	1426, 1400	243, 168
2	1643, 1594	1424, 1404	239, 170
3	1643, 1594	1428, 1402	241, 166
4	1646, 1595	1428, 1405	241, 167

The 1:1 molar ratios of Tb^{3+}/Eu^{3+} in a mixed Ln^{3+} complex **4** were further confirmed by EDS analysis (Eu/Tb = 1.02; Figure 3.2 and Table 3.2).

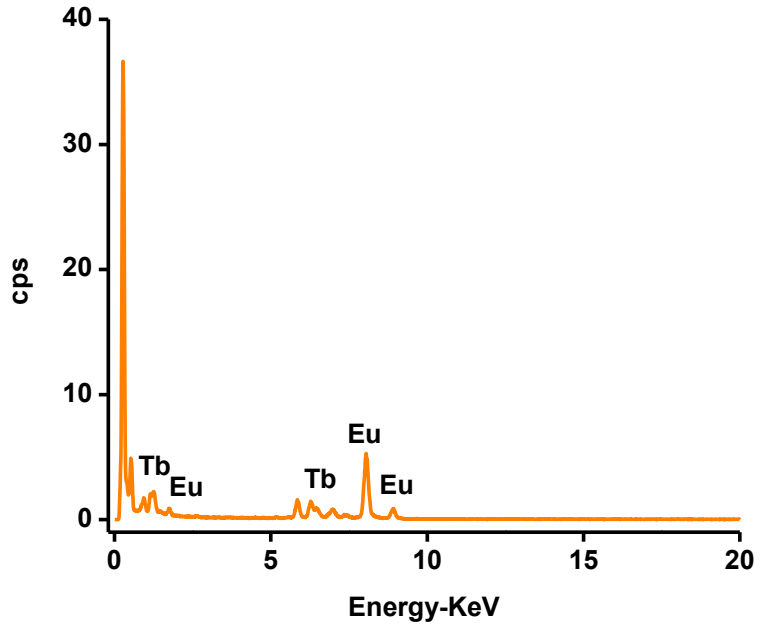

Figure 3.2. EDS spectrum of $\{[Eu_{0.5}Tb_{0.5}(L)_3(H_2O)_2]\}_n$ (**4**).

Table 3.2. EDS analysis results for the complex $\{[Eu_{0.5}Tb_{0.5}(L)_3(H_2O)_2]\}_n$ (**4**).

Complex	Element	Wt %	Eu/Tb molar ratio (EDS)	Eu/Tb molar ratio (cacld.)
$\{[Eu_{0.5}Tb_{0.5}(L)_3(H_2O)_2]\}_n$(4)	Eu	50.7	1.02	1
	Tb	49.3		

The powder XRD patterns of complexes **1–4** are similar to each other, thus implying that these complexes are isostructural (Figure 3.3).

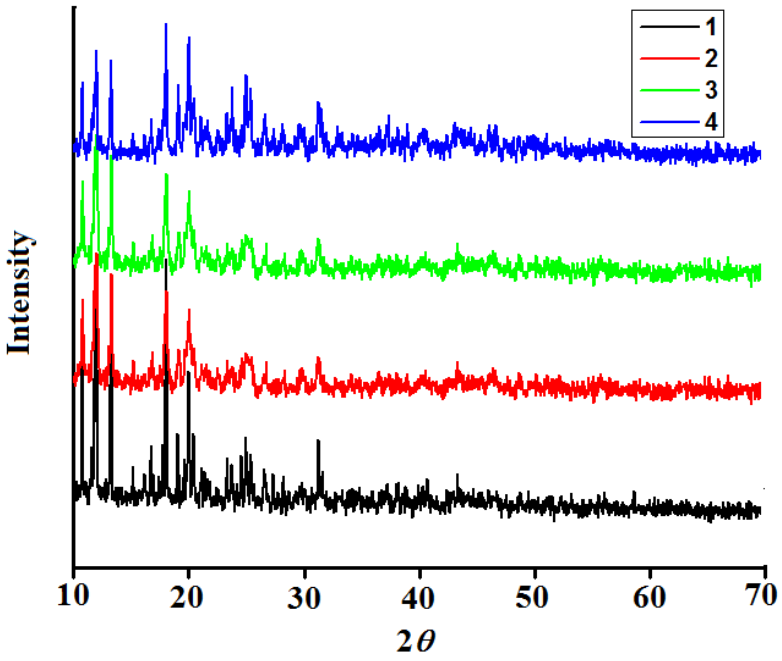

Figure 3.3. Powder XRD patterns for complexes **1**–**4**.

The thermal stabilities of complexes **1, 2,** and **4** were examined by TGA in the 30-1000 °C range, and the corresponding thermograms are depicted in Figure 3.4. It is interesting to note that compounds **1** and **2** are thermally stable up to ~ 450 °C, with a first weight loss between 90 and 200 °C in complex **1** (found, 4.70%**;** calcd, 5.01%), corresponding to the release of one uncoordinated and two coordinated water molecules. On the other hand, the loss of two water molecules was noted in the case of complex **2** (found, 3.40%**;** calcd, 3.38%) due to the elimination of one lattice and one coordinated water molecules. It can be noted from the thermogram of complex **4** that it is stable up to ~ 430 °C, with a first weight loss (found, 3.30%**;** calcd, 3.39%), which accounts for the elimination of two coordinated water molecules. The second weight loss, between 450 and 850 °C for complex **1** (found, 79.80%; calcd, 80.87%), is attributed to the thermal decomposition of three ligand molecules.

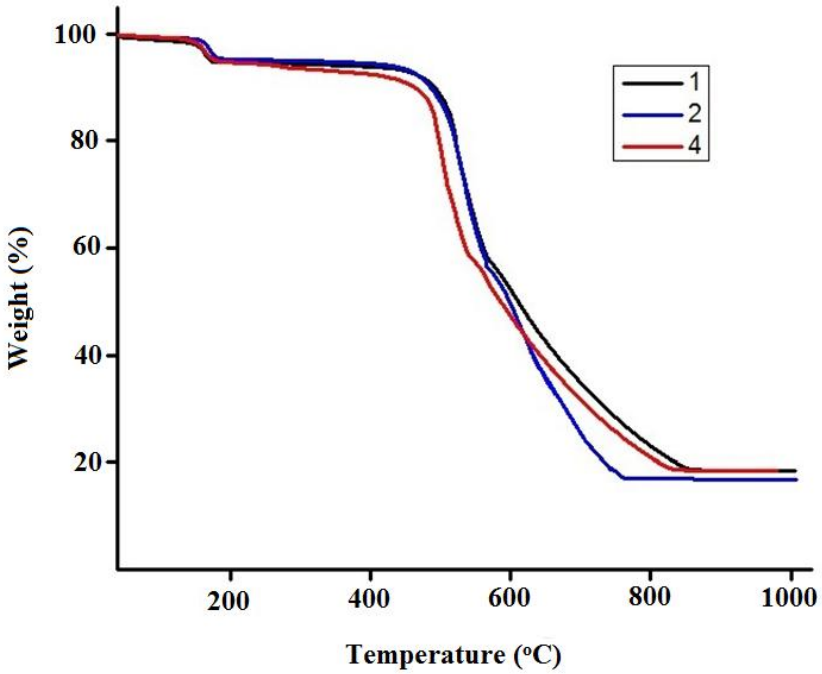

Figure 3.4. TG analysis of complexes **1, 2** and **4**.

On the other hand, in the case of complex **2,** the second weight loss noted between 450 and 770 °C (found, 81.90%; calcd, 81.71%) and the loss occuring between 450 and 850 °C (found, 81.20%; calcd, 81.98%) in complex **4** can also be due to the loss of three ligand moieties. The total weight losses are compatible with formulas, and the masses of the final products correspond to the complete combustion of the complexes to their corresponding metal oxides (Eu_2O_3 or Tb_4O_7). The differences observed in TGA of complexes **1** and **2** are essentially due to the different hydration states of the Ln^{3+} cations and also can be attributed to lanthanide contraction (Mahata *et al.* 2008; Soares-Santos *et al.* 2010).

3.4.2. X-ray crystal structures

Single-crystal X-ray diffraction studies reveal the 1D coordination polymeric nature of the complexes **1**, **2** and **3** (Figures 3.5, 3.6 and 3.7). However, these complexes have different coordination environments. The pertinent data collection parameters and a listing of significant bond distances and angles for both compounds are depicted in Tables 3.3 and 3.4, respectively. Compounds **1**, **2** and **3** crystallize in the monoclinic space group $C2/c$. The lanthanide centers in all the compounds are doubly bridged by carboxylate groups of the 4-(di(pyridin-2-yl)amino)benzoate ligands and thereby form infinite 1D chains. It is interesting to note that compound **2** forms a 1D wavelike strand; and on the other hand, compounds **1** and **3** form a straight chain. This may be due to the differences in their coordination environments. The Ln1 center of **1** and **3** are coordinated to four carboxylate oxygen atoms of the bridging 4-(di(pyridin-2-yl)amino)benzoate ligands, two carboxylate oxygen atoms of the chelating 4-(di(pyridin-2-yl)amino)benzoate ligand, and two water molecules. The coordination geometry around the Eu1 and Gd1 centres can be described as a distorted bicapped trigonal prism with O-Ln1-O bond angle ranging from 51.79° to 163.42° for Eu^{3+} and 52.14° to 162.99° for Gd^{3+}. In contrast to the Ln1 center in **1** and **3,** the Tb1 center of **2** is surrounded by seven oxygen atoms in a distorted pentagonal-bipyramidal arrangement with O-Tb1-O bond angles ranging from 53.69° to 156.2°. The Tb1 center in **2** is coordinated to four carboxylate oxygen atoms from the bridging benzoate ligands, two carboxylate oxygen atoms from the chelating benzoate ligand and one oxygen atom from the water molecule.

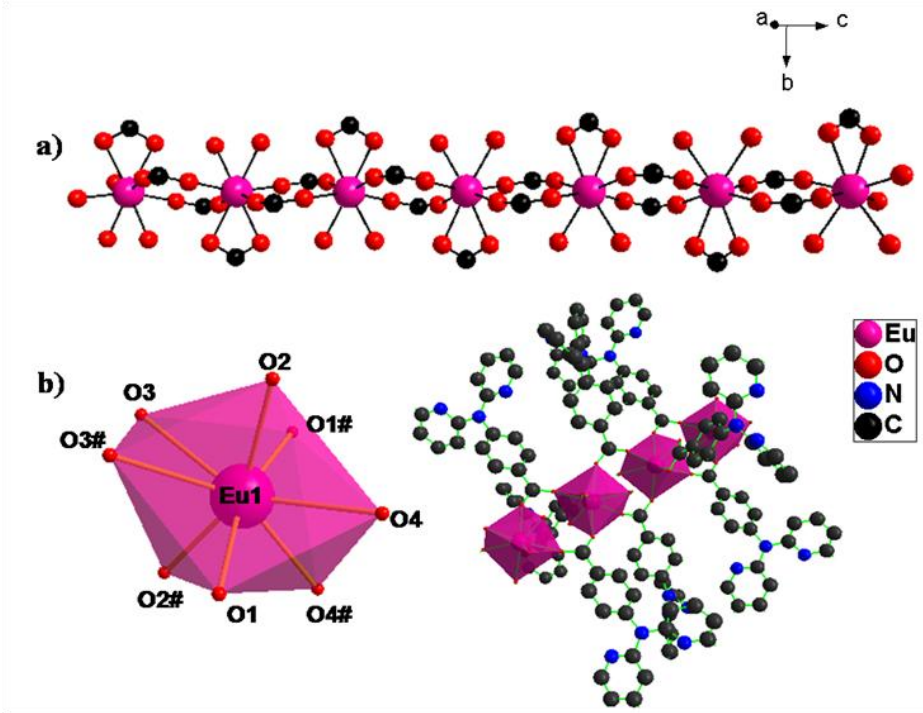

Figure 3.5. a) 1D coordination polymer chain of complex **1**. b) Coordination environment of complex **1.** All hydrogen atoms are omitted for clarity.

The longest Ln1-O bonds involve the oxygen atoms of the bidentate chelating ligands [Eu1–O(3): 2.514 Å; Eu1–O(3#): 2.514 Å; Tb–O(2): 2.428 Å; Tb–O(2#): 2.428 Å; Gd1–O(33): 2.502 Å; Gd1–O(33#): 2.502 Å] and the shortest bonds are associated with bridging carboxylate ligands [Eu–O(1): 2.312 Å; Eu–O(2): 2.330 Å; Eu–O(1#): 2.312 Å; Eu–O(2#): 2.330 Å; Tb–O(1): 2.240 Å; Tb–O(1#): 2.240Å; Tb–O(3): 2.325 Å; Tb–O(3#): 2.325 Å; Gd1–O(31): 2.318 Å; Gd1–O(27): 2.294 Å; Gd1–O(31#): 2.318 Å; Gd1–O(27#): 2.294 Å]. These trends in the distances are found to be same as those observed in lanthanide carboxylate complexes featuring bidentate chelating and bridging modes (Deacon *et al.* 2007; Liu *et al.* 2008). The carboxylate bridges also adopt a *syn-anti* confirmation in all the

three complexes to exhibit a Ln1-Ln1 distance of 5.122 Å in **1,** 5.278 Å in **2** and 5.109 Å in **3**.

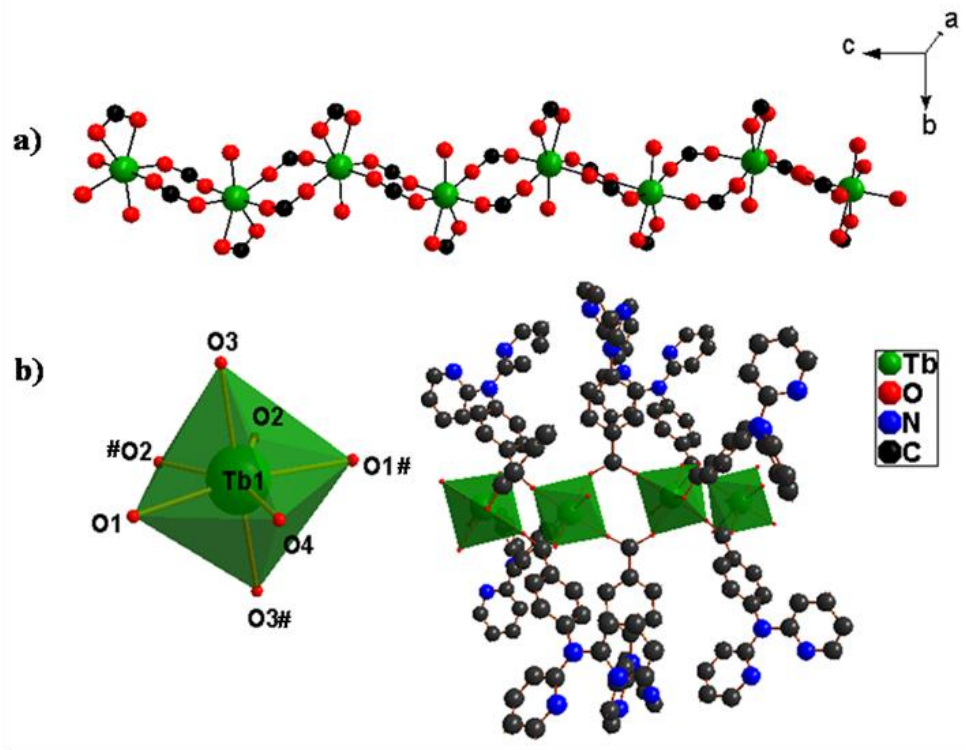

Figure 3.6. a) 1D coordination polymer chain of complex **2**. b) Coordination environment of complex **2.** All hydrogen atoms are omitted for clarity.

The distance between adjacent Tb centers is found to be larger than Eu1-Eu1 and Gd1-Gd1 distance. This can be attributed to the differences in their coordination environments in view of the presence of two inner sphere water molecules in complexes **1** and **3,** while complex **2** has only one. The most noteworthy structural features of these compounds are the presence of free Lewis basic pyridyl sites within the 1D coordination polymers, which may have a potential utility of these compounds for the recognition and sensing of metal ions.

Table 3.3. Crystallographic and refinement data for **1**–**3**.

	1	**2**	**3**
formula	$C_{51}H_{40}N_9O_8Eu$	$C_{51}H_{36}N_9O_9Tb$	$C_{51}H_{40}N_9O_8Gd$
fw	1058.88	1077.81	1064.17
cryst sys	Monoclinic	Monoclinic	Monoclinic
space group	C2/*c*	C 2/c	C2/*c*
cryst size	0.12 × 0.04 × 0.03	0.12× 0.03× 0.02	0.30× 0.20 × 0.20
Temp/K	296 K	293 K	300 K
a/(Å)	30.2598(9)	29.502(3)	30.229 (8)
b/(Å)	14.9444(4)	15.9006(10)	14.919(3)
c/(Å)	10.2439(3)	10.0813(8)	10.217(3)
α (°)	90	90	90
B (°)	102.862(1)	102.716(9)	102.947(3)
γ (°)	90	90	90
V/Å^3	4516.2(2)	4613.2(6)	4490.5(19)
Z	4	4	4
D_{calcd}, g cm^{-1}	1.557	1.552	1.574
μ/(Mo,Kα)mm^{-1}	1.457	1.602	1.545
F(000)	2144.0	2168.0	2148.0
R1 [*I*> 2σ(*I*)]	0.0178	0.0770	0.0282
w*R2* [*I*> 2σ(*I*)]	0.0448	0.1547	0.0651
R1 (all data)	0.0226	0.1070	0.0403
w*R2* (all data)	0.0475	0.1691	0.0709
gof	1.039	0.974	1.020

Table 3.4. Selected bond lengths (Å) and angles (°) for **1**– **3**.

1		**2**		**3**	
Eu1–Eu1	5.122	Tb1–Tb1	5.278	Gd1– Gd 1	5.109
Eu1–O1	2.312(2)	Tb1–O1	2.240(2)	Gd1–O27	2.294(19)
Eu1–O2	2.330(2)	Tb1–O2	2.428(2)	Gd1–O31	2.318(18)
Eu1–O3	2.514(2)	Tb1–O3	2.325(2)	Gd1–O33	2.502(17)
Eu1–O4	2.539(2)	Tb1–O4	2.349(2)	Gd1–O36	2.518(19)
Eu1–O1 #	2.312(2)	Tb1–O1#	2.240(2)	Gd1–O27 #	2.294(19)
Eu1–O2 #	2.330(2)	Tb1–O2#	2.428(2)	Gd1–O31 #	2.318(18)
Eu1–O3 #	2.514(2)	Tb1–O3#	2.325(2)	Gd1–O33 #	2.502(17)
Eu1–O4 #	2.539(2)			Gd1–O36 #	2.518(19)
O1– Eu1–O1	153.60(7)	O2–Tb1–O2	53.69(2)	O31– Gd1–O31	162.99(9)
O1– Eu1–O2	82.59(5)	O1–Tb1–O3	91.55(2)	O33– Gd1–O33	52.14(8)
O1– Eu1–O2	101.23(5)	O3–Tb1–O3	156.2(2)	O27– Gd1–O27	153.50(11)
O2– Eu1–O2	163.42(7)	O1–Tb1–O4	87.94(12)	O36– Gd1–O36	68.80(10)
O1–Eu1–O3	74.45(5)	O3–Tb1–O4	78.10(12)	O31– Gd1–O33	73.69(6)
O1–Eu1–O3	81.79(5)	O1–Tb1–O2	91.3(2)	O31– Gd1–O33	123.13(6)
O2–Eu1–O3	73.68(4)	O3–Tb1–O2	75.05(17)	O33– Gd1–O36	150.06(7)
O3–Eu1–O3	51.79(6)	O3–Tb1–O2	128.74(16)	O27– Gd1–O33	81.77(7)
O1–Eu1–O4	134.22(5)	O2–Tb1–O4	153.15(11)	O27– Gd1–O31	82.90(7)
O4–Eu1–O4	68.77(6)			O27– Gd1–O36	134.38(7)

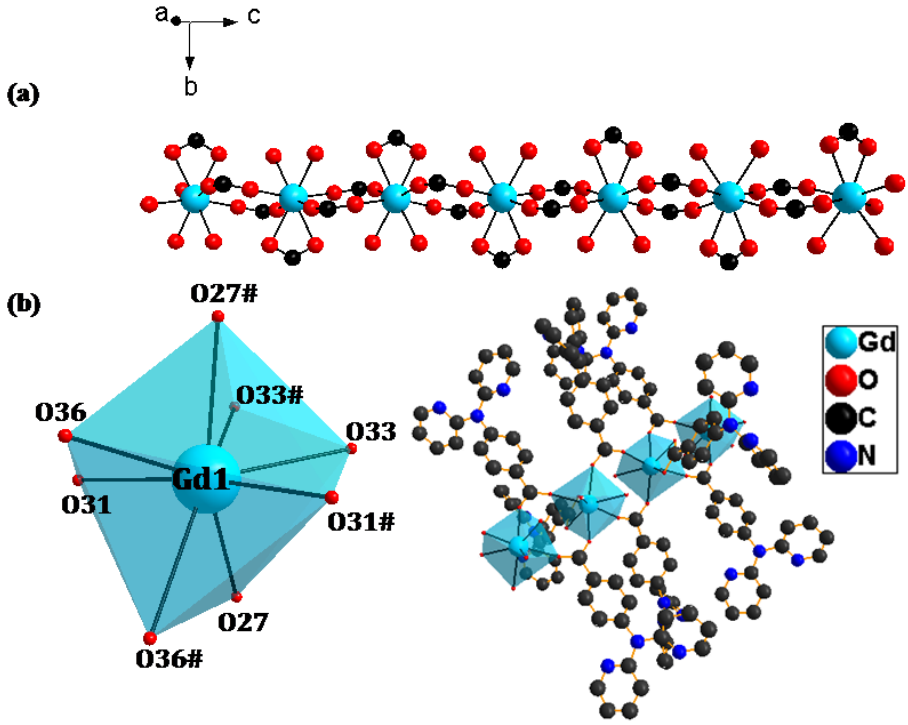

Figure 3.7. a) 1D coordination polymer chains of complex **3**. b) Coordination environment of complex **3**. All hydrogen atoms are omitted for clarity.

3.4.3. Electronic states of the ligand and complexes

The absorption spectra of the free ligand and the corresponding Ln^{3+} complexes (**1–4)** have been recorded in CH_3CN/water mixture (CH_3CN, 60%; water, 40%; *c* = 2 × 10^{-5} M) at 298 K and are depicted in Figure 3.8. The ligand displays an absorption band localized in the UV region with a molar absorption coefficient (ε_{max}) of 1.2 × 10^4 L mol^{-1} cm^{-1} (λ_{max} = 305 nm) that is classically observed for $\pi\pi^*$ transitions of benzoic acid ligands. The trends in the absorption spectra of the complexes are identical with those observed for the free ligand. The molar absorption coefficients of **1–4** are found to be 3.5 × 10^4, 3.7 × 10^4, 3.8 × 10^4 and 3.4 × 10^4 L mol^{-1} cm^{-1}, respectively, showing the strong ability of the complexes

to absorb light in the 250-350 nm region, with maxima at 305 nm. The absorption coefficients for the complexes are about 3 times higher compared that to the free ligand, in line with the formation of 3:1 (ligand/metal) complexes. These features point to the ligand being an adequate light-harvesting chromophore for the sensitization of lanthanide luminescence.

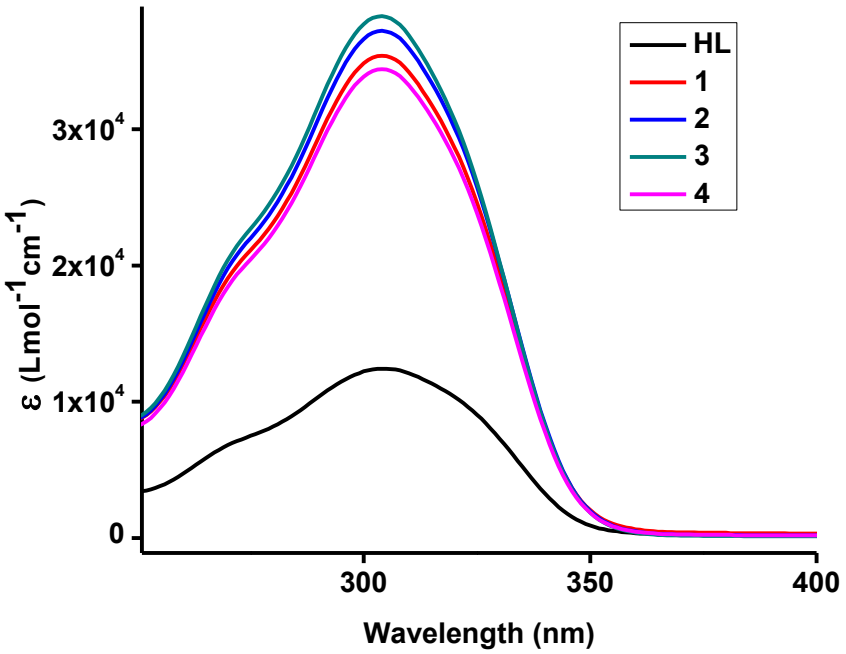

Figure 3.8. UV–vis absorption spectra of the ligand HL and complexes **1**–**4** in CH_3CN/water mixture (CH_3CN, 60%; water, 40%; c = 2 × 10^{-5} M).

3.4.4. Photophysical properties

In the present study, the Gd^{3+}-4-(di(pyridin-2-yl)aminobenzoate complex (**3**) has been utilized to probe the triplet energy level of the newly developed sensitizer 4-(di(pyridin-2-yl) amino)benzoate to assess its efficiency in the energy-transfer process to the lanthanides. It is widely recognized that Gd^{3+} complexes are a popular choice for elucidating triplet energy levels of the ligand for the following reasons: (1) Because of its heavy atom effect, the Gd^{3+} ion

increases the rate of intersystem crossing. (2) The first excited-state electronic levels of Gd^{3+} are at high energies (^5I_J at around 36900 cm^{-1}), there is no gadolinium emission in the visible range, and all luminescence observed is due to the ligand part of the complex. Thus, radiative decay from a triplet excited state becomes the predominant energy migration pathway. Compound **3** exhibits ligand phosphorescence as a broad band centered at 435 nm after excitation at 305 nm at 77 K (Figure 3.9). The triplet energy level ($^3\pi\pi^*$) of the ligand was estimated by reference to its lower-wavelength emission edge (422 nm; 23697 cm^{-1}) of the low-temperature phosphorescence spectrum of the Gd^{3+} complex **3**. It can be noted that the triplet energy level of the ligand is found to be higher than that of the emitting levels of both $^5D_4$ of Tb^{3+} or $^5D_0$ of Eu^{3+}, thus indicating that the designed ligand can act as antenna for the photosensitization of these Ln^{3+} ions (Latva *et al.* 1997). To elucidate the energy migration pathways in Ln^{3+} complexes, it was also necessary to determine the singlet energy level ($^1\pi\pi^*$) of the ligand. The singlet ($^1\pi\pi^*$) energy level of this ligand was determined by reference to the UV-vis upper absorption edge of the Gd^{3+} complex **3** (Figure 3.8) and the value was found to be 346 nm (28900 cm^{-1}). It is well documented that an efficient ligand-to-metal energy transfer requires a good intersystem crossing efficiency, which is maximized when the energy difference between singlet and triplet states, ΔE ($^1\pi\pi^* - {}^3\pi\pi^*$), is close to 5000 cm^{-1} (Steemers *et al.* 1995). Thus, in the present study it amounts to 5203 cm^{-1}, and therefore the newly developed ligand has a good intersystem-crossing efficiency.

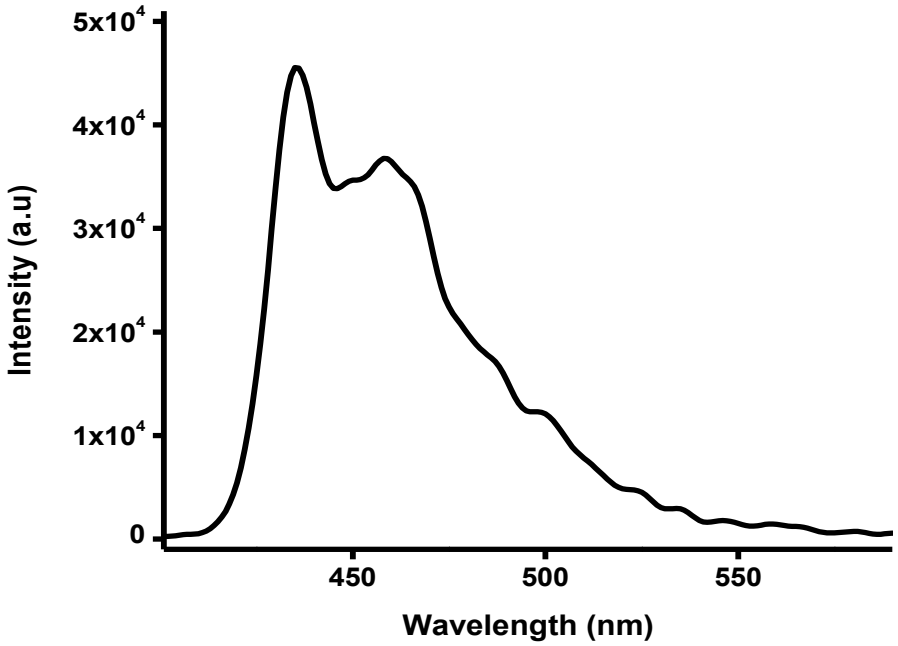

Figure 3.9. Phosphorescence spectrum of gadolinium complex **3** at 77 K.

The excitation spectrum of the Eu^{3+} complex **1** (in the solid state) at room temperature, monitored around the peak of the intense $^5D_0 \rightarrow {}^7F_2$ transition consists of a broad band and several narrow bands (Figure 3.10). The broad band peaking at 355 nm is attributed to the $\pi\pi^*$ ligand transition, and the narrow bands are assigned to transitions of the Eu^{3+} intra-$^4F_6$ ion, from $^7F_0$ to $^5L_6$ (394 nm), $^5D_3$ (414 nm), and $^5D_2$ (464 nm) levels (Armelao *et al.* 2010; Biju *et al.* 2006; Zhang *et al*. 2010; Wan *et* al. 2009). However, these transitions are weaker than the absorption of the organic ligand and are overlapped by a broad excitation band, which proves that luminescence sensitization *via* excitation of the ligand is much more efficient than the direct excitation of the Eu^{3+} ion absorption level. The emission spectrum of **1** was recorded under the maximum excitation wavelength at 355 nm. The emission spectrum is composed of the first excited state, $^5D_0$, and the ground septet, ^7F_J (J = 0–4) of Eu^{3+} (Divya *et al.*

2010; Francis *et al.* 2010; Raj *et al.* 2010). The transition $^5D_0 \rightarrow {}^7F_0$ is very weak and is situated at 582 nm. The moderately strong transition $^5D_0 \rightarrow {}^7F_1$ splits into three peaks at 589, 592 and 596 nm.

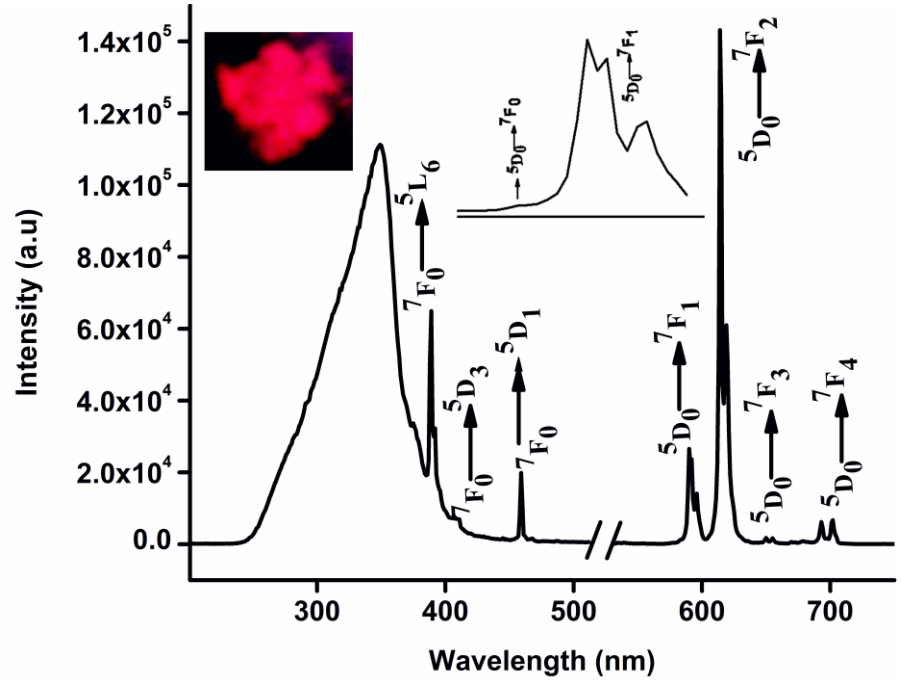

Figure 3.10. Room-temperature excitation and emission spectra for complex **1** (λ_{ex}= 355 nm) with emission monitored at approximately 612 nm.

The hypersensitive transition $^5D_0 \rightarrow {}^7F_2$ consists of a strong band at 614 nm, resulting in red luminescence. The peaks at about 650 and 656 nm correspond to the characteristic $^5D_0 \rightarrow {}^7F_3$ transition. It is also noted that four splitting peaks of the $^5D_0 \rightarrow {}^7F_4$ transition occurs at 693, 697, 701 and 705 nm.

The steady state excitation and emission spectra of Tb^{3+} complex **2** at room temperature are depicted in Figure 3.11. The excitation spectrum of **2** monitored around the peak of the intense $^5D_4 \rightarrow {}^7F_5$ transition of the Tb^{3+} ion displays a broad band between the 250–400 nm range with a maximum at

approximately 355 nm, which can be assigned to the $^1\pi\pi^*$ transition of the antenna molecule.

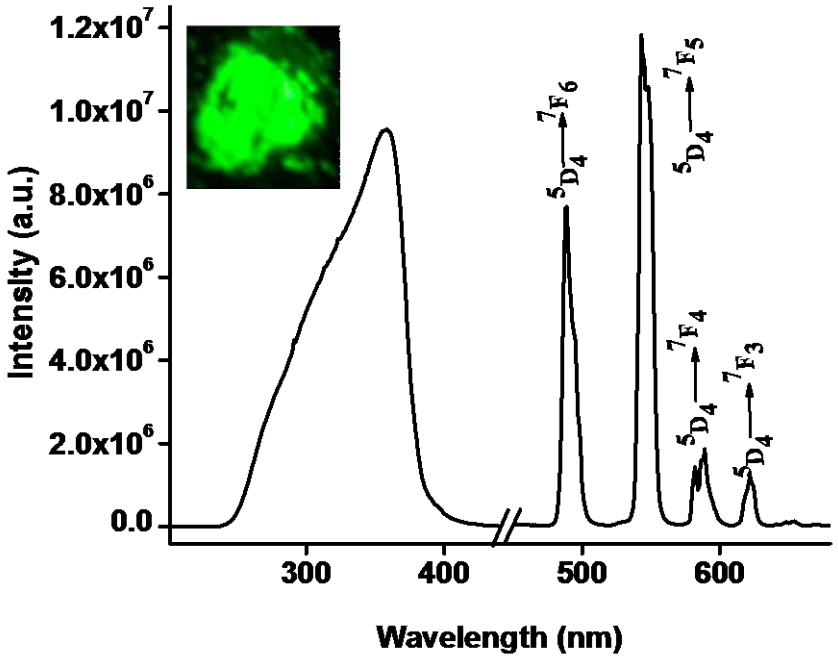

Figure 3.11. Room-temperature excitation and emission spectra for complex **2** (λ_{ex}= 355 nm) with emission monitored at approximately 545 nm.

The absence of any absorption bands due to the f–f transitions of the Tb^{3+} cation proves that luminescence sensitization *via* excitation of the ligand is more sensitive than the direct excitation of the Tb^{3+} ion. The room temperature emission spectrum of Tb^{3+} complex exhibits the characteristic emission bands of Tb^{3+} (λ_{ex}= 355 nm) centered at 490, 545, 585, and 620 nm, which result from deactivation of $^5D_4$ excited state to the corresponding ground state ^7F_J (J = 6, 5, 4, 3) of the Tb^{3+} ion (Biju *et al.* 2009; Remya *et al.* 2008; Xia *et al.* 2007; Dieke 1968). The more intense transition centered at 545 nm corresponds to the transition of $^5D_4 \rightarrow {}^7F_5$. Moreover, the ligand-centered emission is not detected,

thus implying the existence of an efficient ligand-to-metal energy transfer process in this complex.

The excited state $^5D_0$ (Eu^{3+}) and $^5D_4$ (Tb^{3+}) lifetime values (τ_{obs}) were measured at both ambient (298 K) (Figure 3.12) and low temperatures (77 K) (Figures 3.13 and 3.14) for the Ln^{3+} complexes **1** and **2**, by monitoring within the more intense lines of the $^5D_0 \rightarrow {}^7F_2$ and $^5D_4 \rightarrow {}^7F_5$ transitions respectively, and the pertinent values are summarized in Table 3.5. The observed luminescent decay profiles correspond to single-exponential functions, thus implying the presence of only one emissive Ln^{3+} center. The shorter $^5D_0$ lifetime (τ_{obs} = 428 ± 2 μs) noted for Eu^{3+} complex **1** at 298 K may be due to the dominant nonradiative decay channels associated with vibronic coupling on account of the presence of two water molecules in the coordination sphere of this complex (Biju *et al.* 2009; Raj *et al.* 2008). This value is essentially temperature dependent, with τ_{obs} (759 ± 7μs) approximately doubled upon going from 298 to 77 K, thereby reflecting the presence of thermally activated deactivation processes. This effect has been well documented for many hydrated europium carboxylate complexes (Sivakumar *et al.* 2011). A longer $^5D_4$ lifetime value at 298K (938 ± 7 μs) has been observed for the Tb^{3+} complex even when the solvent molecules are present in the first coordination sphere because they are well known to be vibrational deactivators of the excited states of the Ln^{3+} ions (Samuel *et* al. 2008; Biju *et al.* 2009; Sivakumar *et al.* 2011).

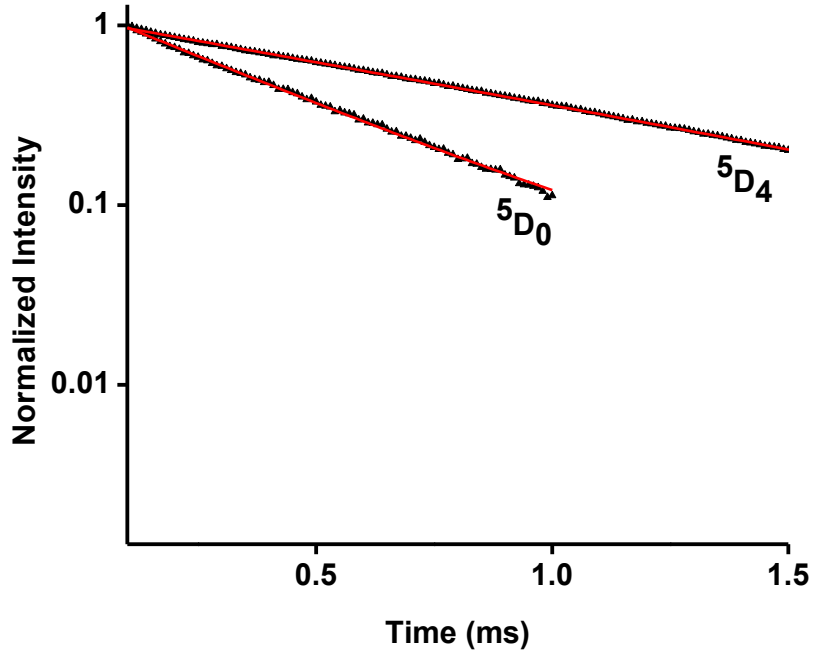

Figure 3.12. Luminescence decay profiles (298K) for complexes **1** and **2** excited at 355 nm and monitored at 612 nm and 545 nm, respectively.

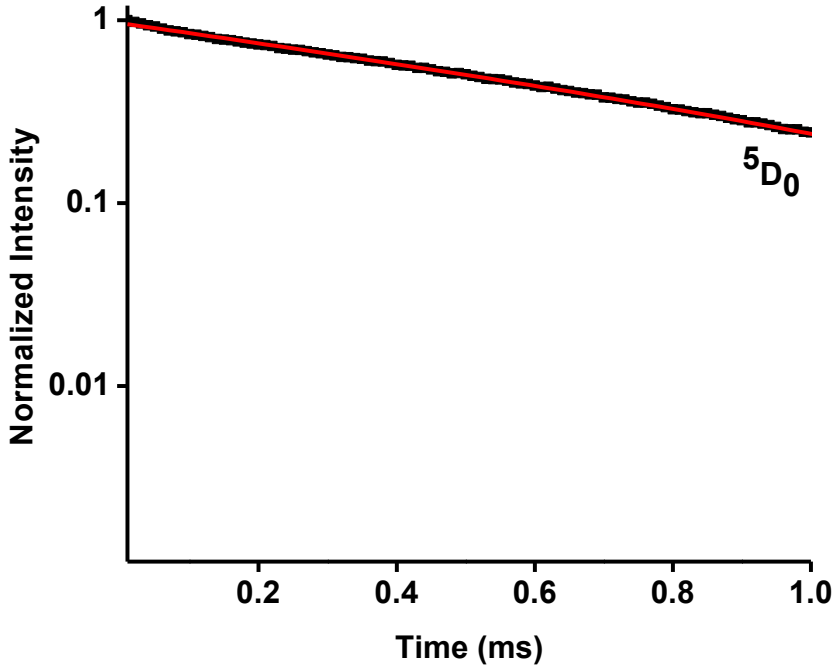

Figure 3.13. Low temperature (77K) luminescence decay profile of complex **1** excited at 355 nm and monitored at approximately 612 nm.

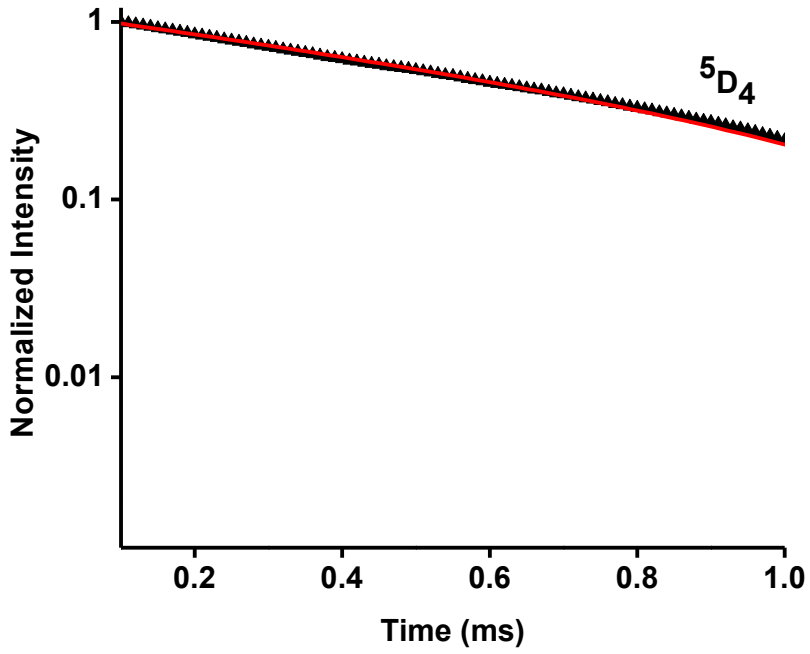

Figure 3.14. Low temperature (77K) luminescence decay profile of complex **2** excited at 355 nm and monitored at approximately 545 nm.

The energy gap between the luminescent and ground state manifolds are approximately 12000 and 14800 cm^{-1} for Eu^{3+} and Tb^{3+}, respectively. Relatively efficient coupling of the Eu^{3+} excited states occurs for the third vibrational overtone of the proximate O–H oscillators (υ_{OH} ~3300–3500 cm^{-1}), and for the fourth harmonic in the case of Tb^{3+}, which is consistent with the less efficient quenching observed in the case of Tb^{3+}, where the Franck-Condon overlap factor is less favourable (Beeby *et al.* 1999; Døssing 2005). The $^5D_4$ lifetime value of Tb^{3+} complex is found to be essentially temperature-independent, with τ_{RAD} (970 ± 7μs) varying by ~3% upon going from 298 to 77 K, thereby reflecting the absence of thermally activated deactivation processes.

In order to understand the photophysical properties of the designed ligand, it was necessary to determine the overall quantum yield which was described in detail in chapter 2. Table 3.5 summarizes the $\Phi_{overall}$, Φ_{Ln}, Φ_{sen}, radiative (A_{RAD}) and nonradiative (A_{NR}) decay rates.

Table 3.5. Radiative (A_{RAD}) and nonradiative (A_{NR}) decay rates, $^5D_0/^5D_4$ lifetimes (τ_{obs}), radiative lifetimes (τ_{RAD}), intrinsic quantum yields (Φ_{Ln}), energy transfer efficiencies (Φ_{sen}), and overall quantum yields ($\Phi_{overall}$) for complexes **1** and **2** ([a] = 77K).

Compl--exes	A_{RAD} /s^{-1}	A_{NR}/s^{-1}	τ_{obs}/ μs	τ_{RAD}/ μs	Φ_{Ln} (%)	Φ_{sen} (%)	$\Phi_{overall}$ (%)
1	282	2071	428 ± 2 759± 7[a]	3540	12	58	7 ± 0.7
2	---	---	938 ± 7	970 ± 7[a]	97	66	64 ± 6

Solid state measurements gave a quantum yield of 64% for the Tb^{3+}-4-(di(pyridin-2-yl) amino)benzoate complex **2**. Conversely, the corresponding Eu^{3+} complex **1** shows poor luminescent efficiency with low quantum yield (7%). A poor sensitization efficiency for the Eu^{3+} complex **1** has been noted for the newly constructed benzoate ligand mainly because of the larger energy gap between the triplet state and $^5D_0$ level of Eu^{3+} ΔE ($^3\pi\pi^*- {}^5D_0$) = 6447 cm^{-1} for **1.** Therefore, a lower quantum yield has been observed in the Eu^{3+} complex. On the other hand, complex **2** exhibits a higher quantum yield ($\Phi_{overall}$ = 64%) and an efficient ligand-to-metal energy transfer (Φ_{sen} = 66%) because of the superior

match of the triplet energy level of ligand to that of the Tb^{3+} emitting level (ΔE ($^3\pi\pi^*-{}^5D_4$) = 3197 cm^{-1}).

3.4.5. Energy Transfer from Tb^{3+} to Eu^{3+} in mixed lanthanide complex

The photoluminescence emission spectrum of compound $[Eu_{0.5}Tb_{0.5}(L)_3(H_2O)_2]_n$ (**4**) is compiled in Figure 3.15 along with the emission spectrum of coordination polymers of complexes **1** and **2**. The mixed lanthanide complex exhibits an enhanced luminescent intensity at 614 nm (5.48 fold) corresponding to $^5D_0 \rightarrow {}^7F_2$ transition of Eu^{3+} ion as compared to isostructural Eu^{3+} complex **1** because of the presence of Tb^{3+} ion in complex **4**. On the other hand, a considerable decrease in the luminescent intensity at 545 nm (22.7 fold) corresponding to $^5D_4 \rightarrow {}^7F_5$ transition compared to the isostructural Tb^{3+} complex **2**, indicating the highest efficiency of Tb^{3+} to Eu^{3+} energy transfer. Furthermore, the colour in the luminescent image of mixed Ln^{3+}-complex shows bright- red emission under UV light.

The lifetime measurements of the Ln^{3+} emissions in mixed lanthanide systems represent an important tool for the demonstration of energy transfer between the Ln^{3+} ions (Ananias *et al.* 2004; Elhabiri *et al.* 1999; Lewis *et al.* 2011; Piguet *et al.* 1993; Sendor *et* al. 2003). Lifetime values for the excited state energy levels for complex **4** were determined from their respective luminescent decay profiles at room temperature (Figure 3.16). The lifetimes of Tb^{3+} and Eu^{3+} emissions in mixed Ln^{3+} system provides further evidence that energy transfer from the Tb^{3+} to Eu^{3+} center is indeed occurring because the lifetime of the Tb^{3+}

emission decreases by approximately 86% (down to 132 ± 1 μs from 938 ± 7 μs in **2**).

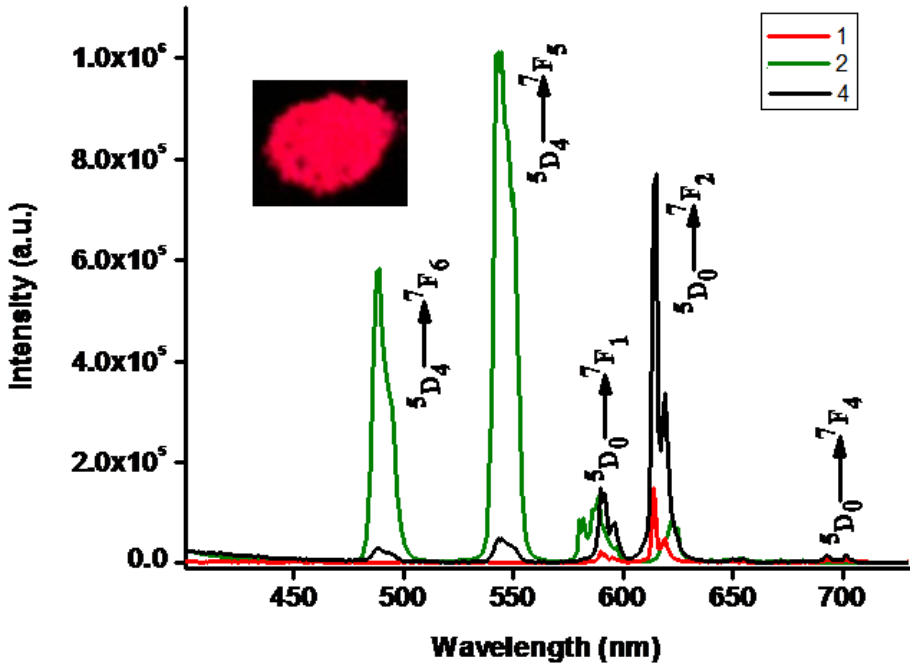

Figure 3.15. Room-temperature emission spectra for complexes **1**, **2** and **4**, excited at 355 nm.

In contrast, the lifetime of the Eu^{3+} emission increases moderately to 525 ± 1 μs (from 428 ± 2μs in **1**). This can be explained as being due to a decrease of the concentration quenching by dilution of the the Eu^{3+} ions. The energy-transfer efficiency (η) for the purely dipole-dipole, through-space-energy-transfer mechanism can be quantified by eqs 1 and 2 (Lewis *et al.* 2011):

$$\eta = 1 - (\tau/\tau_0) \qquad (1)$$

$$\eta = 1/[1 + (R/R_0)^6] \qquad (2)$$

where τ and τ_0 are the lifetimes of luminescence of the donor in the presence and absence of the acceptor, R_0 is the distance required for 50% energy transfer, and R is the actual distance between donor and acceptor. The energy-transfer efficiency estimated as per the eq 1 was found to be 86% when τ = 132 ± 1 μs and τ_0 = 938 ± 7 μs. On the other hand, as per eq 2, the energy-transfer efficiency of η = 96% was obtained when it has been assumed that R = 5.2 Å and R_0 = 9.0 Å (the value for R_0 usually lies between 8 and 10 Å for Eu^{3+}-Tb^{3+} pairs in helicates (Piguet *et al.* 1993)). This efficiency is approximately similar to the value calculated experimentally for the mixed complex $[Eu_{0.5}Tb_{0.5}(L)_3(H_2O)_2]_n$ (**4**) system based on lifetime values. It is therefore a strong possibility that intrachain energy transfer occurs predominantly *via* a dipole-dipole mechanism. The efficiency of energy-transfer observed in the present system is comparable to that of heterometallic lanthanide helicates developed by Piguet and Bünzli and co-workers, which display superior energy-transfer yields of 72% and 82% (Piguet *et al.* 1993).

In addition to the above- mentioned Ln → Ln energy transfer pathways, it is well demonstrated that the general mechanism for the sensitization of Ln^{3+} ion luminescence *via* the "antenna effect" involves the following steps: (i) UV absorption by the organic chromophore, which results in excitation to the first excited singlet state (S_1); (ii) intersystem crossing from singlet to the triplet state (T_1); (iii) intermolecular energy transfer from the ligand centered triplet state to the excited 4f states of the Ln^{3+} ions; (iv) radiative transition from the Ln^{3+} ion emissive states to lower energy states, which results in the

characteristic Ln^{3+} emission (Binnemans 2009; Bünzli 2010; Bunzli *et al.* 2000; Piguet *et al.* 1993).

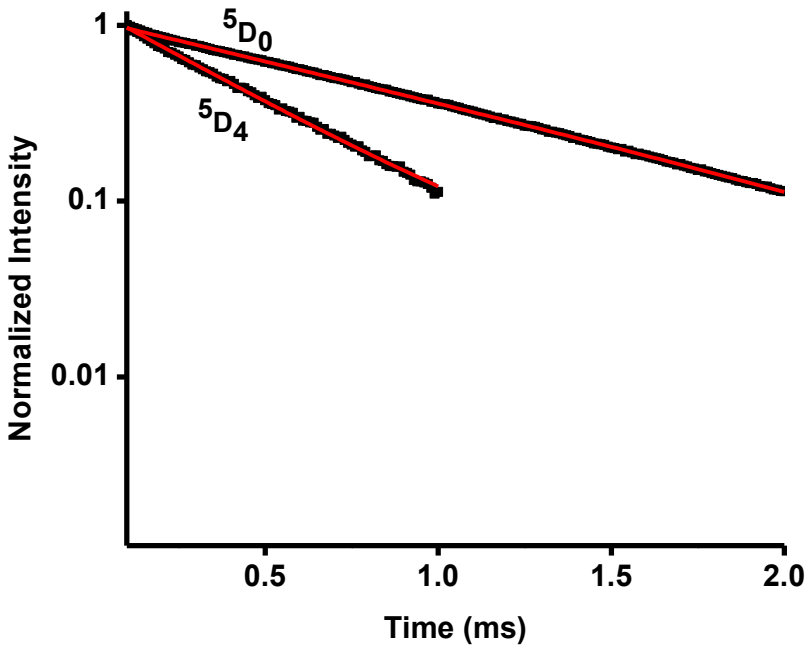

Figure 3.16. $^5D_0$ and $^5D_4$ decay profiles (298K) for complex **4** excited at 355 nm and emission monitored around 612 nm for $^5D_0$ and 545 nm for $^5D_4$.

Thus, the intramolecular energy migration efficiency from the organic chromophore ligand to the central Ln^{3+} ion is one of the key factors that influence the luminescent properties of these Ln^{3+} complexes. Taking the mixed Ln^{3+} complex **4** as a typical example, the schematic diagram representing energy transfer pathways is summarized in Figure 3.17.

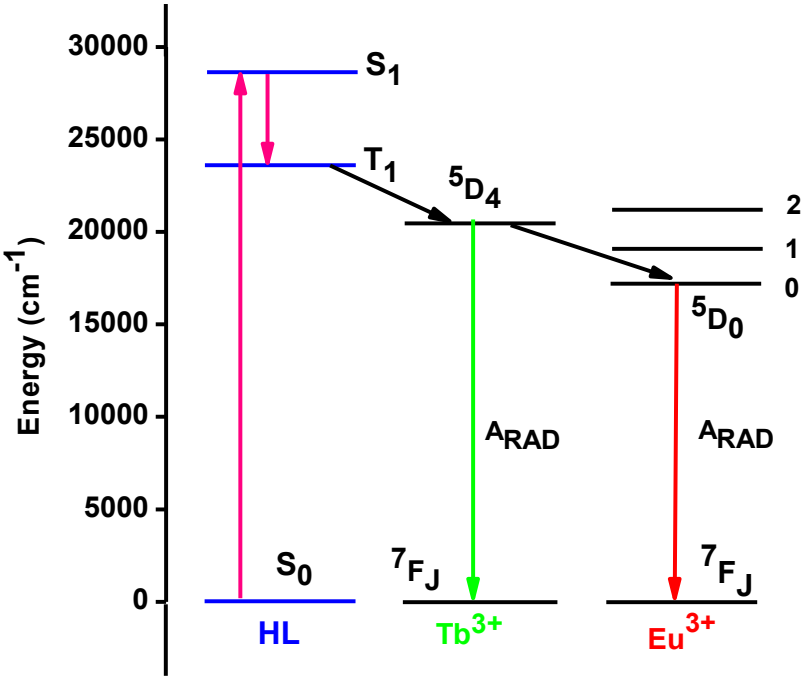

Figure 3.17. Schematic representation of the energy transfer mechanism for complex **4**.

3.5. CONCLUSIONS

- In summary, we have demonstrated the design, synthesis, and characterization of a new class of highly luminescent thermally stable lanthanide coordination polymers that utilizes a novel 4-(di(pyridin-2-yl)amino)benzoic acid ligand to indirectly excite the lanthanide metal center.
- All the three complexes were structurally authenticated by single-crystal X-ray diffraction and were found to exist as infinite 1D coordination polymers.
- The terbium coordination polymer shows high quantum yield ($\Phi_{overall}$ = 64 ± 6%) and long lifetime (τ_{obs} = 938 ± 7 μs), supporting the hypothesis

that the superior match of the triplet state of the ligand with that of the $^5D_4$ excited state level of the metal ion.

- In contrast to the foregoing, the Eu^{3+} coordination polymer features a weak luminescence efficiency ($\Phi_{overall}$ = 7 ± 0.7 %) due to poor matching of the triplet state of the ligand with the emissive excited states of the metal ion.
- Another noteworthy feature from the current study is an efficient Tb^{3+}-to-Eu^{3+} energy transferability in heteronuclear lanthanide complex, (η = 86%), and hence it is a potential candidate for applications in the field of colour displays, luminescence sensors, and structural probes.

CHAPTER 4

Tunable White-Light Emission from a Mixed Lanthanide (Eu^{3+}, Gd^{3+}, Tb^{3+}) Coordination Polymers Derived from 4-(Dipyridin-2-yl)amino benzoate

4.1. ABSTRACT

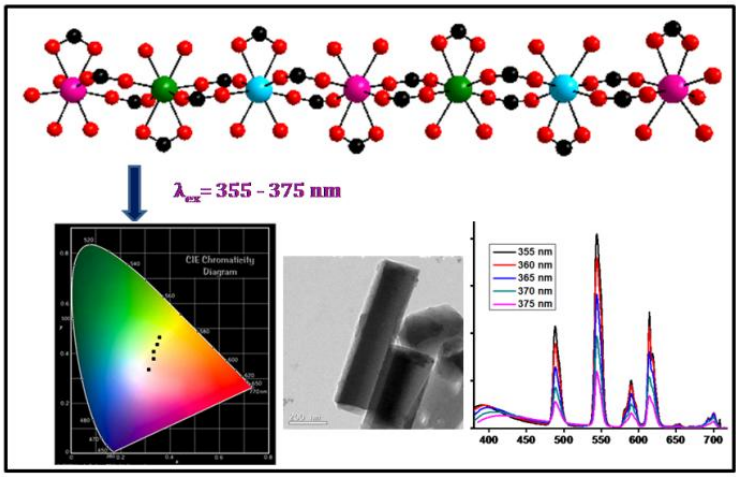

Herein, we have developed a series of isostructural mixed Ln^{3+}–4-(dipyridin-2-yl)aminobenzoate coordination polymers [Ln^{3+} = Eu^{3+} (**1**), Tb^{3+} (**2**), and Gd^{3+} (**3**)], characterized and investigated their photophysical properties. The results demonstrated that by gently tuning the excitation wavelength of these mixed lanthanide complexes, white light emission can be realized with the Commission Internationale de I'Eclairage coordinates (0.32, 0.34). Furthermore, by changing the concentration profiles of lanthanide ions stiochiometrically in mixed-lanthanide complexes and exciting at particular wavelength, various emission colours can also be successfully obtained. The antenna ligand, 4-(dipyridin-2-yl)aminobenzoic acid provides an efficient energy transfer for the sensitization of Eu^{3+} and Tb^{3+} complexes and exhibits red and green emissions, respectively.

Most importantly, due to the high energy (32150 cm^{-1}) of the Gd^{3+} ion lowest-lying emission level, the corresponding Gd^{3+} complex displays ligand-centered visible emission in blue light region, and hence it acts as a blue emitter. Therefore, Eu^{3+} and Tb^{3+} complexes in conjunction with Gd^{3+} complex is a suitable choice to obtain tunable white-light-emission from Ln^{3+} coordination polymers. The morphological analyses of the mixed lanthanide coordination polymers by Transmission Electron Microscopy (TEM) discloses that these compounds exist as unique crystalline nano-rods with an average diameter of 200 nm. The developed mixed lanthanide complexes also exhibit high thermal stability (~ 420 °C).

Ramya, A. R.; Sunil Varughese; Reddy, M. L. P. *Dalton Trans.*, **2014**, *43*, 10940-10946.

4. 2. INTRODUCTION

White-light emitting materials and devices have recently attracted considerable interest because of their potential applications in solid-state lighting, low-cost back-lighting and full-color displays (Reineke *et al.* 2009; Zhu *et al*. 2011; Liu *et al*. 2012; Farinola and Ragni 2011). The lanthanide based molecular materials display unique optical properties such as sharp and intense luminescence, long excited state life times, emissions in the primary color range (red, green and blue) that fully spans in the entire visible spectrum and therefore can be well suitable for designing white-light emitting materials (Guo *et al.* 2010; Rocha *et al*. 2011; Shunmugam and Tew 2008; Eliseeva and Bünzli 2010; Song *et al*. 2013). Interestingly, Eu^{3+} and Tb^{3+} ions emit intense red and green light, respectively. On the other hand, Gd^{3+} complex emits in the blue region in view of its high lowest emitting level (32,150 cm^{-1}). Consequently, mixed lanthanide complexes (Gd^{3+}, Tb^{3+} and Eu^{3+}) have potential applications in generating white-light emission (Dang *et al*. 2012; Balmurugan *et al*. 2009; Zhang *et al*. 2014; Tang *et al*. 2014). The aromatic carboxylate ligands not only play a role as new building blocks for the coordination networks of lanthanides, but also act as efficient sensitizers for Ln^{3+} ions via an "antenna effect" (Reddy *et al.* 2013). Zhang and co-workers have reported a strong white-light emission based on isostructural mixed-lanthanide metal–organic complexes by varying the stoichiometric ratio of the lanthanide ions (Zhang *et al.* 2013). Previously, efforts have been made to generate white-light emission by adjusting the doping concentration of Eu^{3+} and Tb^{3+} ions in the Gd^{3+}-coordination polymer constructed based on

benzimidazole-5,6-dicarboxylic acid, and 1,10-phenanthroline (Ma *et al.* 2012). In recent years, metal–organic frameworks (MOFs) with exceptional tenability and structural diversity, represent a new class of light-emitting materials, with the possibility of color tuning of the light emission, including the production of white light (Rao *et al*. 2012; Zhang *et al*. 2014; Ma *et al*. 2013). Single-phase white light emitters based on MOFs have also been reported (Liu *et al.* 2012). However, developing suitable lanthanide coordination compounds capable of generating white light is still a challenging task because the blue and yellow light emitters or blue, green and red light emitters should compensate exactly through the dichromatic and trichromatic approaches, respectively.

In this work, we report the preparation of a series of mixed lanthanide complexes based on earlier reported three new Ln^{3+}-4-(dipyridin-2-yl)amino benzoate coordination polymers [Ln^{3+} = Eu^{3+} (**1**), Tb^{3+} (**2**), and Gd^{3+} (**3**)] (Ramya *et al*. 2012). In these complexes, 4-(dipyridin-2-yl)aminobenzoate is utilized, not only as an energy absorption antenna for the red Eu^{3+} and green Tb^{3+} emissions, but also as a blue emission source. To maximize the blue emission, the composition percentage of Gd^{3+} is much higher than the other two components to dilute the other two lanthanide ions in the solid state. With careful adjustment of the relative concentration of the lanthanide ions and excitation wavelength, the color of the luminescence can be modulated, and white light-emission can indeed be achieved. The mechanisms possibly responsible for the observed photophysical properties of these mixed complexes are also discussed.

4.3. EXPERIMENTAL SECTION

4.3.1. Materials

The following chemicals were procured commercially and used without subsequent purification: Europium(III) nitrate hexahydrate, 99.9%, terbium(III) nitrate hexahydrate, 99.9% and gadolinium(III) nitrate hexahydrate , 99.9% were procured from Triebacher. Methyl 4-aminobenzoate, 98%, and 2-bromopyridine, 99.9% were purchased from Sigma-Aldrich and used without further purification. All the other chemicals used were of analytical reagent grade.

4.3.2. Characterization and spectroscopic techniques

TEM and SEM were used to determine the morphology and particle size. TEM analyses were done on a JEOL 2010 (300 kV). A pinch of material was suspended in acetone and sonicated for 10 min, then dropped in a carbon-coated grid and allowed to dry at room temperature. Scanning electron microscopy (SEM) was performed on a ZEISS EVO-18 Cryo-SEM instrument.

4.3.3. Synthesis of the ligand and lanthanide complexes

The ligand 4-(dipyridin-2-yl-amino)benzoic acid and their corresponding lanthanide complexes (**1**–**3**) were synthesized in our lab and has been characterized by various spectral techniques as described in chapter 3. The mixed lanthanide complexes **4**–**11** were synthesized by means of the following general procedure: 1 mmol of the lanthanide nitrate mixture (Ln = Eu^{3+}, Tb^{3+} and Gd^{3+}) in 2 mL of ethanol was added to an ethanolic solution of 3 mmol of ligand and 3 mmol of NaOH in 5 mL of water. Precipitation took place

immediately, and the reaction mixture was stirred subsequently for 12 h at room temperature. The product was collected on a filter, washed with ethanol, and dried in vacuo. The resulting complexes were then purified by recrystallization from a dichloromethane/methanol solvent mixture.

The molar ratios of $Gd^{3+}/Eu^{3+}/Tb^{3+}$ in the resulting mixed-lanthanide complexes is exclusively confirmed by energy-dispersive spectrometry (EDS) analysis.

4.4. RESULTS AND DISCUSSION

4.4.1. Synthesis and Characterization of ligand and Ln^{3+} complexes 1–3

The elemental analysis data of the complexes **4–11** revealed that in each case the Ln^{3+} ion had reacted with the corresponding benzoate ligand in a metal-to-ligand mole ratio of 1:3 (Table 4.1). The metal compositions of the designed mixed lanthanide complexes were confirmed by energy-dispersive spectrometry (EDS) analysis and found to be matching with the initial compositions of the metal ions (Figure 4.1 and Table 4.2). The FT-IR spectrum of the coordinated benzoate ligand exhibits two intense bands at approximately 1434 and 1699 cm^{-1}, which are attributable to the symmetric ν_s(C=O) and *anti*-symmetric ν_{as}(C=O) vibration modes, respectively. The coordination of the ligand to the respective lanthanide ion in compound **6** was confirmed by the absence of the ν(COOH) absorption bands of the ligand at ~1699 cm^{-1}. Moreover, the asymmetric and symmetric stretching vibrational modes of the benzoate ligand in complex **6** further split into two peaks [ν_s(C=O): 1428, 1407 cm^{-1}; ν_{as}(C=O): 1648, 1595 cm^{-1}].

Table 4.1. Elemental analysis for mixed complexes **4**–**11**.

Compounds	Elemental Analyses : Calcd (Found)		
	C	H	N
4	56.27 (56.15)	3.88 (3.95)	11.58 (11.40)
5	56.68 (56.77)	3.92 (3.78)	11.66 (11.44)
6	56.67 (56.68)	3.92 (3.74)	11.66 (11.38)
7	56.67 (56.77)	3.92 (3.77)	11.66 (11.64)
8	56.62 (56.58)	3.91 (3.80)	11.65 (11.42)
9	56.79 (57.05)	3.92 (3.90)	11.68 (11.61)
10	56.62 (56.60)	3.91 (3.81)	11.65 (11.47)
11	56.62 (56.55)	3.91 (3.85)	11.65 (11.59)

Table 4.2. Molar ratios of multi component $Gd^{3+}/Eu^{3+}/Tb^{3+}$ for complexes **4**–**11** by EDS analysis.

Compounds	Molar ratios of multi-components		
	Gd	Tb	Eu
4	0.208	0.602	0.190
5	0.283	0.555	0.162
6	0.520	0.392	0.088
7	0.570	0.132	0.298
8	0.665	0.245	0.091
9	0.755	0.121	0.124
10	0.828	0.102	0.070
11	0.870	0.068	0.062

The difference between the asymmetric and symmetric stretching vibration modes ($\Delta\nu_{(C=O)} = \nu_{as} - \nu_s$) is 241 and 167 cm^{-1}, which indicates that carboxylate

groups are coordinated to Ln^{3+} ions in a bidentate bridging and chelating modes. A broad band observed above 3000 cm^{-1} (maximum at 3400 cm^{-1}) in the FT-IR spectrum of the typical complex **6** is attributed to the characteristic ν(OH) stretching vibration and is indicative of the presence of water molecules.

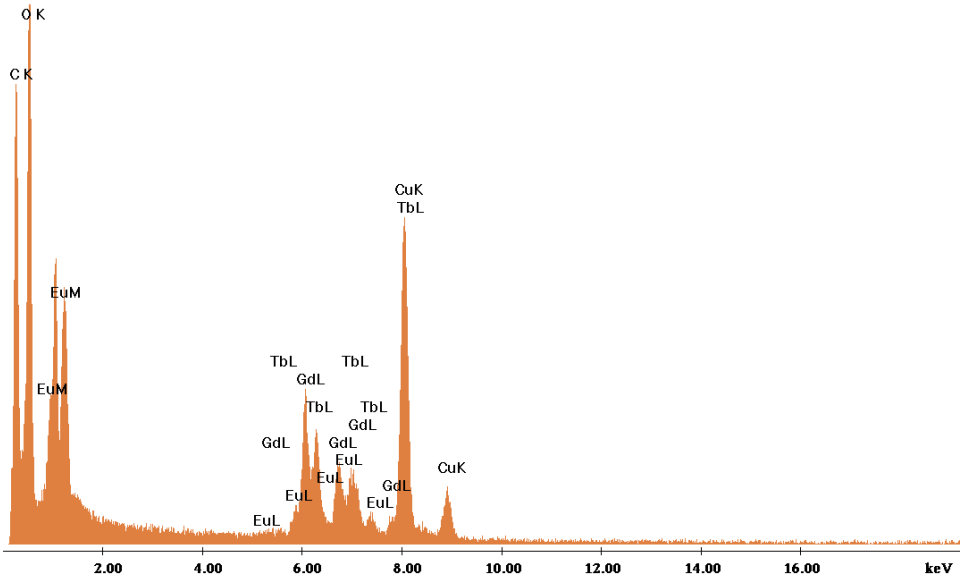

Figure 4.1. EDS spectrum for complex **6**.

The thermal stability of the typical mixed lanthanide complex **6** was examined by means of thermogravimetric analysis (TGA) in the temperature range 30–1000 °C and the corresponding thermogram is depicted in Figure 4.2.

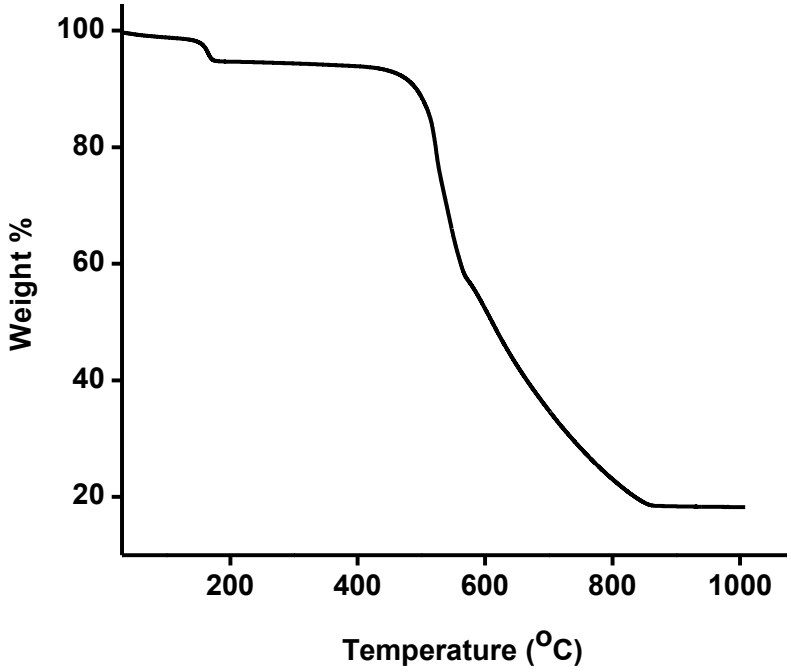

Figure 4.2. Thermogravimetric plot for complex **6**.

The onset of weight loss occurs between 100 and 260 °C (Found: 4.65%) for compound **6.** This weight loss corresponds to the release of lattice and coordinated water molecules (Calcd: 4.99%). The second weight loss, between 420 and 830 °C for complex **6** (found, 77.35%; calcd, 80.67%), is attributed to the thermal decomposition of three ligand molecules. The final residue for each complex corresponds to the formation of the respective lanthanide oxide. The mixed lanthanide complex is found to be thermally stable up to ~420 °C.

The powder XRD pattern of typical mixed complex **6** was found to be similar to that of complexes **1**–**3**, thus implying that all these complexes are isostructural (Figure 4.3)

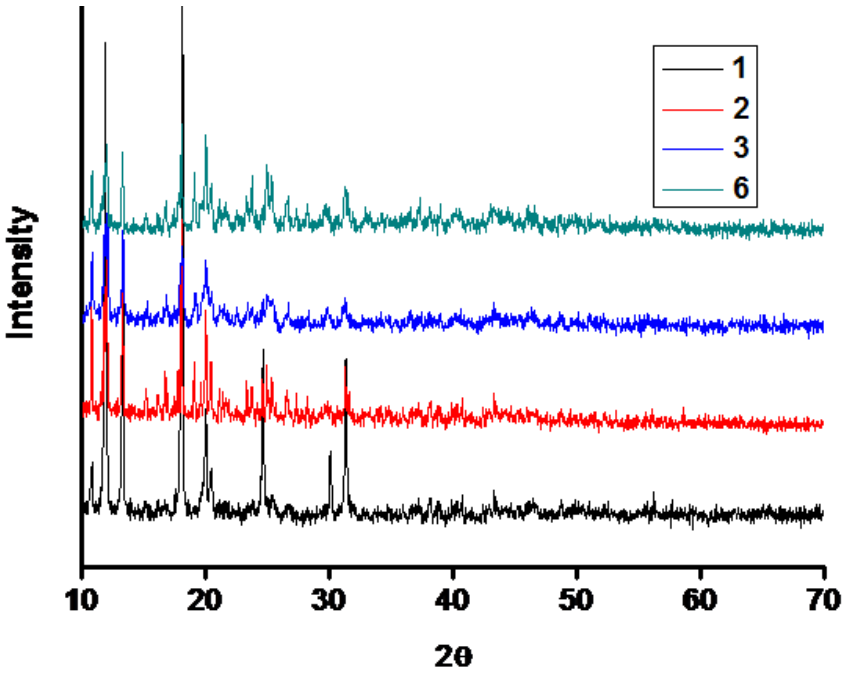

Figure 4.3. PXRD patterns for complexes **1, 2, 3** and **6**.

The SEM and TEM micrographs of Gd complex **3** and mixed lanthanide complex **6** are displayed in Figure 4.4 and 4.5, respectively. It is interesting to note that both the complexes exhibit a rod-like morphology with an average diameter of 200 nm. Thus, this observation suggests that the flexible coordination mode of the 4-(dipyridin-2-yl)aminobenzoic acid ligand in combination with the high coordination number of the Ln^{3+} ions favours the formation of a 1D rod-like structure.

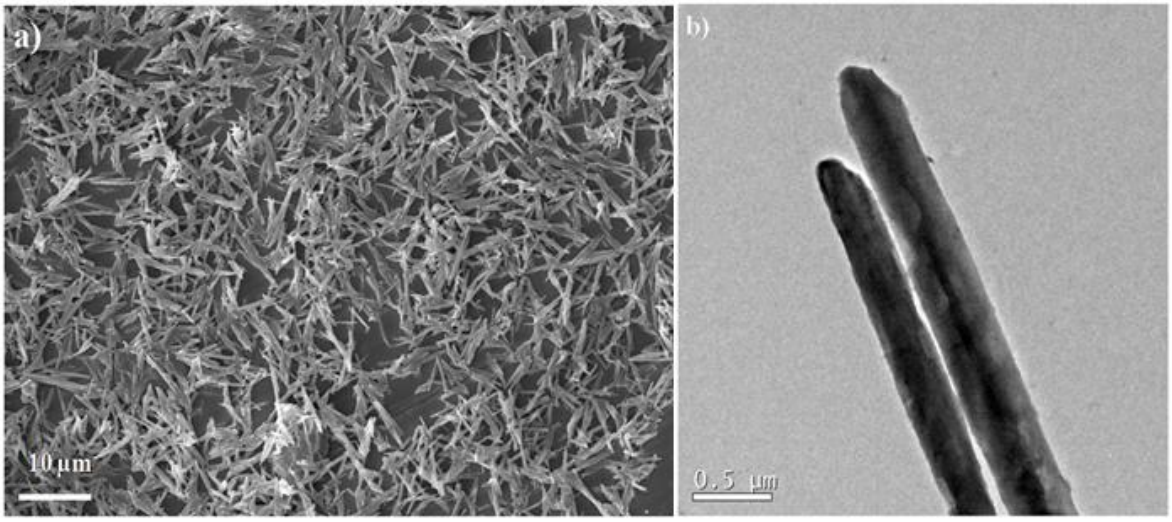

Figure 4.4. a) SEM and b) TEM micrographs of complex **3**.

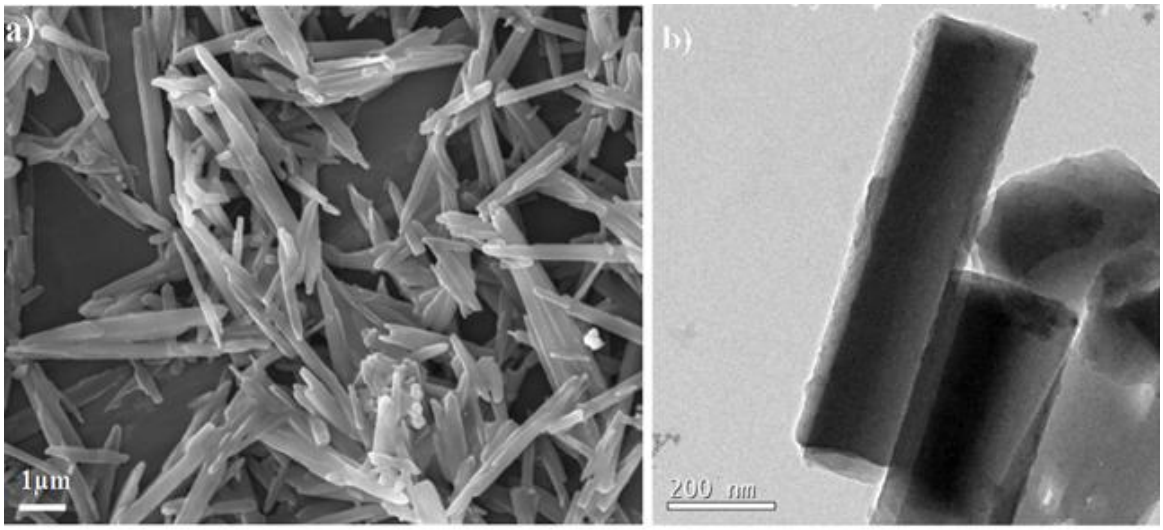

Figure 4.5. a) SEM and b) TEM micrographs of complex **6**.

4.4.2. Photophysical properties

The solid-state excitation and emission spectra of Eu^{3+}, Tb^{3+} and Gd^{3+} coordination polymers (**1**–**3**) recorded at room-temperature are displayed in Figure 4.6. The red emission of the pure Eu^{3+} compound **1** is due to the most intense peak at 614 nm for a $^5D_0 \rightarrow {}^7F_2$ transition, and the green colour of the pure Tb^{3+} compound **2** is due to the most intense peak at 545 nm for a $^5D_4 \rightarrow {}^7F_5$ transition. Compound **1** exhibits emission peaks at 582, 590, 614, 655, and 701 nm related to $^5D_0 \rightarrow {}^7F_J$ transitions of Eu^{3+}, where J = 0–4, respectively when excited at λ_{ex}= 355 nm (Raj *et al.* 2010). On the other hand, the compound **2** displays typical emission bands at 490, 545, 585, and 620 nm, corresponding to transitions from $^5D_4 \rightarrow {}^7F_J$ (where J = 6–3, respectively) of Tb^{3+} (λ_{ex}= 355 nm) (Sivakumar *et al.* 2011; Sivakumar *et al.* 2010). Gd^{3+} compound **3** shows a broad violet-blue emission band between 380 to 430 nm. As the lowest excited states of the Gd^{3+} ($^6P_{7/2}$) are too high to accept energy from the ligand, its characteristic 4f–4f transition at 311 nm is not visible and hence the broad violet-blue emission noted can be assigned to the ligand emission. Furthermore, the absence of ligand-centered emission bands in the emission spectra of **1** and **2**, indicating the efficient ligand-to-Ln^{3+} ion energy transfer in these complexes. The antenna ligand, 4-(dipyridin-2-yl)aminobenzoic acid has a high efficiency of light absorption (λ_{max} = 305 nm, ε = 1.2 × 10^4 L mol^{-1} cm^{-1}) and the energy of its triplet excited state (23697 cm^{-1}) is higher than the lowest emitting level of the Eu^{3+} (17500 cm^{-1}) and Tb^{3+} (20500 cm^{-1}). However, it is lower than that of Gd^{3+} (32150 cm^{-1}). Thus the terbium compound **2** exhibits higher quantum

yield ($\Phi_{overall}$ = 64%) and lifetime values (938 ± 7 μs) because of the superior match of the triplet state of the 4-(dipyridin-2-yl)aminobenzoic acid ligand to that of the Tb^{3+} emitting level ($^5D_4$) as compared to compound **1**. The Eu^{3+} compound displays a moderate quantum yield ($\Phi_{overall}$ = 7%) and life time (428 ± 2μs) values because of the poor match of the triplet energy level of the ligand with that of $^5D_0$ excited state level as described in chapter 3 (Ramya *et al*. 2012).

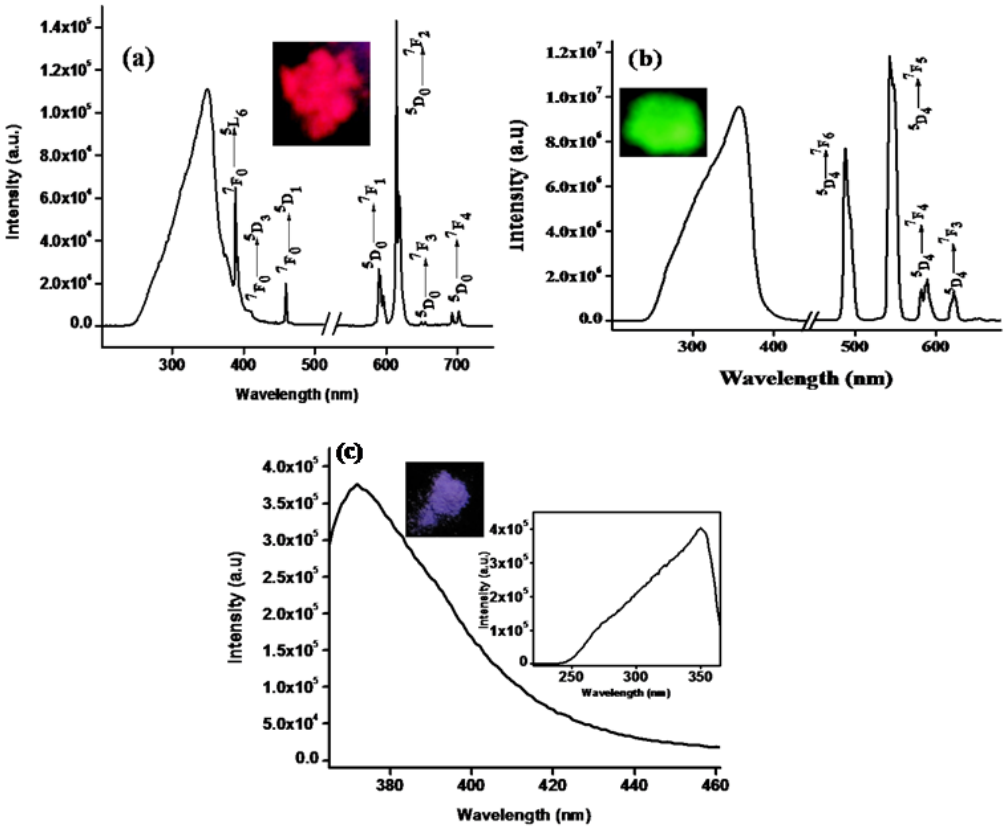

Figure 4.6. The room-temperature excitation and emission profiles of complexes **1**(a), **2**(b) and **3**(c) [(c) Room-temperature excitation (inset)].

The emission profiles of mixed lanthanide compounds **4**–**11** excited at 355 nm are shown in Figure 4.7. The mixed lanthanide compounds consists of multiple luminescent dopants display mixed emission patterns with different relative peak intensities depending on the ratios of the Tb^{3+}, Eu^{3+} and Gd^{3+} ions, resulting in a fluent change of their visible photoluminescence emission colours between green, blue and red. Multiple colours from green, greenish yellow, yellow, yellowish orange, orange yellow, pink to red were thus realized by varying the intensity ratio of RGB emissions. The emission colours for **4**–**11** are illustrated in the CIE chromaticity diagram (Figure 4.8), while their CIE colour coordinates are listed in Table 4.3.

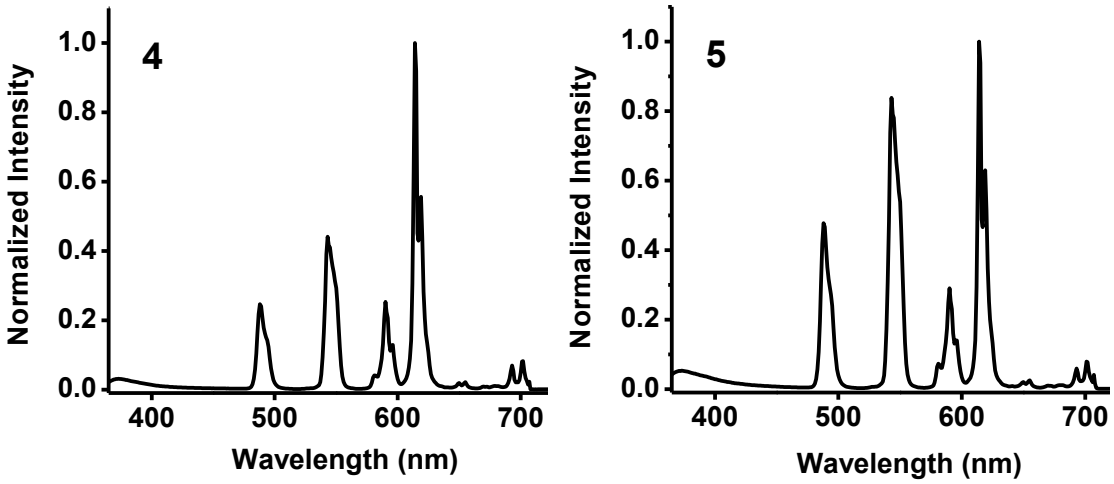

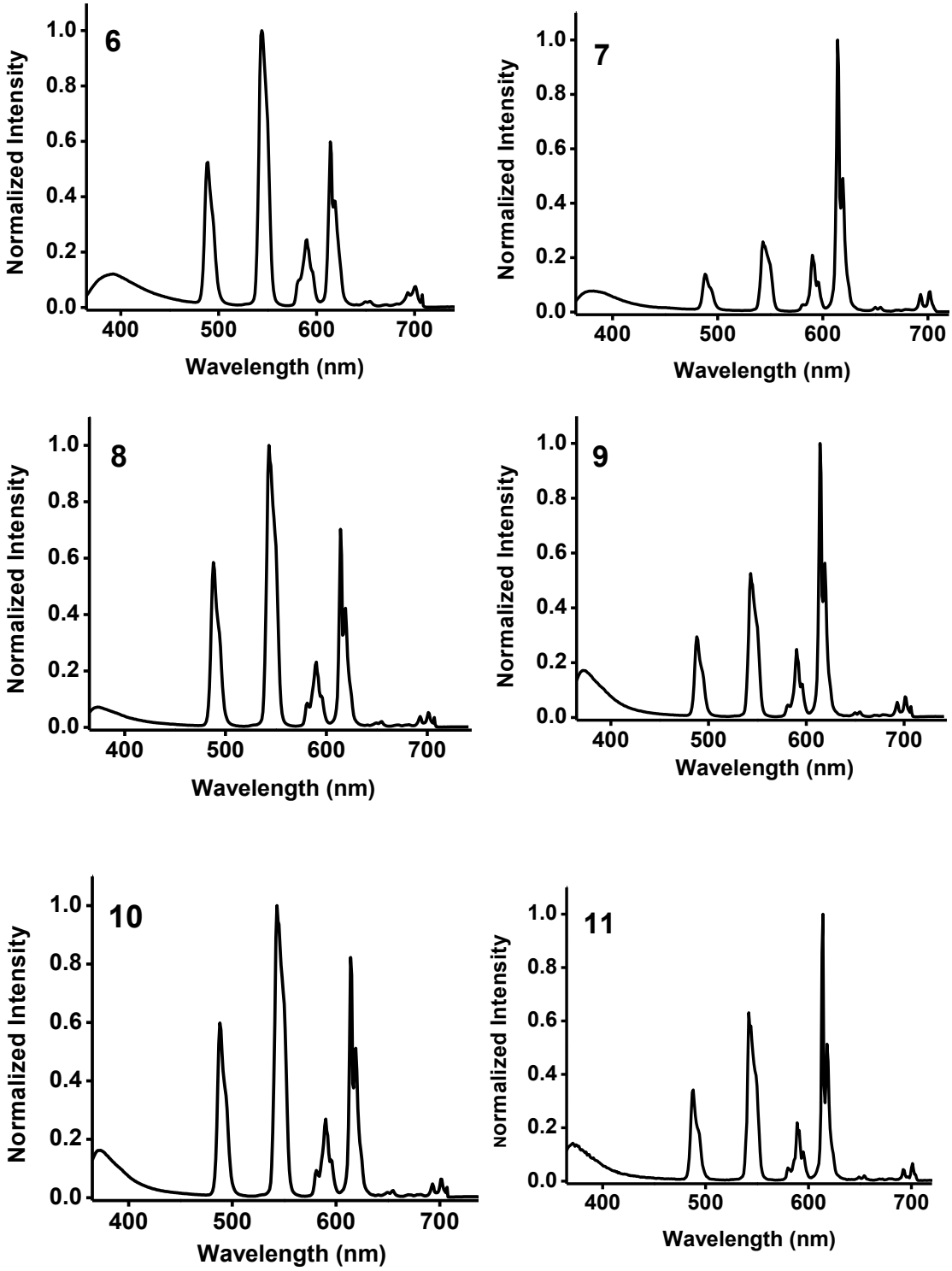

Figure 4.7. Emission spectra for compounds **4**–**11**, excited at 355 nm.

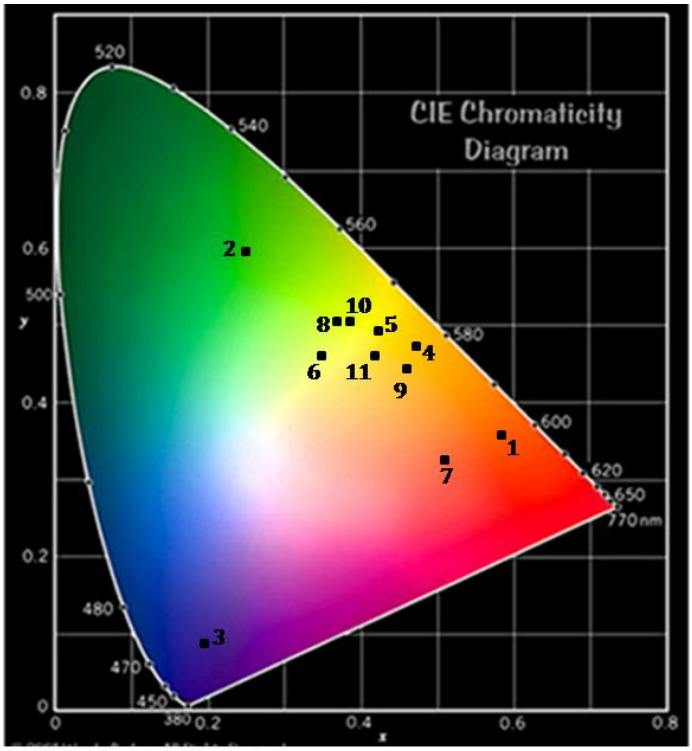

Figure 4.8. CIE chromaticity diagram showing the location of the multi-coloured lanthanide mixed complexes (excited at 355 nm).

The emission behaviour of mixed lanthanide compound **6** has been investigated by varying the excitation wavelength between 355 and 375 nm and the resulting emission profiles are displayed in Figure 4.9. As shown in Figure 4.9, when excited at 355 nm, light yellow emission with CIE coordinate of (0.36, 0.46) is obtained. With the increase in excitation wavelength, the relative intensity of green and red emissions gradually decreases and at the same time the blue emission increases and as a result white emission with the CIE coordinate (0.32, 0.34) emerges upon excitation at 375 nm. The current concept of excitation dependent photoluminescence tuning in the blue, yellow and white regions is controlled by different energy transfer processes.

Table 4.3. Colour coordinates of **1**–**11** according to CIE 1931 at 355 nm excitation wavelength with the approximate colour regions.

Complexes	CIE coordinates	Approximate colour regions
1	(0.60, 0.33)	Red
2	(0.30, 0.58)	Green
3	(0.17, 0.08)	Bluish violet
4	(0.48, 0.45)	Orange yellow
5	(0.42, 0.48)	Yellow
6	(0.36, 0.46)	Light yellow
7	(0.50, 0.29)	Pink
8	(0.37, 0.50)	Greenish Yellow
9	(0.46, 0.43)	Yellowish orange
10	(0.38, 0.50)	Greeish Yellow
11	(0.41, 0.45)	Yellow

In the case of higher energy absorption, the usual "antenna effect" dominates, which generates a yellow light emission. On the other hand, when the absorbed energy is too low to allow intersystem crossing to occur, the ligand fluorescence in the blue region dominates. Thus, a white light emission can be realized through a combination of the usual triplet pathway and a ligand fluorescence process, when an intermediate energy is absorbed. White-light emission thus can be obtained by precisely controlling the concentration profiles of Gd/Eu/Tb and excitation wavelengths.

a)

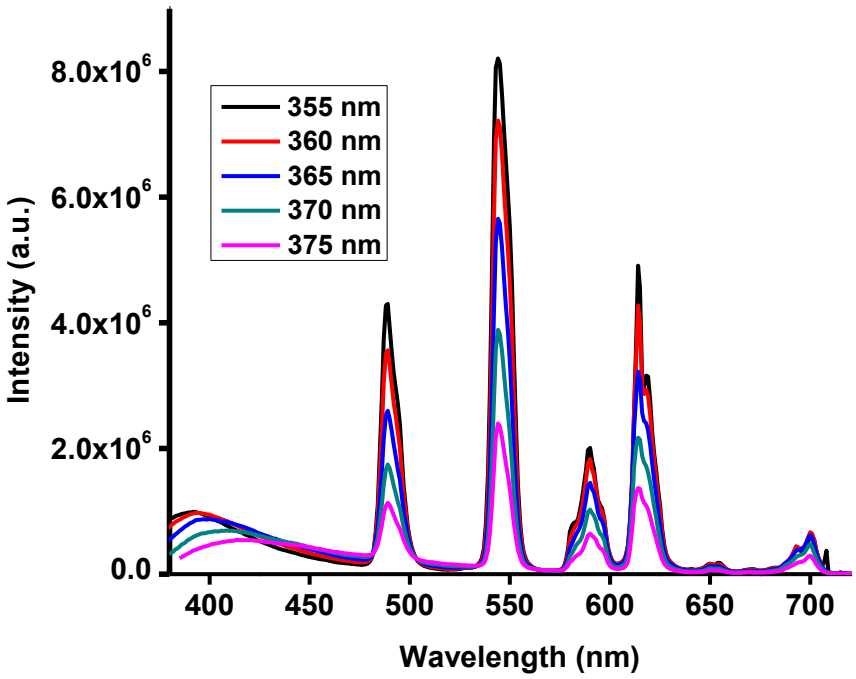

b)

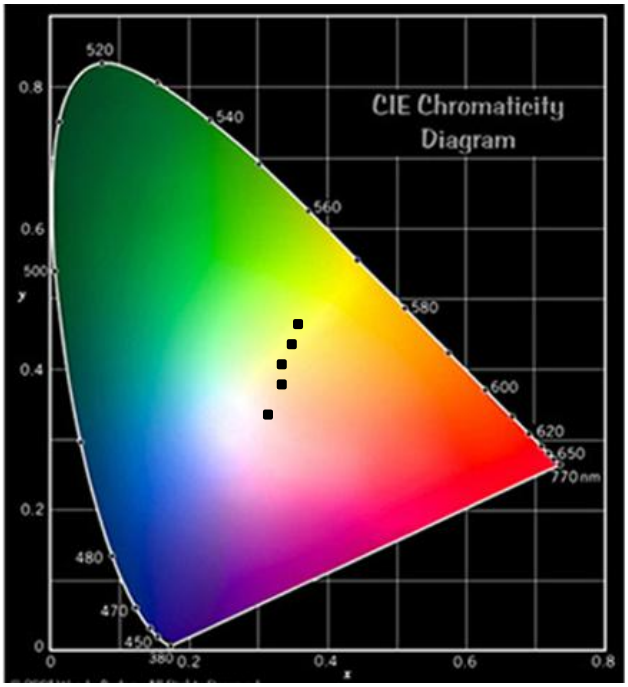

Figure 4.9. a) Emission spectra for compound **6** at 355-375 nm excitation wavelengths. b) Variation of colour coordinate value [355 nm: (0.36, 0.46), 360 nm: (0.36, 0.44), 365 nm: (0.35, 0.40), 370 nm: (0.36, 0.38), 375 nm: (0.32, 0.34)].

a)

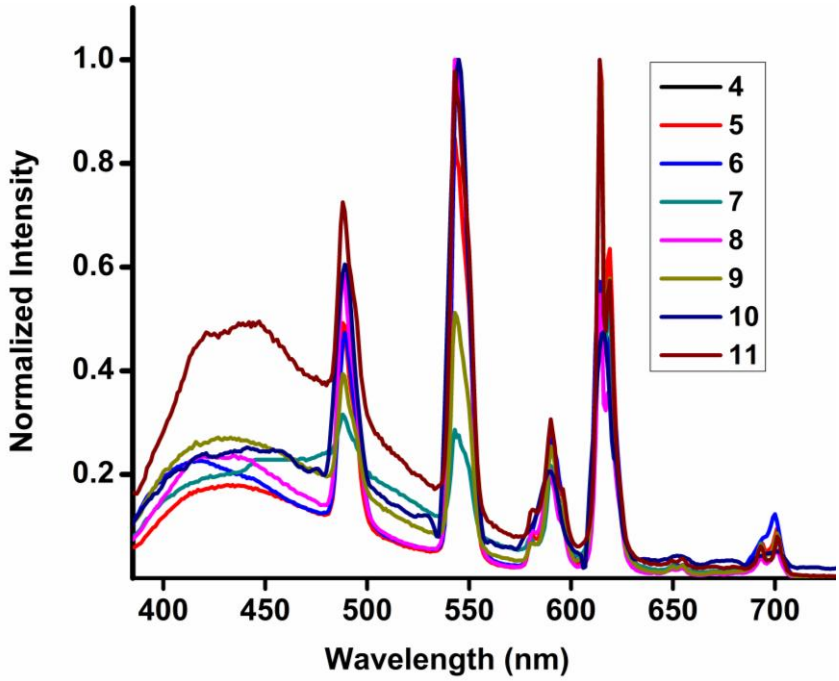

b)

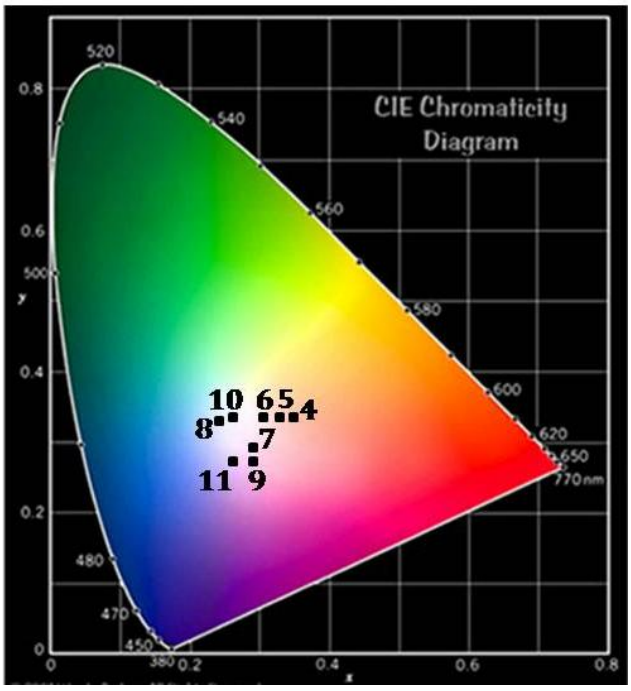

Figure 4.10. a) Emission spectra for compounds **4**–**11**, excited at 375 nm. b) The CIE coordinates characteristic to the emission for **4**–**11** at 375nm.

The CIE chromaticity coordinates of **6** are found to be (0.32, 0.34), which is very close to that for pure white light (0.33, 0.33) according to the 1931 CIE coordinate diagram. Furthermore near white-light is generated by all the mixed-lanthanide complexes (irrespective of their composition), when excited them at 375 nm (Figure 4.10 and Table 4.4). Hence, the chromaticity coordinates of white light are depending on the excitation wavelength (λ_{ex}), enabling a potential approach to regulate the white-light property by means of such dual-emissive compound.

Table 4.4. Colour coordinates of **4**–**11** according to CIE 1931 at 375 nm excitation wavelength with the approximate colour regions.

Complexes	CIE coordinates	Approximate colour regions
4	(0.36, 0.34)	Near white
5	(0.33, 0.34)	White
6	(0.32, 0.34)	White
7	(0.29, 0.28)	Near white
8	(0.27, 0.33)	Near white
9	(0.29, 0.27)	Near white
10	(0.27, 0.34)	Near white
11	(0.26, 0.27)	Near white

The present investigation highlights that development of full-colour photo-luminescent materials based on mixed-lanthanide metal–organic complexes would be a promising strategy in the design of RGB-photo luminescent materials for use in the display devices.

4.5. CONCLUSIONS

- A new series of mixed lanthanide metal–organic complexes [Eu^{3+}/Tb^{3+}/ Gd^{3+}] were synthesized based on novel a aromatic carboxylate ligand, namely, 4-(dipyridin-2-yl)aminobenzoic acid.
- All lanthanide metal–organic complexes are isostructural based upon the analyses of single crystal and powder X-ray diffractions.
- The designed mixed lanthanide metal–organic complexes are thermally stable and exhibit unique nano-rod like morphology.
- Most importantly, by varying concentration profiles of Ln^{3+} in mixed lanthanide metal–organic complexes and also varying the excitation wavelengths, white-light emission was achieved.
- In particular, precisely tuning the white-light emission of RGB-color systems will lead to promising applications in color displays, sensing and labelling.

List of Publications

List of Publications

1. **Ramya A. R**, M. L. P. Reddy, Alan H. Cowley and Kalyan V. Vasudevan. "Synthesis, crystal structure and photoluminescence of homodinuclear lanthanide 4-(dibenzylamino)benzoate complexes." ***Inorg. Chem.,*** 2010, *49*, 2407-2415.

2. **Ramya A. R**, Debajit Sharma, Srinivasan Natarajan and M. L. P. Reddy. "Highly luminescent and thermally stable lanthanide coordination polymers designed from 4-(di(pyridin-2-yl)amino)benzoate: Efficient energy transfer from Tb^{3+} to Eu^{3+} in mixed lanthanide coordination compound." ***Inorg. Chem.,*** 2012, *51*, 8818-8826.

3. **Ramya A. R**, Sunil Varughese and M. L. P. Reddy. "Tunable white-light emission from a mixed lanthanide (Eu^{3+}, Gd^{3+}, Tb^{3+}) coordination polymers derived from 4-(dipyridin-2-yl)amino benzoate." ***Dalton Trans.***, 2014, *43*, 10940-10946.

Contributions to academic conferences

1. **Ramya A. R**, M. L. P. Reddy, Alan H. Cowley and Kalyan V. Vasudevan. "Synthesis, crystal structure and photoluminescence of homodinuclear lanthanide 4-(dibenzylamino)benzoate complexes." International conference on materials for the new millennium, MatCon 2010, CUSAT, Kerala.

2. **Ramya A. R**, Debajit Sharma, Srinivasan Natarajan and M. L. P. Reddy. "Highly luminescent lanthanide cordination polymer based on 4-(dipyridin-2-ylamino)benzoic acid," 3rd Asian conference on coordination chemistry, ACCC-3, 2011, New Delhi.

REFERENCES

Ananias, D.; Kostova, M.; Almeida Paz, F. A.; Ferreira, A.; Carlos, L. D.; Klinowski, J.; Rocha, J. "Photoluminescent layered lanthanide silicates," *J. Am. Chem. Soc.*, *126*, **2004**, 10410-10417.

Armelao, L.; Quici, S.; Barigelletti, F.; Accorsi, G.; Bottaro, G.; Cavazzini, M.; Tondello, E. "Design of luminescent lanthanide complexes: From molecules to highly efficient photo-emitting materials," *Coord. Chem. Rev.*, *254*, **2010**, 487-505.

Artizzu, F.; Marchio, L.; Mercuri, M.; Pilia, L.; Serpe, A.; Quochi, F.; Orru, R. ;Cordella, F.; Mura, A.; Bongiovanni, G.; Deplano, P." New Insights on Near-Infrared Emitters Based on Er-quinolinolate Complexes: Synthesis, Characterization, Structural, and Photophysical Properties," *Adv. Funct. Mater., 17,* **2007**, 2365–2376.

Balamurugan, A.; Reddy, M. L. P.; Jayakannan, M. "Single Polymer Photosensitizer for Tb3+ and Eu3+ Ions: An Approach for White Light Emission Based on Carboxylic-Functionalized Poly(*m*-phenylenevinylene)s," *J. Phys. Chem. B.*, *113*, **2009**, 14128–14138.

Beeby, A.; Clarkson, I. M.; Dickins, R. S.; Faulkner, S.; Parker, D.; Royle, L.; de Sousa, A. S; Williams, J. A. G.; Woods, M. "Non-radiative deactivation of the excited states of europium, terbium and ytterbium complexes by proximate energy-matched OH, NH and CH oscillators: An improved luminescence method for establishing solution hydration states," *J. Chem. Soc. Perkin Trans., 2*, **1999**, 493-504.

Bettinelli, M.; Flint, C. D. " Non-resonant energy transfer between Tb^{3+} and Eu^{3+} in the cubic hexachloroelpasolite crystals $Cs_2NaTb_{1-x}Eu_xCl_6$ (x=0.01-0.15)," *J. Phys. Condens. Mater., 2*, **1990**, 8417–8426.

Biju, S.; Raj, D. B. A.; Reddy, M. L. P.; Kariuki, B. M. "Synthesis, crystal structure, and luminescent properties of novel Eu^{3+} heterocyclic *β*-diketonate complexes with bidentate nitrogen donors," *Inorg. Chem.*, *45*, **2006**, 10651-10660.

[a]Biju, S.; Reddy, M. L. P.; Cowley, A. H.; Vasudevan, K. V. "3-Phenyl-4-acyl-5-isoxazolonate complex of Tb^{3+} doped into poly-*β*-hydroxybutyrate matrix as a promising light-conversion molecular device," *J. Mater. Chem.*, *19*, **2009**, 5179-5187.

[b]Biju, S.; Raj, D. B. A.; Reddy, M. L. P.; Jayasankar, C. K.; Cowley, A. H.; Findlater, M. "Dual emission from stoichiometrically mixed lanthanide complexes of 3-phenyl-4-benzoyl-5-isoxazolonate and 2,2'-bipyridine," *J. Mater. Chem.*, *19*, **2009**, 1425-1432.

[c]Biju, S.; Reddy, M. L. P.; Cowley, A. H.; Vasudevan, K. V. "Molecular ladders of lanthanide-3-phenyl-4-benzoyl-5-isoxazolonate and bis(2-(diphenylphosphino)phenyl) ether oxide complexes: The role of the ancillary ligand in the sensitization of Eu^{3+} and Tb^{3+} luminescence," *Cryst. Growth. Des.*, *9*, **2009**, 3562-3569.

Binnemans, K. "Lanthanide-based luminescent hybrid materials," *Chem. Rev.*, *109*, **2009**, 4283-4374.

Binnemans, K.; Gorller-Walrand, C."Lanthanide-containing liquid crystals and surfactants," *Chem. Rev., 102*, **2002**, 2303-2345.

Bo, S; Juan, P.; Xiaotian, G.; Jianbo, Y.; Yanhui, Z.; Ying, Z.; Yunyou, W. "Synthesis and fluorescence studies on novel complexes of Tb(III) and Eu(III) with 4-(9H-carbazol-9-yl) benzoic acid," *J. Alloys Compd.*, *426*, **2006**, 363-367.

Bredol, M.; Kynast, U.; Ronda, C. "Designing luminescent materials," *Adv. Mater.*, *3*, **1991**, 361-367.

Bril, A.; de Jager-Veenis, A. W. "Quantum efficiency standard for ultraviolet and visible excitation," *J. Electrochem. Soc.*, *123*, **1976**, 396-398.

Brunet, E.; Juanes, O.; Rodriguez-Ubis, J. C. "Supramolecularly organized lanthanide complexes for efficient metal excitation and luminescence as sensors in organic and biological applications," *Curr. Chem. Biol.*, *1*, **2007**, 11-39.

Bünzli, J. C. G.; Piguet, C. "Taking advantage of luminescent lanthanide ions," *Chem. Soc. Rev.*, *34*, **2005**, 1048-1077.

Bünzli, J.-C. G. "Benefiting from the unique properties of lanthanide ions," *Acc. Chem. Res.*, *39*, **2006**, 53-61.

Bünzli, J.-C. G. "Lanthanide luminescence for biomedical analyses and imaging," *Chem. Rev.*, *110*, **2010**, 2729-2755.

Bünzli, J.-C. G.; Charbonniere, L. J.; Ziessel, R. F. "Structural and photophysical properties of Ln(III) complexes with 2,2'-bipyridine-6,6'-

dicarboxylic acid: Surprising formation of a H-bonded network of bimetallic entities," *J. Chem. Soc., Dalton Trans.*, **2000**, 1917-1923.

Bünzli, J.-C. G; Daiguebonne, C.; Kerbellec, N.; Guillou, O.; Gumy, F.; Catala, L.; Mallah, T.; Audebrand, N.; Gérault, Y.; Bernot, K.; Calvez, G. "Structural and luminescent properties of micro- and nanosized particles of lanthanide terephthalate coordination polymers," *Inorg. Chem., 47*, **2008**, 3700-3708.

Bünzli, J.-C. G.; Eliseeva, S. V. "Intriguing aspects of lanthanide luminescence," *Chem. Sci*., *4*, **2013**, 1939–1949.

Bünzli, J.-C. G.; Piguet, C. "Lanthanide-containing molecular and supramolecular polymetallic functional assemblies," *Chem. Rev.*, *102*, **2002**, 1897-1928.

Bunzli, J.-C. G. "Lanthanide probes in life, chemical and earth sciences: Theory and practice, ed. J.-C. G. Bunzli and G. R. Choppin, Elsevier, New York, **1989**, p. 219.

Busskamp, H.; Deacon, G. B.; Hilder, M.; Junk, P. C.; Kynast, U. H.; Lee, W. W.; Turner, D. R. "Structural variations in rare earth benzoate complexes Part I. lanthanum," *Cryst. Eng. Commun.*, *9*, **2007**, 394-411.

Cai, Y.-P.; Zhang, H.-X.; Xu, A.-W.; Su, C.-Y.; Chen, C.-L.; Liu, H.-Q.; Zhang, L.; Kang, B.-S. "Self-assembly of silver(I) polymers with single strand double-helical structures containing the ligand O,O'-bis(8-quinolyl)-1,8-dioxaoctane," *J. Chem. Soc., Dalton Trans.*, **2001**, 2429-2434.

Cambridge Structural Database, version 5.27. http//www.ccdc.ac.uk.

Carlos, L. D.; de Mello Donega, C.; Albuquerque, R. Q.; Alves, S.; Menezes, J. F. S.; Malta, O. L. "Highly luminescent europium(III) complexes with naphtoiltrifluoroacetone and dimethyl sulphoxide," *Mol. Phys.*, *101*, **2003**, 1037-1045.

Carnall, W. T. "In handbook on the physics and chemistry of rare earths," eds. K. A. Gschneidner, L. Eyring, Elsevier, Amsterdam, The Netherlands, **1987**, (Vol. 3), Chapter 24, 171.

Carnall, W. T.; Gruen, D. M.; McBeth, R. L." The Near-Infrared transitions of the trivalent lanthanide in solution. 1. praseodymium(III), neodymium (III), samarium(III), and europium(III) ions," *J. Phys. Chem., 66*, **1962**, 2159–2164.

Carnall, W. T. "The Near-Infrared transitions of the trivalent lanthanide in solution. II. Tb^{+3}, Dy^{+3}, Ho^{+3}, Er^{+3}, Tm^{+3}, and Yb^{+3}," *J. Phys. Chem., 67*, **1963**, 1206–1211.

Carnall, W. T.; Fields, P. R.; Wybourne, B. G. "Spectral Intensities of the Trivalent Lanthanides and Actinides in Solution. I. Pr^{3+}, Nd^{3+}, Er^{3+}, Tm^{3+}, and Yb^{3+}," *J. Chem. Phys., 42*, **1965,** 3797–3806.

Chen, B.; Yang, Y.; Zapata, F.; Qian, G.; Luo, Y.; Zhang, J.; Lobkovsky, E. B. "Enhanced near-infrared–luminescence in an erbium tetrafluoroterephthalate framework," *Inorg. Chem.*, *45*, **2006**, 8882-8886.

Chen, B.; Yang, Y.; Zapata, F.; Lin, G.; Qian, G.; Lobkovsky, E. B. "Luminescent open metal sites within a metal–organic framework for sensing small molecules," *Adv. Mater.*, *19*, **2007**, 1693-1696.

Chen, X. -F.; Zhu, X. -H.; Xu, Y. -H.; S. S. S. Raj.; Öztürk, S.; Fun, H. K.; Ma, J.; You, X. -Z. "Triboluminescence and crystal structures of non-ionic europium complexes," *J. Mater. Chem*., *9*, **1999**, 2919–2922.

Chen, X.-Y.; Bretonnière, Y.; Pécaut, J.; Imbert, D.; Bünzli, J.-C. G.; Mazzanti, M. "Selective self-assembly of hexameric homo- and heteropolymetallic lanthanide wheels: Synthesis, structure, and photophysical studies," *Inorg. Chem.*, *46*, **2007**, 625-637.

Choi, C. -L.; Yen, Y. -F.; Sung, H. H. -Y.; Siu, A. W. -H.; Jayarathne, S. T.; Wong, K. S.; Williams, I. D. "Quantifying enhanced photoluminescence in mixed-lanthanide carboxylate polymers: sensitization *versus* reduction of self-quenching," *J. Mater. Chem., 21*, **2011**, 8547–8549.

Cölle, M.; Gmeiner, J.; Milius, W.; Hillebrecht, H.; Brütting, W. "Preparation and characterization of blue-luminescent tris(8-hydroxyquinoline)aluminum (Alq_3)," *Adv. Funct. Mater.*, *13*, **2003**, 108-112.

Comby, S.; Imbert, D.; Chauvin, A.-S.; Bünzli, J.-C. G.; Charbonnière, L. J.; Ziessel, R. F. "Influence of anionic functions on the coordination and photophysical properties of lanthanide(III) complexes with tridentate bipyridines," *Inorg. Chem.*, *43*, **2004**, 7369-7379.

Comby, S.; Scopelliti, R.; Imbert, D.; Charbonniere, L.; Ziessel, R. F.; Bünzli, J.-C. G. "Dual Emission from Luminescent Nonalanthanide Clusters," *Inorg. Chem., 45*, **2006**, 3158-3160.

Cotton, S. "John Wiley & Sons Ltd, Lanthanide and Actinide Chemistry," *Uppingham* School, Uppingham, Rutland*, UK*, **2006**, p. 51.

Dang, S.; Zhan, J. -H.; Sun, Z. -M. "Tunable emission based on lanthanide(III) metal–organic frameworks: an alternative approach to white light," *J. Mater. Chem*., 22, **2012**, 8868–8873.

Deacon, G. B.; Hein, S.; Junk, P. C.; Jüstel, T.; Lee, W.; Turner, D. R. "Structural variations in rare earth benzoate complexes: Part II. yttrium and terbium," *Cryst. Eng. Commun.*, *9*, **2007**, 1110-1123.

Deacon, G. B.; Phillips, R. J. "Relationships between the carbon-oxygen stretching frequencies of carboxylato complexes and the type of carboxylate coordination," *Coord. Chem. Rev., 33*, **1980**, 227-250.

de Bettencourt-Dias, A. "Lanthanide-based emitting materials in light-emitting diodes," *Dalton Trans.,* **2007**, 2229-2241.

de Bettencourt-Dias, A. "Isophthalato-based 2D coordination polymers of Eu(III), Gd(III), and Tb(III): Enhancement of the terbium-centered luminescence through thiophene derivatization," *Inorg. Chem.*, *44*, **2005**, 2734-2741.

de Bettencourt-Dias, A.; Viswanathan, S. "Nitro-functionalization and luminescence quantum yield of Eu(III) and Tb(III) benzoic acid complexes," *Dalton Trans.*, **2006**, 4093-4103.

de Bettencourt Dias, A.; Viswanathan, S. "Luminescent Ln^{3+} nitrobenzoato complexes: First examples of sensitization of green and red emission," *Chem. Commun.*, **2004**, 1024-1025.

de Lill, D. T.; Cahill, C. L. " An unusually high thermal stability within a novel lanthanide 1,3,5-cyclohexanetricarboxylate framework: synthesis, structure, and thermal data," *Chem.Commun*., *47*, **2006**, 4946–4948.

de Lill, D. T.; de Bettencourt-Dias, A.; Cahill, C. L. "Exploring Lanthanide Luminescence in Metal-Organic Frameworks: Synthesis, Structure, and Guest-Sensitized Luminescence of a Mixed Europium/Terbium-Adipate Framework and a Terbium-Adipate Framework," *Inorg.Chem*., *46*, **2007**, 3960-3965.

de Mello Donega, C.; Junior, S. A.; De Sa, G. F. "Europium(III) mixed complexes with β-diketones and O-phenanthroline-N-oxide as promising light-conversion molecular devices," *Chem. Commun.*, **1996**, 1199-1200.

de Mello, J. C.; Wittmann, H. F.; Friend, R. H. "An improved experimental determination of external photoluminescence quantum efficiency," *Adv. Mater.*, *9*, **1997**, 230-232.

de Sá, G. F.; Malta, O. L.; de Mello Donegá, C.; Simas, A. M.; Longo, R. L.; Santa-Cruz, P. A.; da Silva Jr, E. F. "Spectroscopic properties and design of highly luminescent lanthanide coordination complexes," *Coord. Chem. Rev.*, *196*, **2000**, 165-195.

De Silva, C. R.; Li, J.; Zheng, Z.; Corrales, L. R. "Correlation of calculated excited-state energies and experimental quantum yields of luminescent Tb(III) *β*-diketonates," *J. Phys. Chem. A.*, *112*, **2008**, 4527-4530.

Dexter, D. L. "A theory of sensitized luminescence in solids," *J. Chem. Phys.*, *21*, **1953**, 836-851.

Divya, V.; Biju, S.; Varma, R. L.; Reddy, M. L. P. "Highly efficient visible light sensitized red emission from europium tris[1-(4-biphenoyl)-3-(2-fluoroyl)propanedione](1,10-phenanthroline) complex grafted on silica nanoparticles," *J. Mater. Chem.*, *20*, **2010**, 5220-5227.

Dieke, G. H. "Spectra and energy levels of rare earth ions in crystals," Interscience, New York, **1968**.

Døssing, A. "Luminescence from lanthanide($^{3+}$) ions in solution," *Eur. J. Inorg. Chem.*, **2005**, 1425-1434.

Eddaudi, M.; Kim, J.; Wachter, J. B.; Chae, H. K.; O'Keeffe, M.; Yaghi, O. M. "Porous metal–organic polyhedra: 25 Å Cuboctahedron constructed from 12 $Cu_2(CO_2)_4$ paddle-wheel building blocks," *J. Am. Chem. Soc.*, *123*, **2001**, 4368-4369.

Elhabiri, M.; Scopelliti, R.; Bünzli, J.-C. G.; Piguet, C. "Lanthanide helicates self-assembled in water: A new class of highly stable and luminescent dimetallic carboxylates," *J. Am. Chem. Soc.*, *121*, **1999**, 10747-10762.

Eliseeva, S. V.; Bünzli, J.-C. G. "Lanthanide luminescence for functional materials and bio-sciences," *Chem. Soc. Rev.*, *39*, **2010**, 189-227.

Eliseeva, S. V.; Kotova, O. V.; Gumy, F.; Semenov, S. N.; Kessler, V. G.; Lepnev, L. S.; Bünzli, J.-C. G.; Kuzmina, N. P. "Role of the ancillary ligand N,N-dimethylaminoethanol in the sensitization of Eu(III) and Tb(III) luminescence in dimeric *β*-diketonates," *J. Phys. Chem. A.*, *112*, **2008**, 3614-3626.

Farinola, G. M.; R. Ragni. "Electroluminescent materials for white organic light emitting diodes," *Chem. Soc. Rev.*, *40*, **2011**, 3467–3482.

Farrugia, J. L. "WinGX suite for small-molecule single-crystal crystallography," *J. App. Crystallogr.*, *32*, **1999**, 837–838.

Feng, J.; Zhang, H. "Hybrid materials based on lanthanide organic complexes: a review," *Chem. Soc. Rev.*, *42*, **2013**, 387–410.

Fiedler, T.; Hilder, M.; Junk, P. C.; Kynast, U. H.; Lezhnina, M. M.; Warzala, M. "Synthesis, structural and spectroscopic studies on the lanthanoid *p*-aminobenzoates and derived optically functional polyurethane composites," *Eur. J. Inorg. Chem.*, **2007**, 291-301.

Fomina, I.; Dobrokhotova, Z.; Aleksandrov, G.; Emelina, A.; Bykov, M.; Malkerova, I.; Bogomyakov, A.; Puntus, L.; Novotortsev, V.; Eremenko, I. "Novel 1D coordination polymer $\{Tm(Piv)_3\}_n$: Synthesis, structure, magnetic properties and thermal behavior," *J. Solid State Chem.*, *185*, **2012**, 49-55.

Francis, B.; Ambili Raj, D. B.; Reddy, M. L. P. "Highly efficient luminescent hybrid materials covalently linking with europium(III) complexes *via* a

novel fluorinated *β*-diketonate ligand: Synthesis, characterization and photophysical properties," *Dalton Trans.*, *39*, **2010**, 8084-8092.

Fratini, A.; Richards, G.; Larder, E.; Swavey, S. "Neodymium, gadolinium, and terbium complexes containing hexafluoroacetylacetonate and 2,2′-bipyrimidine: Structural and spectroscopic characterization," *Inorg. Chem.*, *47*, **2008**, 1030-1036.

Froidevaux, P.; Bünzli, J.-C. G. "Energy-transfer processes in lanthanide dinuclear complexes with p-tert- butylcalix[8]arene: an example of dipole-dipolar mechanism," *J. Phys. Chem., 98*, **1994**, 532-536.

Fu, L.; Sa Ferreira, R. A.; Silva, N. J. O.; Fernandes, J. A.; Ribeiro-Claro, P.; Goncüalves, I. S.; de Zea Bermudez, V.; Carlos, L. D. "Structure-photoluminescence relationship in Eu(III) *β*-diketonate-based organic-inorganic hybrids: Influence of the synthesis method: Carboxylic acid solvolysis versus conventional hydrolysis," *J. Mater. Chem., 15*, **2005**, 3117-3125.

Glover, P. B.; Bassett, A. P.; Nockemann, P.; Kariuki, B. M.; Van Deun, R.; Pikramenou, Z. "Fully fluorinated imidodiphosphinate shells for visible- and NIR-emitting lanthanides: Hitherto unexpected effects of sensitizer fluorination on lanthanide emission properties," *Chem. Eur. J.*, *13*, **2007**, 6308-6320.

Georges, J; Arnaud, N. "Influence of pH, surfactant and synergic agent on the luminescent properties of terbium chelated with benzoic acid derivatives in aqueous solutions," *Analyst*., *125*, **2000**, 1487-1490.

Gulgas, C. G.; Reineke, T. M. "Synthesis, characterization, and luminescence properties of a new series of Eu^{3+}-containing macrocycles," *Inorg. Chem.*, *44*, **2005**, 9829-9836.

Guo, H.; Zhu, Y.; Qiu, S.; Lercher, J. A.; Zhang, H. "Coordination Modulation Induced Synthesis of Nanoscale $Eu_{1-x}Tb_x$-Metal-Organic Frameworks for Luminescent Thin Films," *Adv. Mater., 22*, **2010**, 4190–4192.

Gunnlaugsson, T.; Leonard, J. P. "Responsive lanthanide luminescent cyclen complexes: from switching/sensing to supramolecular architectures," *Chem. Commun.*, **2005**, 3114-3131.

Hao, J.; Studenikin, S. A.; Cocivera, M. "Blue, green and red cathodoluminescence of Y_2O_3 phosphor films prepared by spray pyrolysis," *J. Lumin., 93*, **2001**, 313-319.

Heffern, M. C.; Matosziuk, L. M.; Meade, T. J. "Lanthanide Probes for Bioresponsive Imaging," *Chem. Rev.*, *114*, **2014**, 4496–4539.

Heine, J.; Muller-Buschbaum, K. "Engineering metal-based luminescence in coordination polymers and metal–organic frameworks," *Chem. Soc. Rev.,* 42, **2013**, 9232–9242.

Hilder, M.; Peter, C. J.; Ulrich, H. K.; Marina, M. L. "Spectroscopic properties of lanthanoid benzene carboxylates in the solid state: Part 1," *J. Photochem. Photobiol. A.*, *202*, **2009**, 10-20.

Hilder, M.; Lezhnina, M.; Cole, M. L.; Forsyth, C. M.; Junk, P. C.; Kynast, U. H. "Spectroscopic properties of lanthanoid benzene carboxylates in the

solid state: Part 2. Polar substituted benzoates," *J. Photochem. Photobiol. A.*, *217*, **2011**, 76-86.

Jaffres, P.m-A; Rueff, J. -M.; Barrier, N.; Boudin, S.; Dorcet, V.; Caignaert, V.; Boullay, P.; Hix, G. B. "Remarkable thermal stability of Eu(4-phosphonobenzoate): Structure investigations and luminescence properties," *Dalton Trans.*, **2009**, 10614-10620.

Jüstel, T.; Nikol, H.; Ronda, C. "New Developments in the Field of Luminescent Materials for Lighting and Displays," *Angew. Chem. Int. Ed., 37*, **1998**, 3084-3103.

Kai, J.; Parra, D. F.; Brito, H. F. "Polymer matrix sensitizing effect on photoluminescence properties of Eu^{3+}-*β*-diketonate complex doped into poly-*β*-hydroxybutyrate (PHB) in film form," *J. Mater. Chem.*, *18*, **2008**, 4549-4554.

Kajiwara, T.; Hasegawa, M.; Ishii, A.; Katagiri, K.; Baatar, M.; Takaishi, S.; Iki, N.; Yamashita, M. "Highly Luminescent Superparamagnetic Diterbium(III) Complex Based on the Bifunctionality of p- tert-Butylsulfonylcalix[4]arene," *Eur. J. Inorg. Chem*., *36***, 2008,** 5565–5568.

Kawa, M.; Fréchet, J. M. J. "Self-assembled lanthanide-cored dendrimer complexes: Enhancement of the luminescence properties of lanthanide ions through site-isolation and antenna effects," *Chem. Mater.*, *10*, **1998**, 286-296.

Kellendonk, F.; Blasse, G. "Luminescence and energy transfer in $EuAl_3B_4O_{12}$," *J. Chem. Phys., 75*, **1981**, 561.

Kerbellec, N.; Kustaryono, D.; Haquin, V.; Etienne, M.; Diaguebonne, C.; Guillou, O. "An Unprecedented Family of Lanthanide-Containing Coordination Polymers with Highly Tunable Emission Properties," *Inorg. Chem.***,** *48*, **2009**, 2837-2843.

Kido, J.; Okamoto, Y. "Organo lanthanide metal complexes for electroluminescent materials," *Chem. Rev.*, *102*, **2002**, 2357-2368.

Kim Anh, T.; Strek, W. "Dynamics of energy transfer in $Tb_{1-x}Eu_xP_5O_{14}$ crystals," *J. Lumin., 42*, **1988**, 205–210.

Kim, Y. H.; Baek, N. S.; Kim, H. K. "Sensitized emission of luminescent lanthanide complexes based on 4-naphthalen-1-yl-benzoic acid derivatives by a charge-transfer process," *ChemPhysChem.*, *7*, **2006**, 213-221.

Kirin, S. I.; Yennawar, H. P.; Williams, M. E. "Synthesis and Characterization of Cu^{II} Complexes with Amino Acid Substituted Di(2-pyridyl)amine Ligands," *Eur. J. Inorg. Chem., 23*, **2007**, 3686–3694.

Kon, K. K.; Hong, Y.-R.; Lee, S.-W.; Jin, J.-I.; Park, Y.; Sohn, B.-H.; Kim, W.-H.; Park, J.-K. "Synthesis and luminescence properties of poly(-phenylenevinylene) derivatives carrying directly attached carbazole pendants," *J. Mater. Chem.*, *11*, **2001**, 3023-3030.

Kuriki, K.; Koike, Y.; Okamoto, Y. "Plastic optical fiber lasers and amplifiers containing lanthanide complexes," *Chem. Rev., 102*, **2002**, 2347-2356.

Lam A. W.-H.; Wong, W.-T.; Gao, S.; Wen, G.; Zhang, X.-X. "Synthesis, crystal structure, and photophysical and magnetic properties of dimeric and polymeric lanthanide complexes with benzoic acid and its derivatives," *Eur. J. Inorg. Chem.*, **2003**, 149-163.

Latva, M.; Takalo, H.; Mukkala, V.-M.; Matachescu, C.; Rodríguez-Ubis, J. C.; Kankare, J. "Correlation between the lowest triplet state energy level of the ligand and lanthanide(III) luminescence quantum yield," *J. Lumin.*, *75*, **1997**, 149-169.

Lehn, J. "Perspectives in supramolecular chemistry-From molecular recognition towards molecular information processing and self-organization," *Angew. Chem. Int. Ed.*, *29*, **1990**, 1304-1319.

Lewis, D. J.; Glover, B. G.; Solomons, M. C.; Pikramenou, Z. "Purely Heterometallic Lanthanide(III) Macrocycles through Controlled Assembly of Disulfide Bonds for Dual Color Emission," *J. Am. Chem. Soc., 133*, **2011**, 1033–1043.

Lewis, G. N.; Kasha, M. "Phosphorescence and the triplet state," *J. Am. Chem. Soc.*, *66*, **1944**, 2100-2116.

Li, H. R.; Lin, J.; Zhang, H. J.; Fu, L. S.; Meng, Q. G.; Wang, S. B. "Preparation and luminescence properties of hybrid materials containing

europium(III) complexes covalently bonded to a silica matrix," *Chem. Mater.*, *14*, **2002**, 3651-3655.

Li, X.; Zhang, Z.-Y.; Zou, Y.-Q. "Synthesis, structure and luminescence properties of four novel terbium 2-fluorobenzoate complexes," *Eur. J. Inorg. Chem.,* **2005**, 2909-2918.

Li, Y.; Zheng, F.-K.; Liu, X.; Zou, W.-Q.; Guo, G.-C.; Lu, C.-Z.; Huang, J.-S. "Crystal structures and magnetic and luminescent properties of a series of homodinuclear lanthanide complexes with 4-cyanobenzoic ligand," *Inorg. Chem.*, *45*, **2006**, 6308-6316.

Liu, M. -S.; Yu, Q. -Y.; Cai, Y. -P.; Su, C. -Y.; Lin, X. -M.; Zhou, X. -X.; Cai, J. -W. "One-, two-, and three-dimensional lanthanide complexes constructed from pyridine-2,6-dicarboxylic acid and oxalic acid ligands," *Cryst. Growth. Des.*, *8*, **2008**, 4083-4091.

Liu, Y.; Pan, M.; Yang, Q. -Y; Fu, L.; Li, K.; Wei, S. -C; Su, C. -Y. "Dual-Emission from a Single-Phase Eu–Ag Metal–Organic Framework: An Alternative Way to Get White-Light Phosphor," *Chem*. *Mater*., *24*, **2012**, 1954–1960.

Louise S. Natrajan, L. S.; Phillipa L. Timmins, P. L.; Matthew Lunn, M.; Heath, S. L. "Luminescent Dinuclear Lanthanide Complexes of 5-Me-HXTA," *Inorg. Chem., 46*, **2007**, 10877–10886.

Lucky, M. V.; Sivakumar, S.; Reddy, M. L. P.; Paul, A. K.; Natarajan, S. "Lanthanide luminescent coordination polymer constructed from unsymmetrical

dinuclear building blocks based on 4-((1H-benzo[d]imidazol-1-yl)methyl)benzoic acid," *Cryst. Growth Des.*, *11*, **2011**, 857-864.

Ma, M. -L.; Ji, C.; Zang, S.-Q. "Syntheses, structures, tunable emission and white light emitting Eu^{3+} and Tb^{3+} doped lanthanide metal–organic framework materials," *Dalton Trans*., 42, **2013**, 10579–10586.

Ma, X.; Li, X.; Cha, Y. -E.; Jin, L. -P. "Highly Thermostable One-Dimensional Lanthanide(III) Coordination Polymers Constructed from Benzimidazole-5,6-dicarboxylic Acid and 1,10-Phenanthroline: Synthesis, Structure, and Tunable White-Light Emission," *Cryst. Growth Des.,* 12, **2012**, 5227–5232.

Mahata, P.; Ramya, K.; Natarajan, S. "Pillaring of $CdCl_2$-like layers in lanthanide metal-organic frameworks: Synthesis, structure, and photophysical properties," *Chem. Eur. J., 14*, **2008**, 5839-5850.

Mech, A.; Monguzzi, A.; Meinardi, F.; Mezyk, J.; Macchi, G.; Tubino, R. "Sensitized NIR erbium(III) emission in confined geometries: A new strategy for light emitters in telecom applications," *J. Am. Chem. Soc.*, *132*, **2010**, 4574-4576.

Melhuish, W.H. “Measurement of quantum efficiencies of fluorescence and phosphorescence and some suggested luminescence standards,” *J. Opt. Soc. Am., 54,* **1964**, 183.

Miyata, K.; Nakagawa, T.; Kawakami, R.; Kita, Y.; Sugimoto, K.; Nakashima, T.; Harada, T.; Kawai, T.; Hasegawa, Y. "Remarkable luminescence

properties of lanthanide complexes with asymmetric dodecahedron structures," *Chem. Eur. J., 17*, **2011**, 521-528.

Moore, E. G.; Samuel, A. P. S.; Raymond, K. N. "From Antenna to Assay: Lessons Learned in Lanthanide Luminescence," *Acc. Chem. Res.*, *42*, **2009**, 542-552.

Nasso, I.; Bedel, S.; Galaup, C.; Picard, C. "A water-stable and strongly luminescent terbium(III) macrocyclic complex incorporating an intracyclic pyrazolylpyridine chromophore," *Eur. J. Inorg. Chem.*, **2008**, 2064-2074.

Nie, D.; Chen, Z.; Bian, Z.; Zhou, J.; Liu, Z.; Chen, F.; Zhao, Y.; Huang, C. "Energy transfer pathways in the carbazole functionalized *β*-diketonate europium complexes," *New J. Chem.*, *31*, **2007**, 1639-1646.

Norton, K.; Kumar, G. A.; Dilks, J. L.; Emge, T. J.; Riman, R. E.; Brik, M. G.; Brennan, J. G. "Lanthanide compounds with fluorinated aryloxide ligands: Near-infrared emission from Nd, Tm, and Er," *Inorg. Chem.*, *48*, **2009**, 3573-3580.

Palsson, L. O.; Monkman, A. P. "Measurements of solid-state photoluminescence quantum yields of films using a fluorimeter," *Adv. Mater.*, *14*, **2002**, 757-758.

Pan, L.; Sander, M. B.; Huang, X.; Li, J.; Smith, M.; Bittner, E.; Bockrath, B.; Johnson, J. K. "Microporous metal organic materials: Promising candidates as sorbents for hydrogen sftorage," *J. Am. Chem. Soc.*, *126*, **2004**, 1308-1309.

Pandya, S.; Yu, J.; Parker, D. "Engineering emissive europium and terbium complexes for molecular imaging and sensing," *Dalton Trans.,* **2006**, 2757-2766.

Parker, D. "Luminescent lanthanide sensors for pH, pO2 and selected anions," *Coord. Chem. Rev.*, *205*, **2000**, 109-130.

Parker, D. "Excitement in f block: Structure, dynamics and function of nine-coordinate chiral lanthanide complexes in aqueous media," *Chem. Soc. Rev., 33*, **2004**, 156-165.

Parker, D.; Williams, J. A. G. "The lanthanides and their interrelation with biosystems," M. Dekker, Inc., New York, **2003**, (Vol. 40), 233.

Pavithran, R.; Reddy, M. L. P.; Junior, S. A.; Freire, R. O.; Rocha, G. B.; Lima, P. P. "Synthesis and luminescent properties of novel Europium(III) heterocyclic *β*-diketone complexes with lewis bases: Structural analysis using the sparkle/AM1 model," *Eur. J. Inorg. Chem.*, **2005**, 4129-4137.

Pavithran, R.; Saleesh Kumar, N. S.; Biju, S.; Reddy, M. L. P.; Junior, S. A.; Freire, R. O. "3-Phenyl-4-benzoyl-5-isoxazolonate complex of Eu^{3+} with tri-n-octylphosphine oxide as a promising light-conversion molecular device," *Inorg. Chem.*, *45*, **2006**, 2184-2192.

Petoud, S.; Cohen, S. M.; Bünzli, J.-C. G.; Raymond, K. N. "Stable lanthanide luminescence agents highly emissive in aqueous solution: Multidentate 2-hydroxyisophthalamide complexes of Sm^{3+}, Eu^{3+}, Tb^{3+}, Dy^{3+}," *J. Am. Chem. Soc.*, *125*, **2003**, 13324-13325.

Pflugrath, J. W. "The finer things in X-ray diffraction data collection," *Acta Crystallogr, Sect. D., 55*, **1999**, 1718–1725.

Picot, A.; D'Aléo, A.; Baldeck, P. L.; Grichine, A.; Duperray, A.; Andraud, C.; Maury, O. "Long-lived two-photon excited luminescence of water-soluble europium complex: Applications in biological imaging using two-photon scanning microscopy," *J. Am. Chem. Soc.*, *130*, **2008**, 1532-1533.

Piguet, C.; Bünzli, J. C. G. "Mono-and polymetallic lanthanide-containing functional assemblies: A field between tradition and novelty," *Chem. Soc. Rev.*, *28*, **1999**, 347-358.

Piguet, C.; Bünzli, J. C. G.; Bernardinelli, G.; Hopfgartner, G.; Williams, A. F. "Self-assembly and photophysical properties of lanthanide dinuclear triple-helical complexes," *J. Am. Chem. Soc.*, *115*, **1993**, 8197-8206.

Quici, S.; Cavazzini, M.; Marzanni, G.; Accorsi, G.; Armaroli, N.; Ventura, B.; Barigelletti, F. "Visible and near-infrared intense luminescence from water-soluble lanthanide [Tb(III), Eu(III), Sm(III), Dy(III), Pr(III), Ho(III), Yb(III), Nd(III), Er(III)] complexes," *Inorg. Chem., 44*, **2005**, 529-537.

Raj, D. B. A.; Biju, S.; Reddy, M. L. P. "One-, two-, and three-dimensional arrays of Eu^{3+}-4,4,5,5,5-pentafluoro-1-(naphthalen-2-yl)pentane-1,3-dione complexes: Synthesis, crystal structure and photophysical properties," *Inorg. Chem.*, *47*, **2008**, 8091-8100.

Raj, D. B. A.; Francis, B.; Reddy, M. L. P.; Butorac, R. R.; Lynch, V. M.; Cowley, A. H. "Highly luminescent poly(methylmethacrylate)-incorporated europium complex supported by a carbazole-based fluorinated *β*-diketonate ligand and a 4,5-bis(diphenylphosphino)-9,9-dimethylxanthene oxide co-ligand," *Inorg. Chem.*, *49*, **2010**, 9055-9063.

Raj, D. B. A; Biju, S.; Reddy, M. L. P. "Highly luminescent europium(iii) complexes containing organosilyl 4,4,5,5,5-pentafluoro-1-(naphthalen-2-yl)pentane-1,3-dionate ligands grafted on silica nanoparticles," *J. Mater. Chem.*, *19*, **2009**, 7976-7983.

Rao, C. N. R.; Natarajan, S.; Vaidhyanathan, R. "Metal Carboxylates with Open Architectures," *Angew. Chem. Int. Ed.*, *43*, **2004**, 1466-1496.

Rao, X.; Huang, Q.; Yang, X.; Cui, Y.; Yang, Y.; Wu, C.; Chen, B.; Qian, G. "Color tunable and white light emitting Tb^{3+} and Eu^{3+} doped lanthanide metal–organic framework materials," *J. Mater. Chem*., 22, **2012**, 3210–3214.

Ramya, A. R.; Reddy, M. L. P.; Cowley, A. H.; Vasudevan, K. V. "Synthesis, crystal structure, and photoluminescence of homodinuclear lanthanide 4-(dibenzylamino)benzoate complexes," *Inorg. Chem.*, *49*, **2010**, 2407-2415.

Ramya, A. R.; Sharma, D.; Natarajan, S.; Reddy, M. L. P. "Highly luminescent and thermally stable lanthanide coordination polymers designed from 4-

(dipyridin-2-yl)aminobenzoate: Efficient energy transfer from Tb^{3+} to Eu^{3+} in a mixed lanthanide coordination compound," *Inorg. Chem.*, *51*, **2012**, 8818-8826.

Raphael, S., Reddy, M. L. P., Vasudevan, K. V., Cowley. A. H. "Synthesis, crystal structure and photophysical properties of lanthanide coordination polymers of 4-[4-(9H-carbazol-9-yl)butoxy]benzoate: The effect of bidentate nitrogen donors on luminescence," *Dalton Trans.*, *48*, **2012,** 14671–14682.

Raphael, S.; Biju, S.; Reddy, M. L. P.; Cowley, A. H.; Findlater, M. "Synthesis, crystal structures, and photophysical properties of homodinuclear lanthanide xanthene-9-carboxylates," *Inorg. Chem.*, *46*, **2007**, 11025-11030.

Raphael, S.; Reddy, M. L. P.; Cowley, A. H.; Findlater, M. "2-Thiopheneacetato-based one-dimensional coordination polymer of Tb^{3+}: Enhancement of terbium-centered luminescence in the presence of bidentate nitrogen donor ligands," *Eur. J. Inorg. Chem.*, **2008**, 4387-4394.

Reddy, M. L. P.; Sivakumar, S. "Lanthanide benzoates: a versatile building block for the construction of efficient light emitting materials," *Dalton Trans.*, *42*, **2013**, 2663-2678.

Remya, P. N.; Biju, S.; Reddy, M. L. P.; Cowley, A. H.; Findlater, M. "1D molecular ladder of the ionic complex of terbium-4-sebacoylbis(1-phenyl-3-methyl-5-pyrazolonate) and sodium dibenzo-18-crown-6: Synthesis,

crystal structure, and photophysical properties," *Inorg. Chem.*, *47*, **2008**, 7396-7404.

Rheingold, A. L.; King, W. "Crystal structures of three brilliantly triboluminescent centrosymmetric lanthanide complexes: piperidinium tetrakis(benzoylacetonato)europate, hexakis(antipyrine)terbium triiodide, and hexaaquadichloroterbium chloride," *Inorg. Chem., 28*, **1989**, 1715–1719.

Reineke, S.; Lindner, F.; Schwartz, G.; Seidler, N.; Walzer, K.; Lussem, B.; Leo, K. "White organic light-emitting diodes with fluorescent tube efficiency," *Nature.*, *459*, **2009**, 234 – 238.

Rocha, J.; Carlos, L. D.; Paza, F. A. A.; Ananias, D. "Luminescent multifunctional lanthanides-based metal-organic frameworks," *Chem. Soc. Rev.*, *40*, **2011**, 926-940.

Roesky, H.; Andruh, M. "The interplay of coordinative, hydrogen bonding and π–π stacking interactions in sustaining supramolecular solid-state architectures: A study case of bis (4-pyridyl)- and bis (4-pyridyl-N-oxide) tectons," *Coord. Chem. Rev.*, *236*, **2003**, 91-119.

Sabbatini, N.; Guardigli, M.; Lehn, J.-M. "Luminescent lanthanide complexes as photochemical supramolecular devices," *Coord. Chem. Rev.*, *123*, **1993**, 201-228.

Sabbatini, N.; Mecati, A.; Guardigli, M.; Balzani, V.; Lehn, J. M.; Zeissel, R.; Ungaro, R. "Lanthanide luminescence in supramolecular species," *J. Lumin.*, *48-49, Part 2*, **1991**, 463-468.

Saleesh Kumar, N. S.; Varghese, S.; Rath, N. P.; Das, S. "Solid state optical properties of 4-alkoxy-pyridine butadiene derivatives: Reversible thermal switching of luminescence," *J. Phys. Chem. C.*, *112*, **2008**, 8429-8437.

Samuel, A. P. S.; Moore, E. G.; Melchior, M.; Xu, J.; Raymond, K. N. "Water-soluble 2-hydroxyisophthalamides for sensitization of lanthanide luminescence," *Inorg. Chem*., 47, **2008**, 7535−7544.

Santos, P. C. R. S.; Nogueira, H. I. S.; Paz, F. A. A.; Ferreira, R. A. S.; Carlos, L. D.; Klinowski, J.; Trindade, T. "Lanthanide complexes of 2,6-dihydroxybenzoic acid: Synthesis, crystal structures and luminescent properties of $[n\mathrm{Bu_4N}]_2[\mathrm{Ln(2,6\text{-}dhb)_5(H_2O)_2}]$ (Ln = Sm and Tb)," *Eur. J. Inorg. Chem.*, *19*, **2003**, 3609-3617.

Sendor, D.; Hilder, M.; Juestel, T.; Junk, P. C.; Kynast, U. H. "One dimensional energy transfer in lanthanoid picolinates. Correlation of structure and spectroscopy," *New J. Chem*., *27*, **2003**, 1070−1077.

Shah, B. K.; Neckers, D. C.; Shi, J.; Forsythe, E. W.; Morton, D. "Anthanthrene derivatives as blue emitting materials for organic light-emitting diode applications," *Chem. Mater.*, *18*, **2006**, 603-608.

[a]Shavaleev, N. M.; Eliseeva, S. V.; Scopelliti, R.; Bünzli, J.-C. G. "Designing simple tridentate ligands for highly luminescent europium complexes," *Chem. Eur. J.*, *15*, **2009**, 10790-10802.

[b]Shavaleev, N. M.; Scopelliti, R.; Gumy, F.; Bünzli, J.-C. G. "Benzothiazole- and benzoxazole-substituted pyridine-2-carboxylates as efficient sensitizers of europium luminescence," *Inorg. Chem.*, *48*, **2009**, 6178-6191.

Shavaleev, N. M.; Eliseeva, S. V.; Scopelliti, R.; Bünzli, J.-C. G. "N-aryl chromophore ligands for bright europium luminescence," *Inorg. Chem.*, *49*, **2010**, 3927-3936.

Sheldrick, G. M. *Siemens Area Correction Absorption Correction Program;* University of Gottingen: Gottingen, Germany, 1994.

Sheldrick, G. M. SHELXL-97 *Program for Crystal Structure Solution and Refinement*; University of Gottingen: Gottingen, Germany, 1997.

Shi, M.; Li, F.; Yi, T.; Zhang, D.; Hu, H.; Huang, C. "Tuning the triplet energy levels of pyrazolone ligands to match the $^5D_0$ level of europium(III)," *Inorg. Chem.*, *44*, **2005**, 8929-8936.

Shunmugam, R.; Tew, G. "White-light emission from mixing blue and red-emitting metal complexes," *Polym. Adv. Technol.*, *19*, **2008**, 596-601.

Sivakumar, S.; Reddy, M. L. P.; Cowley, A. H.; Butorac, R. R. "Lanthanide-based coordination polymers assembled from derivatives of 3,5-dihydroxy

benzoates: Syntheses, crystal structures, and photophysical properties," *Inorg. Chem.*, *50*, **2011**, 4882-4891.

Sivakumar, S.; Reddy, M. L. P.; Cowley, A. H.; Vasudevan, K. V. "Synthesis and crystal structures of lanthanide 4-benzyloxy benzoates: Influence of electron-withdrawing and electron-donating groups on luminescent properties," *Dalton Trans.*, *39*, **2010**, 776-786.

Sivakumar, S; Reddy, M. L. P. "Bright green luminescent molecular terbium plastic materials derived from 3,5-bis(perfluorobenzyloxy)benzoate," *J. Mater. Chem*., *22*, **2012**, 10852-10859.

SMART (version 5.628), SAINT (version 6.45a), XPREP, SHELXTL; Bruker AXS Inc.: Madison, WI, 2004.

Soares-Santos, P. C. R.; Cunha-Silva, L.; Paz, F. A. A.; Ferreira, R. A. S.; Rocha, J.; Carlos, L. D.; Nogueira, H. I. S. "Photoluminescent lanthanide-organic bilayer networks with 2,3-pyrazinedicarboxylate and oxalate," *Inorg. Chem.*, *49*, **2010**, 3428-3440.

Song, S.; Li, X.; Zhang, Y. -H. "White light emission of an Eu(III)-doped Gd(III) complex with 3-sulfobenzoate and 1H-imidazo[4,5-f][1,10]-phenanthroline," *Dalton Trans*., 42, **2013**, 10409–10412.

Song, X.; Zhou, X.; Liu, W.; Dou, W.; Ma, J.; Tang, X.; Zheng, J. "Synthesis, structures, and luminescence properties of lanthanide complexes

with structurally related new tetrapodal ligands featuring salicylamide pendant arms," *Inorg. Chem.*, *47*, **2008**, 11501-11513.

Stanley, J. M.; Zhu, X.; Yang, X.; Holliday, B. J. "Europium complexes of a novel ethylenedioxythiophene-derivatized bis(pyrazolyl)pyridine ligand exhibiting efficient lanthanide sensitization," *Inorg. Chem.*, *49*, **2010**, 2035-2037.

Steemers, F. J.; Verboom, W.; Reinhoudt, D. N.; van der Tol, E. B.; Verhoeven, J. W. "New sensitizer-modified calix[4]arenes enabling near-UV excitation of complexed luminescent lanthanide ions," *J. Am. Chem. Soc.*, *117*, **1995**, 9408-9414.

Sun, H.-L.; Ye, C.-H.; Wang, X.-Y.; Li, J.-R.; Gao, S.; Yu, K.-B. "Lanthanide contraction and pH value controlled structural change in a series of rare earth complexes with *p*-aminobenzoic acid," *J. Mol. Struct., 702*, **2004**, 77-83.

Sun, L.-N.; Yu, J.-B.; Zheng, G.-L.; Zhang, H.-J.; Meng, Q.-G.; Peng, C.-Y.; Fu, L.-S.; Liu, F.-Y.; Yu, Y.-N. "Syntheses, structures and near-IR luminescent studies on ternary lanthanide (Er^{III}, Ho^{III}, Yb^{III}, Nd^{III}) complexes containing 4,4,5,5,6,6,6-heptafluoro-1-(2-thienyl)hexane-1,3-dionate," *Eur. J. Inorg. Chem.*, **2006**, 3962-3973.

Tang, Q .; Liu, S .; Liu, Y .; He, D .; Miao, J .; Wang, X .; Ji, Y .; Zheng, Z. "Color tuning and white light emission *via* in situ doping of luminescent lanthanide metal−organic frameworks," *Inorg. Chem*., *53*, **2014**, 289−293.

Teotonio, E. E. S.; Brito, H. F.; Felinto, M. C. F. C.; Thompson, L. C.; Young, V. G.; Malta, O. L. "Preparation, crystal structure and optical spectroscopy of the rare earth complexes (RE^{3+} = Sm, Eu, Gd and Tb) with 2-thiopheneacetate anion," *J. Mol. Struct.*, *751*, **2005**, 85-94.

Tsaryuk, V.; Zhuravlev, K.; Zolin, V.; Gawryszewska, P.; Legendziewicz, J.; Kudryashova, V.; Pekareva, I. "Regulation of excitation and luminescence efficiencies of europium and terbium benzoates and 8-oxyquinolinates by modification of ligands," *J. Photochem. Photobiol. A.*, *177*, **2006**, 314-323.

Viswanathan, S.; de Bettencourt-Dias, A. "Eu(III) and Tb(III) luminescence sensitized by thiophenyl-derivatized nitrobenzoato antennas," *Inorg. Chem.*, *45*, **2006**, 10138-10146.

Wan, Y. –H.; Zheng, X. –J.; Wang, F. –Q.; Zhou, X. –Y.; Wang, K. -Z.; Jin, L. –P. "Water cluster supported architecture of lanthanide coordination polymers with pyrazinetricarboxylic acid," *Cryst. Eng. Comm*., *11*, **2009**, 278-283.

Werts, M. H. V.; Jukes, R. T. F.; Verhoeven, J. W. "The emission spectrum and the radiative lifetime of Eu^{3+} in luminescent lanthanide complexes," *Phys. Chem. Chem. Phys., 4*, **2002**, 1542-1548.

Wong, W.-T.; Lam, A. W.-H.; Gao, S.; Wen, G.; Zhang, X.-X. "Synthesis, crystal structure, and photophysical and magnetic properties of dimeric and

polymeric lanthanide complexes with benzoic acid and its derivatives," *Eur. J. Inorg. Chem.*, **2003**, 149-163.

Wrighton, M.S.; Ginley, D.S.; Morse, D.L. "Technique for the determination of absolute emission quantum yields of powdered samples," *J. Phys. Chem*., 78, **1974**, 2229–2233.

Xia, J.; Zhao, B.; Wang, H.-S.; Shi, W.; Ma, Y.; Song, H.-B.; Cheng, P.; Liao, D.-Z.; Yan, S.-P. "Two- and three-dimensional lanthanide complexes: Synthesis, crystal structures, and properties," *Inorg. Chem.*, *46*, **2007,** 3450-3458.

Xiao, M.; Selvin, P. R. "Quantum yields of luminescent lanthanide chelates and far-red dyes measured by resonance energy transfer," *J. Am. Chem. Soc.*, *123*, **2001**, 7067-7073.

Xin, H.; Shi, M.; Gao, X. C.; Huang, Y. Y.; Gong, Z. L.; Nie, D. B.; Cao, H.; Bian, Z. Q.; Li, F. Y.; Huang, C. H. "The effect of different neutral ligands on photoluminescence and electroluminescence properties of ternary terbium complexes," *J. Phys. Chem. B.*, *108*, **2004**, 10796-10800.

Yan, B. "Recent progress in photofunctional lanthanide hybrid materials," *RSC Adv.*, *2*, **2012**, 9304-9324.

Zhan, C.-H.; Wang, F.; Kang, Y.; Zhang, J. "Lanthanide-thiophene-2,5-dicarboxylate frameworks: Ionothermal synthesis, helical structures, photoluminescent properties, and single-crystal-to-single-crystal guest exchange," *Inorg. Chem., 51*, **2012**, 523-530.

Zhang, H.; Shan, X .; Ma, Z.; Zhou, L.; Zhang, M.; Lin, P.; Hu, S.; Ma, E.; Lia R.; Du, S. "A highly luminescent chameleon: fine-tuned emission trajectory and controllable energy transfer," *J. Mater. Chem. C.*, *2*, **2014**, 1367.

Zhang, H.; Shan, X .; Zhou, L.; Lin, P.; Li, R.; Ma, X.; Guo, X. Du, S. "Full-colour fluorescent materials based on mixed-lanthanide(III) metal–organic complexes with high-efficiency white light emission" *J. Mater. Chem*., C., *1*, **2013**, 888.

Zhang, L.; Xu, D.; Zhou, Y.; Jiang, F. "Design of 3-D europium(III)-organic frameworks based on pyridine carboxylate N-oxide and acyclic binary carboxylate: Syntheses, structures, and luminescence properties," *New J. Chem.*, *34*, **2010**, 2470-2478.

Zheng, Y.; Cardinali, F.; Armaroli, N.; Accorsi, G. "Synthesis and photoluminescence properties of heteroleptic europium(III) complexes with appended carbazole units," *Eur. J. Inorg. Chem.*, **2008**, 2075-2080.

Zhong, R.-Q.; Zou, R.-Q.; Du, M.; Jiang, L.; Yamada, T.; Maruta, G.; Takeda, S.; Xu, Q. "Metal-organic coordination architectures with 3-pyridin-3-yl-benzoate: Crystal structures, fluorescent emission and magnetic properties," *CrystEngComm.*, *10*, **2008**, 605-613.

Zhou, X.-X.; Cai, Y.-P.; Zhu, S.-Z.; Zhan, Q.-G.; Liu, M.-S.; Zhou, Z.-Y.; Chen, L. "Self-Assembly of Two Novel Cadmium(II) Complexes: One from Tripodal Imine–Phenol Ligand and the Other from In situ Partial Degradation

of Dipolar Imine–Phenol Ligand," *Cryst. Growth Des.*, **2008**, *8*, 2076–2079.

Zhu, Y. C.; Zhou, L.; Li, H. Y.; Xu, Q. L.; Teng, M. Y.; Zheng, Y. X.; Zou, J. L.; Zhang, H. J.; You, X. Z. "Highly Efficient Green and Blue-Green Phosphorescent OLEDs Based on Iridium Complexes with the Tetraphenylimidodiphosphinate Ligand," *Adv. Mater.*, *23*, **2011**, 4041–4046.

Zucchi, G.; Maury, O.; Thuéry, P.; Gumy, F.; Bünzli, J.-C. G.; Ephritikhine, M. "2,2′-Bipyrimidine as efficient sensitizer of the solid-state luminescence of lanthanide and uranyl ions from visible to near-infrared," *Chem. Eur. J.*, *15*, **2009**, 9686-9696.